FACILITY TO STUDY THE CONTROL OF FLEXIBLE SPACE STRUCTURES

DETAILED DESIGN (Preliminary)

[DOC-CR-SP-83-026]

DYNACON

DYNACON Enterprises Ltd.
DYNAMICS AND CONTROL ANALYSIS
18 Cherry Blossom Lane Thornhill, Ontario L3T 3B9 (416) 889-9260

(2)

FACILITY TO STUDY THE CONTROL OF FLEXIBLE SPACE STRUCTURES

DETAILED DESIGN (Preliminary)

[DOC-CR-SP-83-026]

(1)
G. B. Sincarsin

March 1983

Dynacon Report DAISY-5

Government of Canada / Gouvernement du Canada

Department of Communications

DOC CONTRACTOR REPORT DOC-CR-SP-83-026

DEPARTMENT OF COMMUNICATIONS - OTTAWA - CANADA

SPACE PROGRAM

TITLE: Facility to Study the Control of Flexible Space Structures — Detailed Design (Preliminary)

AUTHOR(S): G. B. Sincarsin

ISSUED BY CONTRACTOR AS REPORT NO: Dynacon Report DAISY-5

PREPARED BY: Dynacon Enterprises Ltd.,
18 Cherry Blossom Lane,
Thornhill, Ontario
L3T 3B9

DEPARTMENT OF SUPPLY AND SERVICES CONTRACT NO: 22ST.36001-2-0727

DOC SCIENTIFIC AUTHORITY: A. H. Reynaud (Communications Research Centre)

CLASSIFICATION: Unclassified

DATE: March 1983

SUMMARY

A detailed model is developed for the dynamics of the flexible structure DAISY. Motion equations are first written for the various substructures comprised by DAISY and then these are combined to obtain an overall dynamics model. A similar procedure is used to derive gravitational and aerodynamic disturbance models and a detailed inertia model. Preliminary detailed designs for each substructure also are presented.

PREFACE

Acknowledgments

The author would like to thank P. C. Hughes for his critical review of the manuscript. Thanks are also due to Mrs J. Hughes for typing this document. Finally, the author is pleased to acknowledge the encouragement and timely advice of A. H. Reynaud of the Communications Research Centre, who acted as the Scientific Authority for this contract.

Proprietary Rights

Dynacon Enterprises Ltd. does not claim "proprietary rights" to the material in this report. Indeed, the hope is that the analyses, results, ideas and opinions in this report will be useful to others. In this event, a reference to this report would be appreciated.

Units and Spelling

This report uses S.I. units and North American spelling.

TABLE OF CONTENTS

LIST OF FIGURES

LIST OF TABLES

1. INTRODUCTION

This report describes the progress made towards completing the detailed design of a facility to study the control of flexible space structures. The conceptual design for this facility has already been described in an earlier report [Sincarsin, 1983]; however, since the present discussion requires a knowledge of the former, a brief review is in order.

1.1 Review of Conceptual Design

It is conceived that the control facility will consist of a highly flexible structure, called DAISY, and a group of primary and secondary actuators and sensors, so arranged as to make achievable the objectives of the control facility development program. In brief, these objectives are as follows:

- The primary objective is to study the stabilization and control of structurally flexible communications satellites.
- Fundamental concepts in the control of flexible space structures must be investigated and evaluated.
- 'Hands-on' experience must be developed with realistic sensors, actuators, structures, and control electronics.
- Control approaches must be developed that are especially adapted to the unusual and challenging requirements of large flexible space structures.
- The results of this research must be of direct relevance to the attitude control of the next generation of Canadian communications satellites.

It is believed that the structure shown in Fig. 1.1 will satisfy the requirements for the control facility. DAISY is approximately 3 m in diameter and consists of a central rigid hub to which are attached 2 n (n odd) 'flexible' ribs. Initially all the rib flexibility is to be localized in the form of spirator springs at the rib-hub inter-

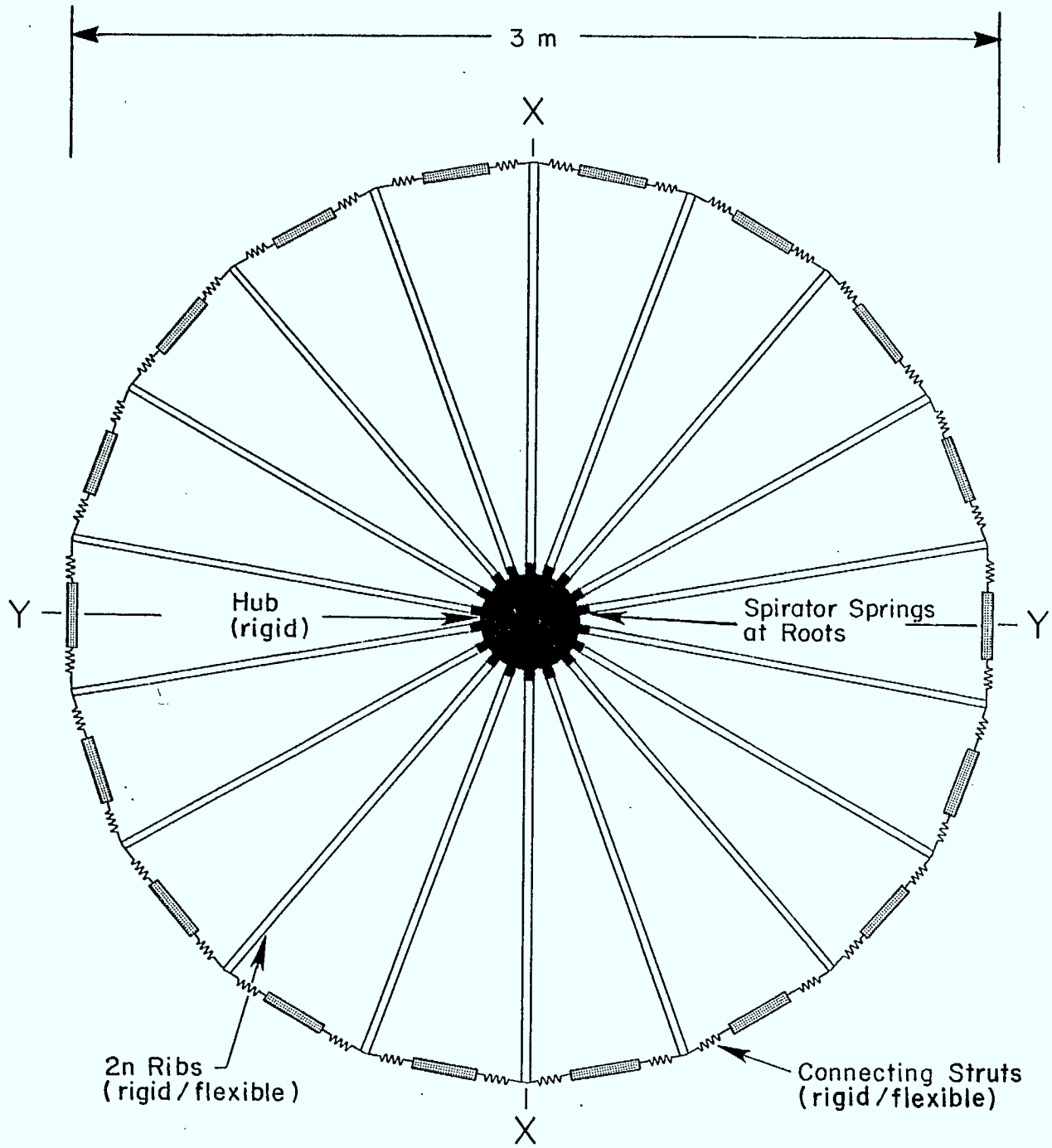

Figure 1.1: Basic Components of Flexible Structure for Control Experiment

face. The ribs are interconnected at their tips via 'flexible' struts. Again, the strut flexibility is localized, as will be seen later in this report. The rib attachments to the hub are adjustable and, in fact, for a horizontal mounting, DAISY's ribs 'droop' under gravity. It is also intended to have the rib attachments designed so that ribs can be interchanged. This permits both geometric and material asymmetries to be introduced by removing certain ribs or replacing a given rib with one made of a different material. Another advantage of the chosen structure is that it is easily discretized into individual substructures, a characteristic that will be exploited in Section 2.

The primary sensors chosen for the control facility are digital encoders and accelerometers. The digital encoders, three to measure angular displacement and three ('tachometers') to measure angular rate, are located at the hub gimbal (see Fig. 1.2). The accelerometers, on the other hand, are to be mounted on the ribs. The secondary sensors, located on the periphery, are linear variable differential transformers. Future possibilities for sensors include gyros and an optical relative-displacement measurement system.

The primary actuators are three reaction wheels located in the hub, and the secondary actuators are solenoid drivers located on the periphery of DAISY (see Fig. 1.2). The former are intended to control DAISY, while the latter will provide known 'external' disturbances. In the future, proof-mass actuators may be placed on the ribs and the rib root adjustment may be automated, using brushless DC motors.

A diagram of the proposed mounting for DAISY and the various sensor and actuator locations is given in Fig. 1.2. A horizontal mounting (with DAISY suspended from below) is chosen to enable the mass center to correspond with the gimbal pivot point. This removes the possibility of a pendulous mode for the structure under gravity. It is notable that the ribs are shown 'drooping' in the figure, for just this reason. The support structure is isolated in the sense that electronic filtering will be required to remove high-frequency background noise. The gimbal is intended eventually to possess three degrees of freedom, but for the present it is restricted not to rotate about the hub symmetry axis. Every attempt will

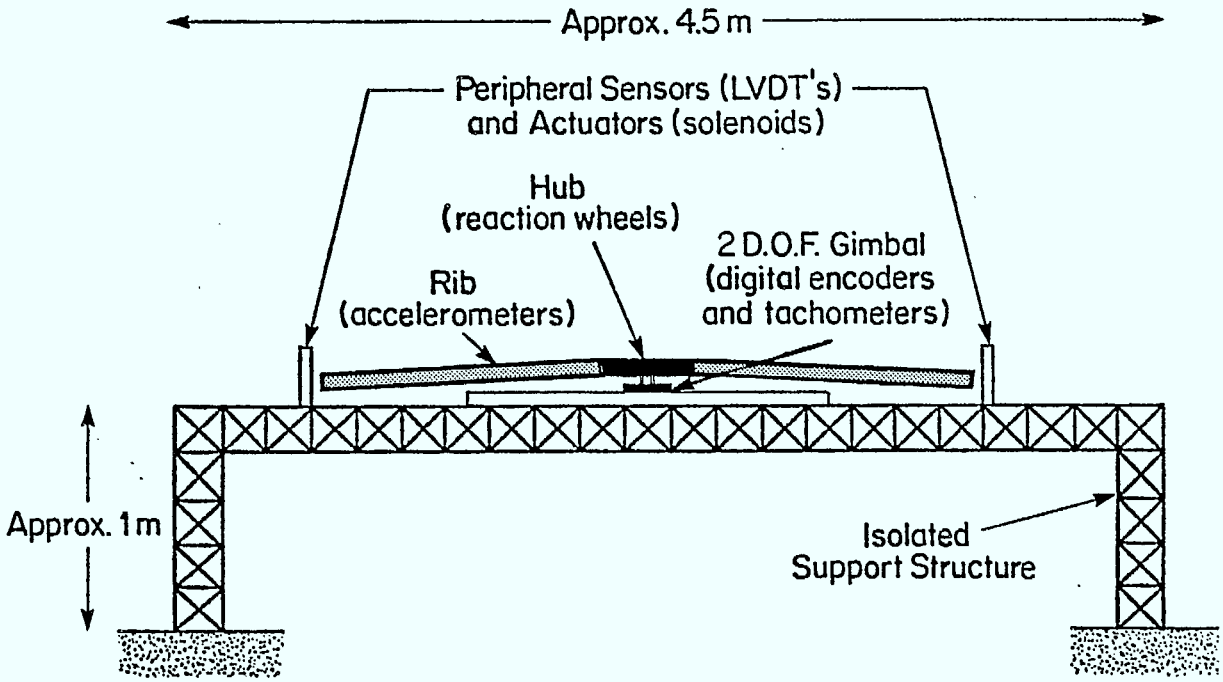

Figure 1.2: Horizontal Mounting for DAISY

be made to keep the gimbal mount a 'universal' mount suitable for use with a variety of structures, not just with DAISY.

1.2 Report Outline

This report consists of three major sections. The first, Section 2, presents a detailed dynamics model for DAISY. The basic technique is first to formulate equations of motion for the individual substructures and then to combine these equations to obtain the overall motion equations. In this regard, Section 2 parallels very closely the presentation given by [Hughes, 1981]. The major differences are these: (i) for DAISY the geometric constraint equations are more complicated, and (ii) the multiplicity of individual substructures necessitates the use of indicial notation.

Section 3, the second major section, deals with disturbance models. Both gravitational and aerodynamic disturbances are modeled for each substructure. The aerodynamic disturbances are inertial air resistance and viscous drag. The general theory behind these models is elaborated upon in [Sincarsin and Hughes, 1983], with results specific for DAISY being the aim of Section 3.

The third and final major section, Section 4, describes the preliminary detailed designs for each substructure and presents an inertia model for each. This is required before the equations derived in Section 2 can be applied to assess structural dynamical characteristics. Some comments on spring placement and design also are included in this section, as is a brief discussion of one potential damper and its most likely location.

2. DYNAMICS MODEL FOR DAISY

In this section a detailed dynamics model for the DAISY structure (shown in Fig. 1.1) is presented in its most general form. The motion equations for the overall structure are derived in terms of the motion equations for the individual substructures comprised by DAISY.

2.1 Basic Considerations

Prior to obtaining motion equations for each substructure, it is necessary to specify in some detail the generic model assumed for DAISY. For example, the flexibility of each substructure must be established. Also, the reference frames and attachment points assumed for the various substructures must be identified, as must the forces and torques acting upon these substructures. Finally, the overall inertia distribution must be determined. These topics are discussed in detail in what follows.

2.1.1 DAISY Substructures

The morphology assumed for DAISY is depicted in Fig. 2.1. It is assumed to consist of $2m + 1$ substructures, where $m = 2n$, $n > 3$ and n odd, is the number of ribs and the number of struts. Since these substructures are repeated components it is necessary to consider only a typical rib and a typical strut. Hence, the substructures of interest are as follows:

Hub,	symbol	R_h,	Rigid
Rib_j,	symbol	E_{r_j},	Elastic
Strut_j,	symbol	E_{s_j},	Elastic

The connection points between the various substructures $\{O_{r_j}, O_{s_j}, O_{c_j}, j = 1,\ldots,m\}$ are also shown in Fig. 2.1. The motion equations will ultimately be written with respect to O_h, an arbitrary reference point in the hub.

2.1.2 Reference Frames

A total of $2(m + 1)$ reference frames are required to formulate the dynamics model: $2m + 1$ explicit frames and one implicit inertial frame, F_I. It is not necessary to consider individually each rib frame F_{r_j} and each strut frame F_{s_j}; only a typical frame need be considered in each case. The remaining reference frame of interest is the hub frame,

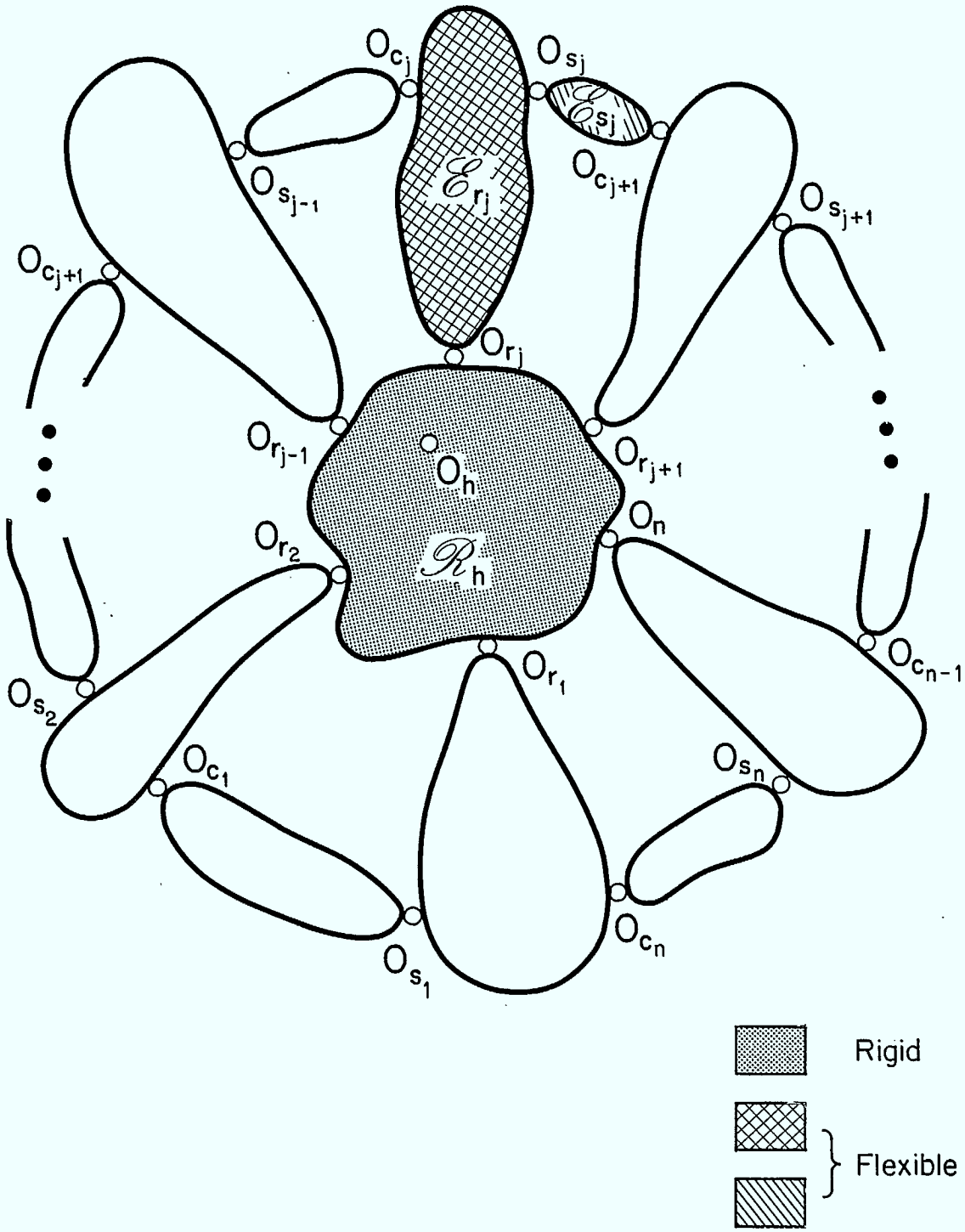

Figure 2.1: Daisy Morphology

F_h. The origin of F_{r_j} is the point O_{r_j}; similarly, the origins of F_{s_j}, F_h and F_I are O_{s_j}, O_h and O_I, as shown in Fig. 2.2.

Each substructure is assigned its own reference frame so that the motion equations of that structure can be written independently of the remaining substructures. It is convenient, therefore, to express absolute displacements (i.e., those relative to F_I) in local reference frames. To be specific, the following symbols indicate absolute translational displacements:

$\underline{w}_h$ - translation of O_h, expressed in F_h

$\underline{w}_{r_j}$ - translation of O_{r_j}, expressed in F_{r_j}

$\underline{w}_{s_j}$ - translation of O_{s_j}, expressed in F_{s_j}

$\underline{w}_{c_{j+1}}$ - translation of $O_{c_{j+1}}$, expressed in F_{s_j}

Furthermore, the absolute angular displacements are as follows:

$\underline{\theta}_h$ - rotation of F_h about O_h, expressed in F_h

$\underline{\theta}_{r_j}$ - rotation of F_{r_j} about O_{r_j}, expressed in F_{r_j}

$\underline{\theta}_{s_j}$ - rotation of F_{s_j} about O_{s_j}, expressed in F_{s_j}

These absolute displacements are not assumed to be necessarily small; however, their first and second time derivatives (i.e. the absolute velocities and accelerations) are assumed to be first-order infinitesimals.

2.1.3 Rotation Matrices

Here we adopt the notation $\underline{C}_{pq}$ for a rotation matrix that transforms the components of a vector expressed in F_q into the components of the same vector expressed in F_p. Since the absolute rotations assumed herein are not small, the rotation matrices between the various substructures of DAISY need not represent small rotations; however, any *changes* to the rotation matrices caused by deformations

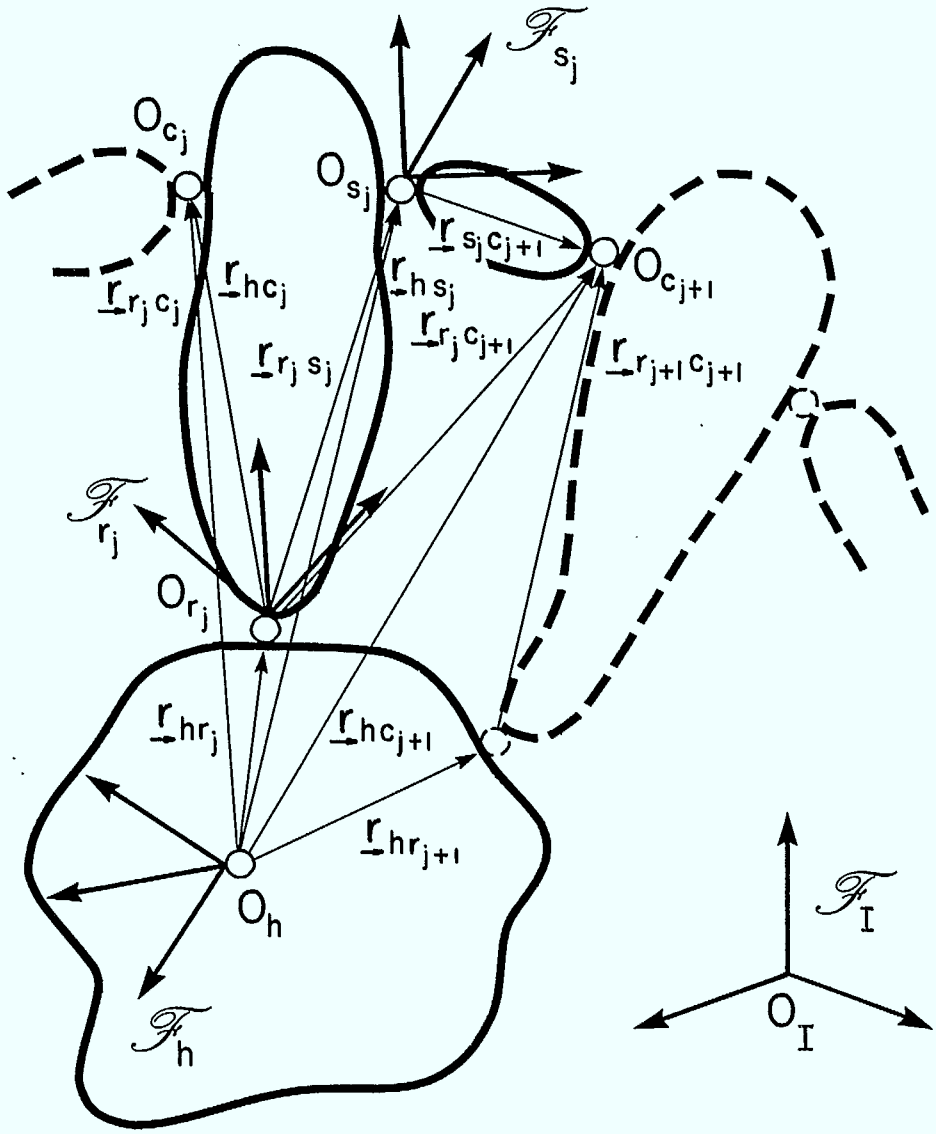

Figure 2.2: A Typical Rib-Strut Pair

of DAISY are first-order infinitesimals. This fact, coupled with the realization that every rotation matrix in the motion equations occurs multiplied by a first-order system coordinate, implies that any change in C_{pq} will result in second-order terms — to be neglected in the linear analysis presented here. Hence, any change in $\underline{C}_{pq}$ can be ignored from the outset and the relationships between the various reference frames established as though DAISY were rigid.

Two useful relationships are the identities

$$\underline{C}_{pq} = \underline{C}_{pb}\underline{C}_{bq} \tag{2.1}$$

and

$$(\underline{C}_{pq}\underline{a})^{x} = \underline{C}_{pq}\underline{a}^{x}\underline{C}_{qp} \tag{2.2}$$

where F_b is some intermediate reference frame and $\underline{a}$ is any 3×1 matrix expressed in F_q. These relations will prove very useful during the derivation of the final motion equations. It is noteworthy that since any change in $\underline{C}_{pq}$ can be ignored, the question as to whether $\underline{a}$ is expressed in an undeformed F_q or in a deformed F_q is inconsequential.

2.1.4 Attachment-Point Vectors

Let the vector attaching the point O_p to O_q be $\underrightarrow{r}_{pq}$. Furthermore, let the components of this vector, denoted $\underline{r}_{pq}$, be expressed in F_p. Then, from Fig. 2.2, it follows that:

$$\underline{r}_{r_j c_{j+1}} = \underline{r}_{r_j s_j} + \underline{C}_{r_j s_j}\underline{r}_{s_j c_{j+1}} \tag{2.3}$$

$$\underline{r}_{hc_j} = \underline{r}_{hr_j} + \underline{C}_{hr_j}\underline{r}_{r_j c_j} \tag{2.4}$$

$$\underline{r}_{hs_j} = \underline{r}_{hr_j} + \underline{C}_{hr_j}\underline{r}_{r_j s_j} \tag{2.5}$$

$$\underline{r}_{hc_{j+1}} = \underline{r}_{hr_j} + \underline{C}_{hr_j}\underline{r}_{r_j c_{j+1}} = \underline{r}_{hs_j} + \underline{C}_{hs_j}\underline{r}_{s_j c_{j+1}} \tag{2.6}$$

Again, these relations will play a key role in formulating the final motion equations.

2.1.5 Forces and Torques

In order to formulate the motion equations for the individual substructures, it is helpful to draw a free-body diagram for the substructure in question. Figure 2.3 shows such diagrams for E_{r_j} and E_{s_j}. A partial free-body diagram for R_h is also shown. Two types of force (and torque) are evident — internal interaction forces that act as external forces applied to the substructures, and truly external forces, which remain after the individual substructural models have been combined. Discussion of the types of external force experienced by DAISY is left until Section 2.3.4.

As shown in Fig. 2.3, the internal force from substructure q on substructure p is denoted $\underset{\rightarrow}{f}_{pq}$. Simlarly, the torque on substructure p from substructure q is $\underset{\rightarrow}{g}_{pq}$. Since these are internal interaction forces and torques, they occur in equal and opposite pairs:

$$\underset{\rightarrow}{f}_{pq} = -\underset{\rightarrow}{f}_{qp} \tag{2.7}$$

$$\underset{\rightarrow}{g}_{pq} = -\underset{\rightarrow}{g}_{qp} \tag{2.8}$$

Here we choose to express $\underset{\rightarrow}{f}_{pq}$ and $\underset{\rightarrow}{g}_{pq}$ in F_p, whence

$$\underline{f}_{hr_j} = -\underline{C}_{hr_j}\underline{f}_{r_jh} \; ; \qquad \underline{g}_{hr_j} = -\underline{C}_{hr_j}\underline{g}_{r_jh}$$

$$\underline{f}_{r_js_j} = -\underline{C}_{r_js_j}\underline{f}_{s_jr_j} \; ; \qquad \underline{g}_{r_js_j} = -\underline{C}_{r_js_j}\underline{g}_{s_jr_j}$$

$$\underline{f}_{r_js_{j-1}} = -\underline{C}_{r_js_{j-1}}\underline{f}_{s_{j-1}r_j} \; ; \qquad \underline{g}_{r_js_{j-1}} = -\underline{C}_{r_js_{j-1}}\underline{g}_{s_{j-1}r_j} \tag{2.9}$$

$$\underline{f}_{s_jr_{j+1}} = -\underline{C}_{s_jr_{j+1}}\underline{f}_{r_{j+1}s_j} \; ; \qquad \underline{g}_{s_jr_{j+1}} = -\underline{C}_{s_jr_{j+1}}\underline{g}_{r_{j+1}s_j}$$

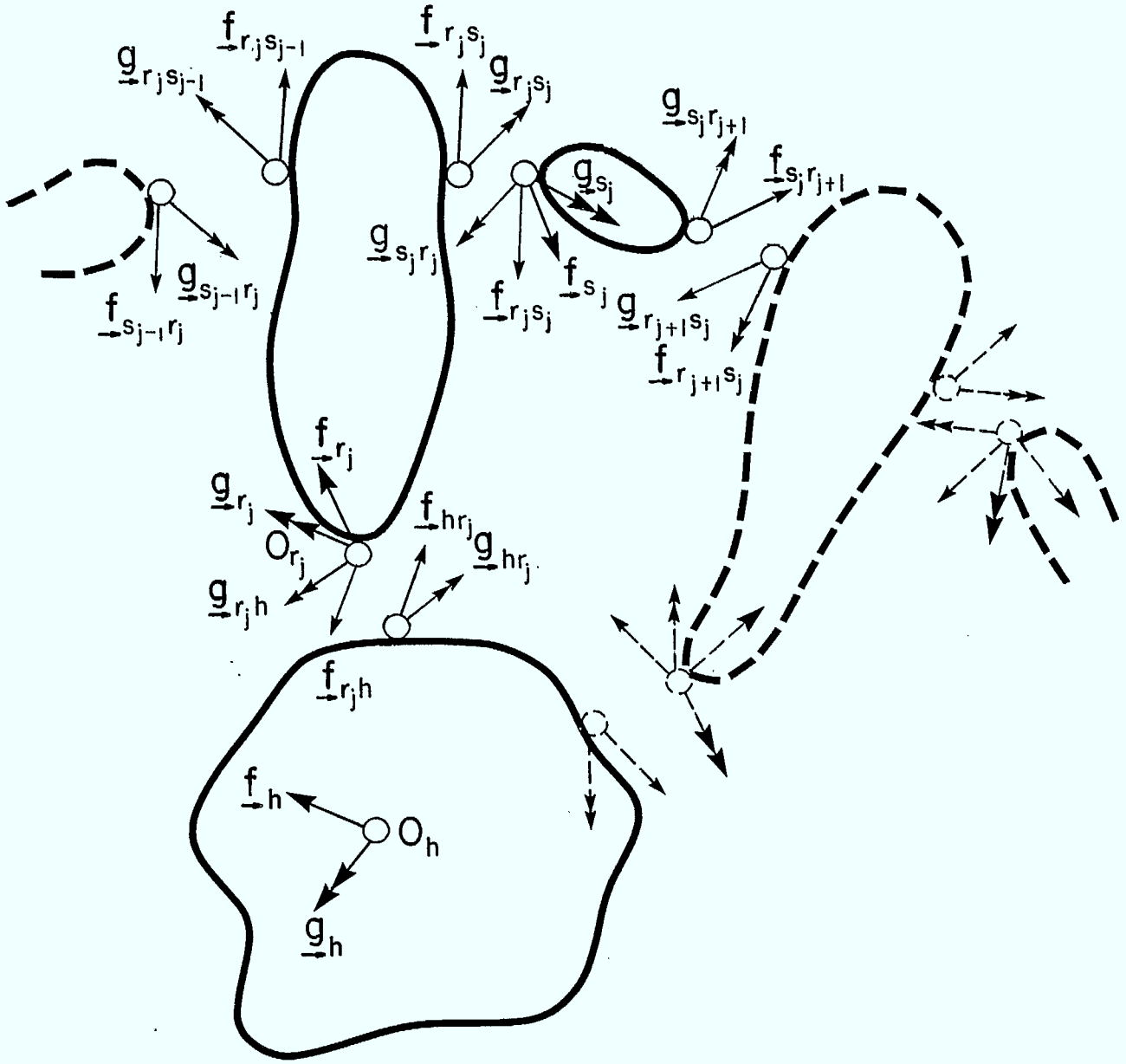

Figure 2.3: Free-Body Diagrams for a Typical Rib-Strut Pair

Of course, these relations can be written in reverse by application of the identity $\underline{C}_{pq}^{-1} = \underline{C}_{qp}$.

The notation adopted here to represent external forces and torques also is highlighted in Fig. 2.3. Simply, the external force acting on substructure p is denoted by $\underline{f}_{\rightarrow p}$, with components expressed in F_p. The external torque about the point O_p for this same substructure is given by $\underline{g}_{\rightarrow p}$, where the components of $\underline{g}_{\rightarrow p}$ also are expressed in F_p. Therefore, to summarize:

$\underline{f}_h$ - external force on R_h, expressed in F_h

$\underline{f}_{r_j}$ - external force on E_{r_j}, expressed in F_{r_j}

$\underline{f}_{s_j}$ - external force on E_{s_j}, expressed in F_{s_j}

$\underline{g}_h$ - external torque on R_h, expressed in F_h

$\underline{g}_{r_j}$ - external torque on E_{r_j}, expressed in F_{r_j}

$\underline{g}_{s_j}$ - external torque on E_{s_j}, expressed in F_{s_j}

Given the above definitions, (2.9), and the geometry from Section 2.1.4, it is possible, by combining the system of forces and torques on the individual substructures, to define the total force and torque (about O_h) acting on DAISY. The total force, expressed in F_h, is

$$\underline{f} = \underline{f}_h + \sum_{j=1}^{m} (\underline{C}_{hr_j} \underline{f}_{r_j} + \underline{C}_{hs_j} \underline{f}_{s_j}) \tag{2.10}$$

while the total torque about O_h, also expressed in F_h, is

$$\underline{g} = \underline{g}_h + \sum_{j=1}^{m} [(\underline{C}_{hr_j} \underline{g}_{r_j} + \underline{r}^{x}_{hr_j} \underline{C}_{hr_j} \underline{f}_{r_j}) + (\underline{C}_{hs_j} \underline{g}_{s_j} + \underline{r}^{x}_{hs_j} \underline{C}_{hs_j} \underline{f}_{s_j})] \tag{2.11}$$

It only remains to consider the inertia distribution for DAISY, before the motion equations for the individual substructures can be formulated.

2.1.6 Inertia Distribution

We denote the masses of the individual substructures as follows:

m_h - mass of R_h

m_{r_j} - mass of E_{r_j}

m_{s_j} - mass of E_{s_j}

The total mass is

$$m = m_h + \sum_{j=1}^{m} (m_{r_j} + m_{s_j}) \tag{2.12}$$

Also, let the first moments of inertia ($\int \underline{r}\, dm$) for the individual substructures be given by

$\underline{c}_h$ - first inertia moment of R_h, about O_h, expressed in F_h

$\underline{c}_{r_j}$ - first inertia moment of E_{r_j}, about O_{r_j}, expressed in F_{r_j}

$\underline{c}_{s_j}$ - first inertia moment of E_{s_j}, about O_{s_j}, expressed in F_{s_j}

Then the first moment of inertia of DAISY about O_h, expressed in F_h, is

$$\underline{c} = \underline{c}_h + \sum_{j=1}^{m} [(m_{r_j} \underline{r}_{hr_j} + \underline{C}_{hr_j} \underline{c}_{r_j}) + (m_{s_j} \underline{r}_{hs_j} + \underline{C}_{hs_j} \underline{c}_{s_j})] \tag{2.13}$$

Finally, denoting the second moment of inertia matrix for each substructure as follows

$\underline{J}_h$ - moment-of-inertia matrix for R_h, about O_h, expressed in F_h

$\underline{J}_{r_j}$ - moment-of-inertia matrix for E_{r_j}, about O_{r_j}, expressed in F_{r_j}

$\underline{J}_{s_j}$ - moment-of-inertia matrix for E_{s_j}, about O_{s_j}, expressed in F_{s_j}

the second moment of inertia matrix for DAISY, about O_h, expressed in F_h,

takes the form

$$\underline{J} = \underline{J}_h + \sum_{j=1}^{m} [(\underline{C}_{hr_j} \underline{J}_{r_j} \underline{C}_{r_j h} - \underline{C}_{hr_j} \underline{c}^{x}_{r_j} \underline{C}_{r_j h} \underline{r}^{x}_{hr_j} - \underline{r}^{x}_{hr_j} \underline{C}_{hr_j} \underline{c}^{x}_{r_j} \underline{C}_{r_j h} - m_{r_j} \underline{r}^{x}_{hr_j} \underline{r}^{x}_{hr_j}) + (\underline{C}_{hs_j} \underline{J}_{s_j} \underline{C}_{s_j h} - \underline{C}_{hs_j} \underline{c}^{x}_{s_j} \underline{C}_{s_j h} \underline{r}^{x}_{hs_j} - \underline{r}^{x}_{hs_j} \underline{C}_{hs_j} \underline{c}^{x}_{s_j} \underline{C}_{s_j h} - m_{s_j} \underline{r}^{x}_{hs_j} \underline{r}^{x}_{hs_j})] \tag{2.14}$$

This expression and (2.13) follow from the repeated use of the parallel-axis theorems governing moments of inertia, as described by [Hughes, 1980].

2.2 Motion Equations for Substructures

The motion equations for each substructure specified in Section 2.1.1 can now be written. Here the equations are presented in a general format so that they will remain valid despite any changes in the design of the various substructures. The only restrictions are that the overall geometry for DAISY be that shown in Fig. 2.1 and that the degrees of freedom assumed for each substructure do not change. These will be elaborated upon in what follows.

2.2.1 Motion Equations for the Hub

As stated in Section 2.1.1, the hub is assumed rigid. Thus the absolute displacement (to first order) anywhere in the hub (located by $\underline{r}_h$ relative to O_h) is given by

$$\underline{d}_h(\underline{r}_h, t) = \underline{w}_h(t) - \underline{r}^{x}_h \underline{\theta}_h(t) \tag{2.15}$$

where $\underline{d}_h$ is expressed in F_h and $\underline{w}_h$ and $\underline{\theta}_h$ are defined in Section 2.1.2. The motion equations governing these six rigid degrees of freedom are well known:

$$m_h \ddot{\underline{w}}_h - \underline{c}_h^{\times} \ddot{\underline{\theta}}_h = \underline{f}_h + \sum_{j=1}^{m} \underline{f}_{hr_j} \tag{2.16}$$

$$\underline{c}_h^{\times} \ddot{\underline{w}}_h + \underline{J}_h \ddot{\underline{\theta}}_h = \underline{g}_h + \sum_{j=1}^{m} (\underline{g}_{hr_j} + \underline{r}_{hr_j}^{\times} \underline{f}_{hr_j}) \tag{2.17}$$

It should be noted that the torque equation (2.17) is written about O_h, and that both (2.16) and (2.17) are expressed in F_h.

2.2.2 Motion Equations for a Typical Rib

For the present analysis each rib is itself rigid; however, the spirator springs at the hub-rib interface (recall Fig. 1.1) necessitates the treatment of each rib as an elastic body. Nine degrees of freedom are associated with each rib — six absolute displacements, $\underline{w}_{r_j}$ and $\underline{\theta}_{r_j}$ and three relative rotations about O_{r_j}, $\underline{\alpha}_j$. These relative rotations activate the springs at the rib root.

The absolute displacement at any point within the rib ($\underline{r}_{r_j}$ measured relative to O_{r_j}) is in general given by

$$\underline{d}_{r_j}(\underline{r}_{r_j},t) = \underline{w}_{r_j}(t) - \underline{r}_{r_j}^{\times} \underline{\theta}_{r_j}(t) + \underline{\Delta}_{r_j}(\underline{r}_{r_j},t) \tag{2.18}$$

where in the present context the deflection from elasticity $\underline{\Delta}_{r_j}(\underline{r}_{r_j},t)$ is just

$$\underline{\Delta}_{r_j}(\underline{r}_{r_j},t) = -\underline{r}_{r_j}^{\times} \underline{\alpha}_j(t) \tag{2.19}$$

Furthermore, as is common practice, we shall assume that $\underline{\Delta}_r(\underline{r},t)$ can be expressed as a superposition of shape functions $\{\underline{\psi}_1(\underline{r}),\underline{\psi}_2(r),\ldots\}$ according to

$$\underline{\Delta}_r(\underline{r},t) = \sum_k \underline{\psi}_k(\underline{r}) q_k(t) \tag{2.20}$$

where $q_k(t)$ is the generalized coordinate associated with the shape function $\underline{\psi}_k(\underline{r})$. Then, defining the rectangular matrix

$$\underline{\Psi}(\underline{r}) = [\underline{\psi}_1(\underline{r}) \quad \underline{\psi}_2(\underline{r}) \quad \ldots], \tag{2.21}$$

(2.20) can be written in the form

$$\underline{\Delta}_r(\underline{r},t) = \underline{\Psi}(\underline{r})\underline{q}(t) \tag{2.22}$$

where

$$\underline{q}(t) = [q_1 \quad q_2 \quad \ldots]^T \tag{2.23}$$

Therefore, for each rib,

$$\underline{\Psi}_{r_j}(\underline{r}_{r_j}) \equiv -\underline{r}^X_{r_j} \; ; \qquad \underline{q}_{r_j} \equiv \underline{\alpha}_j \tag{2.34}$$

Given these facts, the linear and angular momentum matrices ($\underline{P}_{\alpha_j}$ and $\underline{H}_{\alpha_j}$) associated with the elastic deflections of the rib can be determined:

$$\underline{P}_{\alpha_j} = \int \underline{\Psi}_{r_j} \, dm_{r_j} \equiv -\underline{c}^X_{r_j} \tag{2.35}$$

$$\underline{H}_{\alpha_j} = \int \underline{r}^X_{r_j} \underline{\Psi}_{r_j} \, dm_{r_j} \equiv \underline{J}_{r_j} \tag{2.36}$$

Also, the mass matrix $\underline{M}_{\alpha_j}$ and the generalized forces $\underline{\mathcal{A}}_{\alpha_j}$ can be written explicitly:

$$\underline{M}_{\alpha_j} = \int \underline{\Psi}^T_{r_j} \underline{\Psi}_{r_j} \, dm_{r_j} \equiv \underline{J}_{r_j} \tag{2.37}$$

$$\underline{\mathcal{A}}_{\alpha_j} = \int \underline{\Psi}^T_{r_j} \hat{\underline{f}}_{r_j}(\underline{r}_{r_j},t) dV_{r_j} \equiv \underline{g}_{r_j} \tag{2.38}$$

A distributed force per unit volume $\hat{\underline{f}}_r(\underline{r},t)$ has been assumed in (2.38). This is consistent with the type of external forces anticipated to be significant for DAISY — gravitational and aerodynamic forces (see Sections 2.3.4 and 2.3.5). In any case, should a different force model be required

(e.g., point forces), the modification of (2.38) is a straightforward matter.

Now recalling the free-body diagram of Fig. 2.3, and summing the applied forces and torques, the motion equations for a typical rib, expressed in F_{r_j}, are

$$m_{r_j}\underline{\ddot{w}}_{r_j} - \underline{c}^{x}_{r_j}\underline{\ddot{\theta}}_{r_j} + \underline{P}_{\alpha_j}\underline{\ddot{\alpha}}_j = \underline{f}_{r_j} + \underline{f}_{r_j h} + \underline{f}_{r_j s_j} + \underline{f}_{r_j s_{j-1}} \tag{2.39}$$

$$\underline{c}^{x}_{r_j}\underline{\ddot{w}}_{r_j} + \underline{J}_{r_j}\underline{\ddot{\theta}}_{r_j} + \underline{H}_{\alpha_j}\underline{\ddot{\alpha}}_j = \underline{g}_{r_j} + \underline{g}_{r_j h} + \underline{g}_{r_j s_j} + \underline{r}^{x}_{r_j s_j}\underline{f}_{r_j s_j} + \underline{g}_{r_j s_{j-1}} + \underline{r}^{x}_{r_j c_j}\underline{f}_{r_j s_{j-1}} \tag{2.40}$$

$$\underline{P}^{T}_{\alpha_j}\underline{\ddot{w}}_{r_j} + \underline{H}^{T}_{\alpha_j}\underline{\ddot{\theta}}_{r_j} + \underline{M}_{\alpha_j}\underline{\ddot{\alpha}}_j + \underline{K}_{\alpha_j}\alpha_j = \underline{\mathcal{f}}_{\alpha_j} + \underline{g}_{r_j s_j} + \underline{r}^{x}_{r_j s_j}\underline{f}_{r_j s_j} + \underline{g}_{r_j s_{j-1}} + \underline{r}^{x}_{r_j c_j}\underline{f}_{r_j s_{j-1}} \tag{2.41}$$

The torque equation (2.40) is written about O_{r_j}. To permit a variety of rib designs without requiring substantial modifications to the final dynamics equations for DAISY, $\underline{P}_{\alpha_j}$, $\underline{H}_{\alpha_j}$, $\underline{M}_{\alpha_j}$ and $\underline{\mathcal{f}}_{\alpha_j}$ are retained in their most general forms in (2.39) through (2.41). However, for the present rib design (see Section 3.2), these matrices are given by (2.35) through (2.38). $\underline{K}_{\alpha_j}$ is the stiffness matrix associated with $\underline{\alpha}_j$.

2.2.3 Motion Equations for a Typical Strut

As for the ribs, each strut is elastic only because of the presence of springs in its design. Of the eight degrees of freedom possessed by each strut, two are associated with elastic (spring) displacements. They are denoted by δ_j and γ_j. The first is a linear displacement along the line

joining the strut connection points O_{s_j} and $O_{c_{j+1}}$. That is, δ_j is the magnitude of the displacement along the unit vector

$$\hat{\underline{r}}_{s_j c_{j+1}} = \underline{r}_{s_j c_{j+1}} / \ell_{s_j} = \underline{1}_{s_j} \tag{2.42}$$

where ℓ_{s_j} is the magnitude of $\underline{r}_{s_j c_{j+1}}$. The second elastic displacement, γ_j, is a rotation about the $\underline{1}_{s_j}$ direction. The remaining six degrees of freedom are the absolute displacements $\underline{w}_{s_j}$ and $\underline{\theta}_{s_j}$ defined in Section 2.1.2.

Given the cited degrees of freedom, the absolute displacement for any point in the strut is

$$\underline{d}_{s_j}(\underline{r}_{s_j},t) = \underline{w}_{s_j}(t) - \underline{r}^{X}_{s_j}\underline{\theta}_{s_j}(t) + \underline{\Delta}_{s_j}(\underline{r}_{s_j},t) \tag{2.43}$$

where $\underline{r}_{s_j}$ is measured relative to O_{s_j} and $\underline{d}_{s_j}$ is expressed in F_{s_j}. Furthermore,

$$\underline{\Delta}_{s_j}(\underline{r}_{s_j},t) = \underline{1}_{s_j}\delta_j - \underline{r}^{X}_{s_j}\underline{1}_{s_j}\gamma_j \tag{2.44}$$

whence

$$\underline{\Psi}_{s_j}(\underline{r}_{s_j}) \equiv [\underline{1}_{s_j} \quad -\underline{r}^{X}_{s_j}\underline{1}_{s_j}] \tag{2.45}$$

$$\underline{q}_{s_j} \equiv [\delta_j \quad \gamma_j]^{T} \tag{2.46}$$

Therefore, conducting the integrations implied by (2.35) through (2.38) with r_j replaced by s_j, it follows that

$$\underline{P}_{s_j} = \begin{bmatrix} \underline{P}_{\delta_j} \\ \underline{P}_{\gamma_j} \end{bmatrix} = \begin{bmatrix} m_{s_j} \underline{1}_{s_j} \\ -\underline{c}^{x}_{s_j} \underline{1}_{s_j} \end{bmatrix} \quad ; \quad \underline{H}_{s_j} = \begin{bmatrix} \underline{H}_{\delta_j} \\ \underline{H}_{\gamma_j} \end{bmatrix} = \begin{bmatrix} \underline{c}^{x}_{s_j} \underline{1}_{s_j} \\ \underline{J}_{s_j} \underline{1}_{s_j} \end{bmatrix}$$

$$\underline{M}_{s_j} = \begin{bmatrix} m_{\delta\delta_j} & m_{\delta\gamma_j} \\ m_{\gamma\delta_j} & m_{\gamma\gamma_j} \end{bmatrix} = \begin{bmatrix} m_{s_j} & \underline{1}^{T}_{s_j} \underline{c}^{x}_{s_j} \underline{1}_{s_j} \\ -\underline{1}^{T}_{s_j} \underline{c}^{x}_{s_j} \underline{1}_{s_j} & \underline{1}^{T}_{s} \underline{J}_{s_j} \underline{1}_{s_j} \end{bmatrix} \tag{2.47}$$

$$\underline{\mathcal{G}}_{s_j} = \begin{bmatrix} \mathcal{G}_{\delta_j} \\ \mathcal{G}_{\gamma_j} \end{bmatrix} = \begin{bmatrix} \underline{1}^{T}_{s_j} \underline{f}_{s_j} \\ \underline{1}^{T}_{s_j} \underline{g}_{s_j} \end{bmatrix}$$

As before, in order to keep the final dynamics model for DAISY as general as possible, these matrices will not be implemented explicitly in the motion equations for the strut.

Once again, referring to the free-body diagrams depicted in Figure 2.3, and summing the applied forces and torques, the motion equations for a typical strut, expressed in F_{s_j}, are

$$m_{s_j} \ddot{\underline{w}}_{s_j} - \underline{c}^{x}_{s_j} \ddot{\underline{\theta}}_{s_j} + \underline{P}_{\delta_j} \ddot{\delta}_j + \underline{P}_{\gamma_j} \ddot{\gamma}_j = \underline{f}_{s_j} + \underline{f}_{s_j r_j} + \underline{f}_{s_j r_{j+1}} \tag{2.48}$$

$$\underline{c}^{x}_{s_j} \ddot{\underline{w}}_{s_j} + \underline{J}_{s_j} \ddot{\underline{\theta}}_{s_j} + \underline{H}_{\delta_j} \ddot{\delta}_j + \underline{H}_{\gamma_j} \ddot{\gamma}_j = \underline{g}_{s_j} + \underline{g}_{s_j r_j} + \underline{g}_{s_j r_{j+1}} + \underline{r}^{x}_{s_j c_{j+1}} \underline{f}_{s_j r_{j+1}} \tag{2.49}$$

$$\underline{P}^{T}_{\delta_j} \ddot{\underline{w}}_{s_j} + \underline{H}^{T}_{\delta_j} \ddot{\underline{\theta}}_{s_j} + m_{\delta\delta_j} \ddot{\delta}_j + m_{\delta\gamma_j} \ddot{\gamma}_j + k_{\delta\delta_j} \delta_j + k_{\delta\gamma_j} \gamma_j = \mathcal{G}_{\delta_j} + \underline{1}^{T}_{s_j} \underline{f}_{s_j r_{j+1}} \tag{2.50}$$

to be consistent with (2.51).

$$\underline{P}_{\gamma_j}^T \ddot{\underline{w}}_{s_j} + \underline{H}_{\gamma_j}^T \ddot{\underline{\theta}}_{s_j} + m_{\gamma\delta_j} \ddot{\delta}_j + m_{\gamma\gamma_j} \ddot{\gamma}_j + k_{\gamma\delta_j} \delta_j + k_{\gamma\gamma_j} \gamma_j = \mathcal{M}_{\gamma_j} + \underline{1}_{s_j}^T \underline{g}_{s_j} r_{j+1} \tag{2.51}$$

Here the torque equation (2.49) is taken about O_{s_j}. Also, it should be noted that the strut stiffness matrix $\underline{K}_{s_j}$ has been partitioned in a manner analogous to $\underline{M}_{s_j}$.

2.2.4 A Comment on Subscripts

To avoid notational difficulties when either rib "1" (j = 1) or strut "m" (j = m) appears in a summation, the following definitions are assumed:

$$\begin{aligned} \underline{\sigma}_{r_{m+1}} &\triangleq \underline{\sigma}_{r_1} \; ; \qquad \underline{\sigma}_{s_{m+1}} \triangleq \underline{\sigma}_{s_1} \; ; \qquad \underline{\sigma}_{c_{m+1}} \triangleq \underline{\sigma}_{c_1} \\ \underline{\sigma}_{r_o} &\triangleq \underline{\sigma}_{r_m} \; ; \qquad \underline{\sigma}_{s_o} \triangleq \underline{\sigma}_{s_m} \; ; \qquad \underline{\sigma}_{c_o} \triangleq \underline{\sigma}_{c_m} \end{aligned} \tag{2.52}$$

Here $\underline{\sigma}$ is any matrix quantity appearing in the motion equations for rib 1 or strut m. These definitions permit a summation over j = 1,...,m without the need to treat rib 1 or strut m as special cases, at least until the final mass and stiffness matrices are assembled.

2.3 Motion Equations for DAISY

The motion equations presented in Section 2.1 for the hub, a typical rib and a typical strut can now be combined to produce a set of motion equations for the dynamics of DAISY. The technique involves forming a number of appropriate linear combinations of the substructure motion equations, after the imposition of several geometric constraints.

2.3.1 Geometric Constraints

In order that the free-body diagrams of Fig. 2.3 can be combined into the single structure shown in Fig. 2.2, a number of geometric constraints

must be satisfied. To be specific, it is necessary that, at the point O_{r_j},

$$\underline{w}_{r_j} = \underline{C}_{r_j h}(\underline{w}_h - \underline{r}^{\times}_{h r_j}\underline{\theta}_h) \tag{2.53}$$

$$\underline{\theta}_{r_j} = \underline{C}_{r_j h}\underline{\theta}_h \tag{2.54}$$

At the point O_{s_j},

$$\underline{w}_{s_j} = \underline{C}_{s_j r_j}[\underline{w}_{r_j} - \underline{r}^{\times}_{r_j s_j}(\underline{\theta}_{r_j} + \underline{\alpha}_j)] \tag{2.55}$$

$$\underline{\theta}_{s_j} = \underline{C}_{s_j r_j}(\underline{\theta}_{r_j} + \underline{\alpha}_j) - \underline{1}^{\times}_{s_j}\underline{1}^{\times}_{s_j}\underline{\beta}_j \tag{2.56}$$

Last, at the point $O_{c_{j+1}}$,

$$\underline{w}_{c_{j+1}} = \underline{w}_{s_j} - \underline{r}^{\times}_{s_j c_{j+1}}\underline{\theta}_{s_j} + \underline{1}_{s_j}\delta_j \tag{2.57}$$

$$\underline{\theta}_{c_{j+1}} = \underline{\theta}_{s_j} + \underline{1}_{s_j}\gamma_j \tag{2.58}$$

The angles $\underline{\beta}_j$ denote three rigid rotations about O_{s_j} of strut s_j relative to rib r_j (expressed in F_{s_j}). We know, however, that an elastic rotational degree of freedom γ_j has been included in the strut model. Hence, to permit DAISY a full range of motions (in-plane, out-of-plane and twist), only two rigid rotations are actually required at O_{s_j}, namely, those perpendicular to $\underline{1}_{s_j}$. To elaborate, using the identity

$$\underline{1} \equiv \underline{1}_{s_j}\underline{1}^{T}_{s_j} - \underline{1}^{\times}_{s_j}\underline{1}^{\times}_{s_j} \tag{2.59}$$

where $\underline{1}$ is the identity matrix, $\underline{\beta}_j$ can be separated into components parallel and perpendicular to $\underline{1}_{s_j}$:

$$\underline{\beta}_j = \underline{\beta}_{j\parallel} + \underline{\beta}_{j\perp} = \underline{1}_{s_j}(\underline{1}_j^T \underline{\beta}_j) - \underline{1}_{s_j}^X \underline{1}_{s_j}^X \underline{\beta}_j \tag{2.60}$$

Now, since γ_j is used to represent any rotation about the $\underline{1}_{s_j}$ direction, only $\underline{\beta}_{j\perp}$ need be incorporated into the angular constraint at O_{s_j}.

Furthermore, the rotations represented by $\beta_{j\perp}$ are not independent degrees of freedom. They are linear combinations of the relative rotations $\underline{\alpha}_{r_j}$ at the rib roots O_{r_j}. To demonstrate this fact, we begin by writing the constraints at $O_{c_{j+1}}$ relative to rib j+1 rather than relative to strut j. Simply, from Fig. 2.2, it follows that

$$\underline{w}_{c_{j+1}} = \underline{C}_{s_j r_{j+1}} [\underline{w}_{r_{j+1}} - \underline{r}_{r_{j+1} c_{j+1}}^X (\underline{\theta}_{r_{j+1}} + \underline{\alpha}_{r_{j+1}})] \tag{2.61}$$

$$\underline{\theta}_{c_{j+1}} = \underline{C}_{s_j r_{j+1}} (\underline{\theta}_{r_{j+1}} + \underline{\alpha}_{j+1}) - \underline{1}_{s_j}^X \underline{1}_{s_j}^X \underline{\phi}_j \tag{2.62}$$

where $\underline{\phi}_j$ is defined analgous to $\underline{\beta}_j$, but about O_{c_j} instead of about O_{s_j}. Now, replace r_j by r_{j+1} in (2.53) and (2.54) and substitute the resulting equations into (2.61) and (2.62). Then given the attachment point vector definitions of Section 2.1.4, one obtains

$$\underline{w}_{c_{j+1}} = \underline{C}_{s_j h} (\underline{w}_h - \underline{r}_{h c_{j+1}}^X \underline{\theta}_h) - \underline{C}_{s_j r_{j+1}} \underline{r}_{r_{j+1} c_{j+1}}^X \underline{\alpha}_{j+1} \tag{2.63}$$

$$\underline{\theta}_{c_{j+1}} = \underline{C}_{s_j h} \underline{\theta}_h + \underline{C}_{s_j r_{j+1}} \underline{\alpha}_{j+1} - \underline{1}_{s_j}^X \underline{1}_{s_j}^X \underline{\phi}_j \tag{2.64}$$

Also, by direct substitution of (2.53) and (2.54) into (2.55) and (2.56), it can be shown that

$$\underline{w}_{s_j} = \underline{C}_{s_j h} (\underline{w}_h - \underline{r}_{h s_j}^X \underline{\theta}_h) - \underline{C}_{s_j r_j} \underline{r}_{r_j s_j}^X \underline{\alpha}_j \tag{2.65}$$

$$\underline{\theta}_{s_j} = \underline{C}_{s_j h} \underline{\theta}_h + \underline{C}_{s_j r_j} \underline{\alpha}_j - \underline{1}_{s_j}^X \underline{1}_{s_j}^X \underline{\beta}_j \tag{2.66}$$

Whence, from (2.57) and (2.58),

$$\underline{w}_{c_{j+1}} = \underline{C}_{s_j h}(\underline{w}_h - \underline{r}^X_{hc_{j+1}}\underline{\theta}_h) - \underline{C}_{s_j r_j}\underline{r}^X_{r_j c_{j+1}}\underline{\alpha}_j + \underline{r}^X_{s_j c_{j+1}}\underline{1}^X_{s_j}\underline{1}^X_{s_j}\underline{\beta}_j + \underline{1}_{s_j}\delta_j \tag{2.67}$$

$$\underline{\theta}_{c_{j+1}} = \underline{C}_{s_j h}\underline{\theta}_h + \underline{C}_{s_j r_j}\underline{\alpha}_j - \underline{1}^X_{s_j}\underline{1}^X_{s_j}\underline{\beta}_j + \underline{1}_{s_j}\gamma_j \tag{2.68}$$

As a consequence, equating (2.63) and (2.67) gives

$$\underline{1}_{s_j}\delta_j + \underline{r}^X_{s_j c_{j+1}}\underline{1}^X_{s_j}\underline{1}^X_{s_j}\underline{\beta}_j = \underline{C}_{s_j r_j}\underline{r}^X_{r_j c_{j+1}}\underline{\alpha}_j - \underline{C}_{s_j r_{j+1}}\underline{r}^X_{r_{j+1} c_{j+1}}\underline{\alpha}_{j+1} \tag{2.69}$$

Now recalling that

$$\ell_{s_j}\underline{1}_{s_j} = \underline{r}_{s_j c_{j+1}} \tag{2.70}$$

and noting from (2.59) that

$$\underline{1}^X_{s_j}\underline{1}^X_{s_j}\underline{1}^X_{s_j} = \underline{1}^X_{s_j}(\underline{1}_{s_j}\underline{1}^T_{s_j} - \underline{1}) = -\underline{1}^X_{s_j} \tag{2.71}$$

(2.69) becomes

$$\underline{1}_{s_j}\delta_j - \ell_{s_j}\underline{1}^X_{s_j}\underline{\beta}_j = \underline{C}_{s_j r_j}\underline{r}^X_{r_j c_{j+1}}\underline{\alpha}_j - \underline{C}_{s_j r_{j+1}}\underline{r}^X_{r_{j+1} c_{j+1}}\underline{\alpha}_{j+1} \tag{2.72}$$

Therefore, forming the cross-product of $\underline{1}_{s_j}$ with (2.72), that is $\underline{1}^X_{s_j}$ (2.72), the desired relationship for $\underline{\beta}_{j\perp}$ results:

$$\underline{\beta}_{j\perp} = - \underline{1}^{X}_{s_j} \underline{1}^{X}_{s_j} \underline{\beta}_j$$

$$= \frac{1}{\ell_{s_j}} \underline{1}^{X}_{s_j} (\underline{C}_{s_j r_j} \underline{r}^{X}_{r_j} c_{j+1} \underline{\alpha}_j - \underline{C}_{s_j r_{j+1}} \underline{r}^{X}_{r_{j+1}} c_{j+1} \underline{\alpha}_{j+1}) \tag{2.73}$$

Furthermore, by forming the dot product of $\underline{1}_{s_j}$ with (2.72), namely $\underline{1}^{T}_{s_j}$(2.72), we obtain the interesting relation

$$\delta_j = \underline{1}^{T}_{s_j} (\underline{C}_{s_j r_j} \underline{r}^{X}_{r_j} c_{j+1} \underline{\alpha}_j - \underline{C}_{s_j r_{j+1}} \underline{r}^{X}_{r_{j+1}} c_{j+1} \underline{\alpha}_{j+1}) \tag{2.74}$$

The implication, not unexpectedly, is that δ_j also is not an independent degree of freedom. Similarly, by forming the dot product of $\underline{1}_{s_j}$ with the equation obtained by equating (2.64) and (2.68), it can be shown that γ_j also is a dependent degree of freedom:

$$\gamma_j = \underline{1}^{T}_{s_j} (\underline{C}_{s_j r_{j+1}} \underline{\alpha}_{j+1} - \underline{C}_{s_j r_j} \underline{\alpha}_j) \tag{2.75}$$

Equation (2.73) also plays a key role in obtaining this result. It should be noted that the defining relationship for $\underline{\phi}_{j\perp}$, namely,

$$\underline{\phi}_{j\perp} = - \underline{1}^{X}_{s_j} \underline{1}^{X}_{s_j} \underline{\phi}_j$$

$$= \underline{1}^{X}_{s_j} [(\underline{C}_{s_j r_{j+1}} + \frac{1}{\ell_{s_j}} \underline{1}^{X}_{s_j} \underline{C}_{s_j r_{j+1}} \underline{r}^{X}_{r_{j+1}} c_{j+1}) \underline{\alpha}_{j+1} \tag{2.76}$$

$$- (\underline{C}_{s_j r_j} + \frac{1}{\ell_{s_j}} \underline{1}^{X}_{s_j} \underline{C}_{s_j r_j} \underline{r}^{X}_{r_j} c_{j+1}) \underline{\alpha}_j]$$

can be found by taking the cross-product of $\underline{1}_{s_j}$ with the same equation as that used to obtain (2.75).

To summarize, the required geometric constraints are, at the point O_{r_j},

$$\underline{w}_{r_j} = \underline{C}_{r_j h}(\underline{w}_h - \underline{r}^{X}_{h r_j}\underline{\theta}_h) \tag{2.77}$$

$$\underline{\theta}_{r_j} = \underline{C}_{r_j h}\underline{\theta}_h \tag{2.78}$$

and, at the point O_{s_j},

$$\underline{w}_{s_j} = \underline{C}_{s_j h}(\underline{w}_h - \underline{r}^{X}_{h s_j}\underline{\theta}_h) - \underline{C}_{s_j r_j}\underline{r}^{X}_{r_j s_j}\underline{\alpha}_j \tag{2.79}$$

$$\begin{aligned}\underline{\theta}_{s_j} = \underline{C}_{s_j h}\underline{\theta}_h + (\underline{C}_{s_j r_j} + \frac{1}{\ell_{s_j}}\underline{1}^{X}_{s_j}\underline{C}_{s_j r_j}\underline{r}^{X}_{r_j c_{j+1}})\underline{\alpha}_j \\ - \frac{1}{\ell_{s_j}}\underline{1}^{X}_{s_j}\underline{C}_{s_j r_{j+1}}\underline{r}^{X}_{r_{j+1} c_{j+1}}\underline{\alpha}_{j+1}\end{aligned} \tag{2.80}$$

with

$$\delta_j = \underline{1}^{T}_{s_j}(\underline{C}_{s_j r_j}\underline{r}^{X}_{r_j c_{j+1}}\underline{\alpha}_j - \underline{C}_{s_j r_{j+1}}\underline{r}^{X}_{r_{j+1} c_{j+1}}\underline{\alpha}_{j+1}) \tag{2.81}$$

and

$$\gamma_j = \underline{1}^{T}_{s_j}(\underline{C}_{s_j r_{j+1}}\underline{\alpha}_{j+1} - \underline{C}_{s_j r_j}\underline{\alpha}_j) \tag{2.82}$$

Given the findings of this section, it is timely to review the various degrees of freedom prior to formulating the motion equations for DAISY.

2.3.2 Degrees of Freedom

Let us begin by summarizing the degrees of freedom associated with each substructure. From Section 2.1.1, we know that the hub has six rigid degrees of freedom — three translational ($\underline{w}_h$) and three rotational ($\underline{\theta}_h$). A typical rib, on the other hand, has nine degrees of freedom, six rigid — three translational ($\underline{w}_{r_j}$) and three rotational ($\underline{\theta}_{r_j}$) — and three elastic — the relative rotations ($\underline{\alpha}_j$) at the rib root. Finally, a typical

strut has eight degrees of freedom, six rigid — three translational ($\underline{w}_{s_j}$) and three rotational ($\underline{\theta}_{s_j}$) — and two elastic — the linear displacement along $\underline{1}_{s_j}$ (δ_j) and the rotation about $\underline{1}_{s_j}$ (γ_j). However, based on the previous section, only the following degrees of freedom are independent:

$$\underline{w}_h,\ \underline{\theta}_h,\ \underline{\alpha}_1,\ \cdots\ \underline{\alpha}_m \tag{2.83}$$

Here m is the number of ribs (and struts) in DAISY. This represents a total of $6 + 3m$ degrees of freedom, six of them rigid and $3m$ of them elastic.

Now, based on the substructure motion equations presented in Sections 2.2.1 through 2.2.3, the total number of available scalar equations is $6 + 17m$. At present, there are $14m$ equations too many. These extra equations will vanish, as will the inter-structure constraint forces, when an appropriate set of $6 + 3m$ linear combinations of the substructure equations (with the 14 geometric constraints (2.77) through (2.82) inserted) are taken.

2.3.3 Linear Combinations of Substructure Equations

In the following, it will be assumed that (2.77) through (2.82) have already been substituted into (2.16), (2.17), (2.39), (2.40), (2.41), (2.48), (2.49), (2.50) and (2.51). Now, form the following linear combinations:

$\underline{w}_h$:
$$(2.16) + \sum_{j=1}^{m} [\underline{C}_{hr_j}(2.39) + \underline{C}_{hs_j}(2.48)]$$

$\underline{\theta}_h$:
$$(2.17) + \sum_{j=1}^{m} [\underline{C}_{hr_j}(2.40) + \underline{r}^{x}_{hr_j}\underline{C}_{hr_j}(2.39) + \underline{C}_{hs_j}(2.49) + \underline{r}^{x}_{hs_j}\underline{C}_{hs_j}(2.48)]$$

$\underline{\alpha}_j$:
$$(2.41) + \underline{C}_{r_js_j}(2.49) + \underline{r}^{x}_{r_js_j}\underline{C}_{r_js_j}(2.48) - \underline{C}_{r_js_j}\underline{1}_{s_j}(2.51) - \underline{r}^{x}_{r_jc_{j+1}}\underline{C}_{r_js_j}\underline{1}_{s_j}(2.50)$$ *(cont'd next page)*

$$+ \underline{C}_{r_j s_{j-1}} \underline{1}_{s_{j-1}} (2.51)^{j-1} + \underline{r}^{x}_{r_j c_j} \underline{C}_{r_j s_{j-1}} \underline{1}_{s_{j-1}} (2.50)^{j-1}$$

$$+ \frac{1}{\ell_{s_j}} \underline{r}^{x}_{r_j c_{j+1}} \underline{C}_{r_j s_j} \underline{1}^{x}_{s_j} (2.49)$$

$$- \frac{1}{\ell_{s_{j-1}}} \underline{r}^{x}_{r_j c_j} \underline{C}_{r_j s_{j-1}} \underline{1}^{x}_{s_{j-1}} (2.49)^{j-1}$$

The notation $(\ )^{j-1}$ implies that j is replaced by j - 1 in the respective equation. The degrees of freedom associated with each resultant motion equation are given in the left margin.

This procedure yields the final set of motion equations for DAISY. In matrix format, they are

$$\underline{M}\ddot{\underline{q}} + \underline{K}\underline{q} = \underline{B}\underline{u}_b + \underline{u}_d \tag{2.84}$$

where

$$\underline{q} = \text{col}\{\underline{w}_h, \underline{\theta}_h, \underline{\alpha}_1, \ldots, \underline{\alpha}_m\} \tag{2.85}$$

$$\underline{u}_b = \text{col}\{\underline{g}_{r_1 s_1}, \underline{g}_{r_2 s_2}, \ldots, \underline{g}_{r_m s_m}, \underline{g}_{r_1 s_m}, \underline{g}_{r_2 s_1}, \underline{g}_{r_3 s_2}, \ldots, \underline{g}_{r_m s_{m-1}}\} \tag{2.86}$$

$$\underline{u}_d = \text{col}\{\underline{f}, \underline{g}, \underline{g}_{\alpha_1}, \ldots, \underline{g}_{\alpha_m}\} \tag{2.87}$$

and $\underline{M}$, $\underline{K}$ and $\underline{B}$ are partitioned as shown in Tables 2.1, 2.3 and 2.5. The expressions for the partitioned elements of $\underline{M}$, $\underline{K}$ and $\underline{B}$ are given in Tables 2.2, 2.4 and 2.6. Also, the expression for $\underline{g}_{\alpha_j}$ used in (2.87) is cited in Table 2.7.

While the mass ($\underline{M}$) and stiffness ($\underline{K}$) matrices given in Tables 2.1 and 2.3 are complete, the input matrix ($\underline{B}$) must be augmented to include the inputs from the actuators listed in Section 1. This is part of

Table 2.1

Partitioning† of the Mass Matrix, $\underline{M}$

$$
\begin{bmatrix}
\underline{M}_{ww} & \underline{M}_{w\theta} & \underline{M}_{w\alpha_1} & \underline{M}_{w\alpha_2} & \underline{M}_{w\alpha_3} & \underline{M}_{w\alpha_4} & \times & \times & \underline{M}_{w\alpha_{m-1}} & \underline{M}_{w\alpha_m} \\
 & \underline{M}_{\theta\theta} & \underline{M}_{\theta\alpha_1} & \underline{M}_{\theta\alpha_2} & \underline{M}_{\theta\alpha_3} & \underline{M}_{\theta\alpha_4} & \times & \times & \underline{M}_{\theta\alpha_{m-1}} & \underline{M}_{\theta\alpha_m} \\
 & & \underline{M}_{\alpha_1\alpha_1} & \underline{M}_{\alpha_1\alpha_2} & \underline{O} & \underline{O} & \cdot & \cdot & \underline{O} & \underline{M}_{\alpha_1\alpha_m} \\
 & & & \underline{M}_{\alpha_2\alpha_2} & \underline{M}_{\alpha_2\alpha_3} & \underline{O} & \cdot & \cdot & \underline{O} & \underline{O} \\
 & & & & \underline{M}_{\alpha_3\alpha_3} & \underline{M}_{\alpha_3\alpha_4} & \cdot & \cdot & \cdot & \cdot \\
 & & & & & \underline{M}_{\alpha_4\alpha_4} & \times & \cdot & \cdot & \cdot \\
 & & & & & & \times & \times & \underline{O} & \underline{O} \\
 & & & & & & & \times & \underline{M}_{\alpha_{m-2}\alpha_{m-1}} & \underline{O} \\
 & \text{(symmetric)} & & & & & & & \underline{M}_{\alpha_{m-1}\alpha_{m-1}} & \underline{M}_{\alpha_{m-1}\alpha_m} \\
 & & & & & & & & & \underline{M}_{\alpha_m\alpha_m}
\end{bmatrix}
$$

†see Table 2.2 for individual elements

× a series of nonzero elements

· a series of zero elements

Table 2.2

Expressions for Partitioned Elements in $\underline{M}$

$$\underline{M}_{ww} = \underline{1}m$$

$$\underline{M}_{w\theta} = -\underline{c}^{x}$$

$$\underline{M}_{w\alpha_j}{}^{\dagger} = \underline{C}_{hr_j}(P_{\alpha_j} - m_{s_j}\underline{r}^{x}_{r_j s_j})$$

$$+ \underline{C}_{hs_j}[(\underline{P}_{\delta_j}\underline{1}^{T}_{s_j} - \frac{1}{\ell_{s_j}}\underline{c}^{x}_{s_j}\underline{1}^{x}_{s_j})\underline{C}_{s_j r_j}\underline{r}^{x}_{r_j c_{j+1}}$$

$$- (\underline{P}_{\delta_j}\underline{1}^{T}_{s_j} + \underline{c}^{x}_{s_j})\underline{C}_{s_j r_j}]$$

$$- \underline{C}_{hs_{j-1}}[(\underline{P}_{\delta_{j-1}}\underline{1}^{T}_{s_{j-1}} - \frac{1}{\ell_{s_{j-1}}}\underline{c}^{x}_{s_{j-1}}\underline{1}^{x}_{s_{j-1}})\underline{C}_{s_{j-1}r_j}\underline{r}^{x}_{r_j c_j}$$

$$- \underline{P}_{\gamma_{j-1}}\underline{1}^{T}_{s_{j-1}}\underline{C}_{s_{j-1}r_j}]$$

$$\underline{M}_{\theta\theta} = \underline{J}$$

$$\underline{M}_{\theta\alpha_j} = \underline{C}_{hr_j}\underline{H}_{\alpha_j} + \underline{r}^{x}_{hr_j}\underline{C}_{hr_j}\underline{P}_{\alpha_j} - m_{s_j}\underline{r}^{x}_{hs_j}\underline{C}_{hr_j}\underline{r}^{x}_{r_j s_j}$$

$$+ \underline{r}^{x}_{hs_j}\underline{C}_{hs_j}[(\underline{P}_{\delta_j}\underline{1}^{T}_{s_j} - \frac{1}{\ell_{s_j}}\underline{c}^{x}_{s_j}\underline{1}^{x}_{s_j})\underline{C}_{s_j r_j}\underline{r}^{x}_{r_j c_{j+1}}$$

$$- (\underline{P}_{\gamma_j}\underline{1}^{T}_{s_j} + \underline{c}^{x}_{s_j})\underline{C}_{s_j r_j}] \qquad \text{[Eq'n cont'd next page]}$$

†Here $j\varepsilon(1,\ldots,m)$, provided that the following definitions are noted: for $j = 1$, $j - 1 \triangleq m$ and for $j = m$, $j + 1 \triangleq 1$.

$$- \underline{r}^{X}_{hs_{j-1}} \underline{C}_{hs_{j-1}} [(\underline{P}_{\delta_{j-1}} \underline{1}^{T}_{s_{j-1}} - \frac{1}{\ell_{s_{j-1}}} \underline{c}^{X}_{s_{j-1}} \underline{1}^{X}_{s_{j-1}}) \underline{C}_{s_{j-1} r_j} \underline{r}^{X}_{r_j c_j}$$

$$- \underline{P}_{\gamma_{j-1}} \underline{1}^{T}_{s_{j-1}} \underline{C}_{s_{j-1} r_j}]$$

$$+ \underline{C}_{hs_j} [(\underline{H}_{\delta_j} \underline{1}^{T}_{s_j} + \frac{1}{\ell_{s_j}} \underline{J}_{s_j} \underline{1}^{X}_{s_j}) \underline{C}_{s_j r_j} \underline{r}^{X}_{r_j c_{j+1}}$$

$$- (\underline{H}_{\gamma_j} \underline{1}^{T}_{s_j} - \underline{J}_{s_j}) \underline{C}_{s_j r_j} - \underline{c}^{X}_{s_j} \underline{C}_{s_j r_j} \underline{r}^{X}_{r_j s_j}]$$

$$- \underline{C}_{hs_{j-1}} [(\underline{H}_{\delta_{j-1}} \underline{1}^{T}_{s_{j-1}} + \frac{1}{\ell_{s_{j-1}}} \underline{J}_{s_{j-1}} \underline{1}^{X}_{s_{j-1}}) \underline{C}_{s_{j-1} r_j} \underline{r}^{X}_{r_j c_j}$$

$$- \underline{H}_{\gamma_{j-1}} \underline{1}^{T}_{s_{j-1}} \underline{C}_{s_{j-1} r_j}]$$

$$\underline{M}_{\alpha_j \alpha_j} = \underline{M}_{\alpha_j} + \underline{C}_{r_j s_j} \underline{J}_{s_j} \underline{C}_{s_j r_j} - m_{s_j} \underline{r}^{X}_{r_j s_j} \underline{r}^{X}_{r_j s_j}$$

$$+ \underline{r}^{X}_{r_j c_{j+1}} \underline{C}_{r_j s_j} (\underline{1}^{X}_{s_j} \underline{J}_{s_j} \underline{1}^{X}_{s_j} - \underline{1}_{s_j} m_{\delta\delta_j} \underline{1}^{T}_{s_j}) \underline{C}_{s_j r_j} \underline{r}^{X}_{r_j c_{j+1}}$$

$$+ \underline{C}_{r_j s_j} \underline{1}_{s_j} m_{\gamma\gamma_j} \underline{1}^{T}_{s_j} \underline{C}_{s_j r_j}$$

$$+ \underline{r}^{X}_{r_j c_j} \underline{C}_{r_j s_{j-1}} (\underline{1}^{X}_{s_{j-1}} \underline{J}_{s_{j-1}} \underline{1}^{X}_{s_{j-1}} - \underline{1}_{s_{j-1}} m_{\delta\delta_{j-1}} \underline{1}^{T}_{s_{j-1}}) \underline{C}_{s_{j-1} r_j} \underline{r}^{X}_{r_j c_j}$$

$$+ \underline{C}_{r_j s_{j-1}} \underline{1}_{s_{j-1}} m_{\gamma\gamma_{j-1}} \underline{1}^{T}_{s_{j-1}} \underline{C}_{s_{j-1} r_j}$$

$$- [\underline{r}^{X}_{r_j c_{j+1}} \underline{C}_{r_j s_j} (\frac{1}{\ell_{s_j}} \underline{1}^{X}_{s_j} \underline{c}^{X}_{s_j} - \underline{1}_{s_j} \underline{P}^{T}_{\delta_j})$$

$$+ \underline{C}_{r_j s_j} (\underline{c}^{X}_{s_j} - \underline{1}_{s_j} \underline{P}^{T}_{\gamma_j})] \underline{C}_{s_j r_j} \underline{r}^{X}_{r_j s_j}$$

$$+ \underline{r}^{X}_{r_j s_j} \underline{C}_{r_j s_j} [(\underline{P}_{\delta_j} \underline{1}^{T}_{s_j} - \frac{1}{\ell_{s_j}} \underline{c}^{X}_{s_j} \underline{1}^{X}_{s_j}) \underline{C}_{s_j r_j} \underline{r}^{X}_{r_j c_{j+1}}$$

$$- (\underline{P}_{\gamma_j} \underline{1}^{T}_{s_j} + \underline{c}^{X}_{s_j}) \underline{C}_{s_j r_j}] \qquad \text{(cont'd)}$$

$$+ [\underline{r}^{X}_{r_j c_{j+1}} \underline{C}_{r_j s_j} (\frac{1}{\ell_{s_j}} \underline{1}^{X}_{s_j} \underline{J}_{s_j} - \underline{1}_{s_j} \underline{H}^{T}_{\delta_j})$$

$$- \underline{C}_{r_j s_j} \underline{1}_{s_j} \underline{H}^{T}_{\gamma_j}] \underline{C}_{s_j r_j}$$

$$+ \underline{C}_{r_j s_j} [(\underline{H}_{\delta_j} \underline{1}^{T}_{s_j} + \frac{1}{\ell_{s_j}} \underline{J}_{s_j} \underline{1}^{X}_{s_j}) \underline{C}_{s_j r_j} \underline{r}^{X}_{r_j c_{j+1}}$$

$$- \underline{H}_{\gamma_j} \underline{1}^{T}_{s_j} \underline{C}_{s_j r_j}]$$

$$+ [\frac{1}{\ell_{s_j}} \underline{r}^{X}_{r_j c_{j+1}} \underline{C}_{r_j s_j} \underline{1}^{X}_{s_j} \underline{H}_{\delta_j} \underline{1}^{T}_{s_j}$$

$$- \underline{C}_{r_j s_j} \underline{1}_{s_j} (\frac{1}{\ell_{s_j}} \underline{H}^{T}_{\gamma_j} \underline{1}^{X}_{s_j} + m_{\delta\gamma_j} \underline{1}^{T}_{s_j})] \underline{C}_{s_j r_j} \underline{r}^{X}_{r_j c_{j+1}}$$

$$- \underline{r}^{X}_{r_j c_{j+1}} \underline{C}_{s_j r_j} [\frac{1}{\ell_{s_j}} \underline{1}_{s_j} \underline{H}^{T}_{\delta_j} \underline{1}^{X}_{s_j} \underline{C}_{s_j r_j} \underline{r}^{X}_{r_j c_{j+1}}$$

$$- (\underline{1}_{s_j} m_{\delta\gamma_j} - \frac{1}{\ell_{s_j}} \underline{1}^{X}_{s_j} \underline{H}_{\gamma_j}) \underline{1}^{T}_{s_j} \underline{C}_{s_j r_j}]$$

$$+ [\frac{1}{\ell_{s_{j-1}}} \underline{r}^{X}_{r_j c_j} \underline{C}_{r_j s_{j-1}} \underline{1}^{X}_{s_{j-1}} \underline{H}_{\delta_{j-1}} \underline{1}^{T}_{s_{j-1}}$$

$$- \underline{C}_{r_j s_{j-1}} \underline{1}_{s_{j-1}} (\frac{1}{\ell_{s_{j-1}}} \underline{H}^{T}_{\gamma_{j-1}} \underline{1}^{X}_{s_{j-1}} m_{\delta\gamma_{j-1}} \underline{1}^{T}_{s_{j-1}})] \underline{C}_{s_{j-1} r_j} \underline{r}^{X}_{r_j c_j}$$

$$- \underline{r}^{X}_{r_j c_j} \underline{C}_{r_j s_{j-1}} [\frac{1}{\ell_{s_{j-1}}} \underline{1}_{s_{j-1}} \underline{H}^{T}_{\delta_{j-1}} \underline{1}^{X}_{s_{j-1}} \underline{C}_{s_{j-1} r_j} \underline{r}^{X}_{r_j c_j}$$

$$- (\underline{1}_{s_{j-1}} m_{\delta\gamma_{j-1}} - \frac{1}{\ell_{s_{j-1}}} \underline{1}^{X}_{s_{j-1}} \underline{H}_{\gamma_{j-1}}) \underline{1}^{T}_{s_{j-1}} \underline{C}_{s_{j-1} r_j}]$$

$$\underline{M}_{\alpha_j \alpha_{j+1}} = [-\underline{r}^{X}_{r_j c_{j+1}} \underline{C}_{r_j s_j} (\frac{1}{\ell_{s_j}} \underline{1}^{X}_{s_j} \underline{J}_{s_j} - \underline{1}_{s_j} \underline{H}^{T}_{\delta_j}) - \underline{C}_{r_j s_j} (\underline{J}_{s_j} - \underline{1}_{s_j} \underline{H}^{T}_{\gamma_j})$$

$$+ \underline{r}^{X}_{r_j s_j} \underline{C}_{r_j s_j} \underline{c}^{X}_{s_j}] \frac{1}{\ell_{s_j}} \underline{1}^{X}_{s_j} \underline{C}_{s_j r_{j+1}} \underline{r}^{X}_{r_{j+1} c_{j+1}} \qquad \text{(cont'd)}$$

$$+ [\underline{r}^{X}_{r_j c_{j+1}} \underline{C}_{r_j s_j} (\frac{1}{\ell_{s_j}} \underline{1}^{X}_{s_j} \underline{H}_{\delta_j} + \underline{1}_{s_j} m_{\delta\delta_j}) - \underline{C}_{r_j s_j} (\underline{H}_{\delta_j} - \underline{1}_{s_j} m_{\delta\gamma_j})$$

$$- \underline{r}^{X}_{r_j s_j} \underline{C}_{r_j s_j} \underline{P}_{\delta_j}] \underline{1}^{T}_{s_j} \underline{C}_{s_j r_{j+1}} \underline{r}^{X}_{r_{j+1} c_{j+1}}$$

$$+ [\underline{r}^{X}_{r_j c_{j+1}} \underline{C}_{r_j s_j} (\frac{1}{\ell_{s_j}} \underline{1}^{X}_{s_j} \underline{H}_{\gamma_j} - \underline{1}_{s_j} m_{\delta\gamma_j}) + \underline{C}_{r_j s_j} (\underline{H}_{\gamma_j} - \underline{1}_{s_j} m_{\gamma\gamma_j})$$

$$+ \underline{r}^{X}_{r_j s_j} \underline{C}_{r_j s_j} \underline{P}_{\gamma_j}] \underline{1}^{T}_{s_j} \underline{C}_{s_j r_{j+1}}$$

Table 2.3

Partitioning† of the Stiffness Matrix, $\underline{K}$

$$
\begin{bmatrix}
\underline{0} & \underline{0} & \underline{0} & \underline{0} & \underline{0} & \underline{0} & \cdot & \cdot & \underline{0} & \underline{0} \\
 & \underline{0} & \underline{0} & \underline{0} & \underline{0} & \underline{0} & \cdot & \cdot & \underline{0} & \underline{0} \\
 & & \underline{K}_{\alpha_1\alpha_1} & \underline{K}_{\alpha_1\alpha_2} & \underline{0} & \underline{0} & \cdot & \cdot & \underline{0} & \underline{K}_{\alpha_1\alpha_m} \\
 & & & \underline{K}_{\alpha_2\alpha_2} & \underline{K}_{\alpha_2\alpha_3} & \underline{0} & \cdot & \cdot & \underline{0} & \underline{0} \\
 & & & & \underline{K}_{\alpha_3\alpha_3} & \underline{K}_{\alpha_3\alpha_4} & \cdot & \cdot & \cdot & \cdot \\
 & & & & & \underline{K}_{\alpha_4\alpha_4} & \times & \cdot & \cdot & \cdot \\
 & & & & & & \times & \times & \underline{0} & \underline{0} \\
 & \text{(symmetric)} & & & & & & \times & \underline{K}_{\alpha_{m-2}\alpha_{m-1}} & \underline{0} \\
 & & & & & & & & \underline{K}_{\alpha_{m-1}\alpha_{m-1}} & \underline{K}_{\alpha_{m-1}\alpha_m} \\
 & & & & & & & & & \underline{K}_{\alpha_m\alpha_m}
\end{bmatrix}
$$

†see Table 2.4 for individual elements

× a series of nonzero elements

· a series of zero elements

Table 2.4

Expressions for Partitioned Elements in $\underline{K}$

(see Table 2.3)

$$\underline{K}_{\alpha_j\alpha_j}{}^{\dagger} = \underline{K}_{\alpha_j}$$

$$- (\underline{C}_{r_j s_j} \underline{1}_{s_j} k_{\delta\gamma_j} + \underline{r}^{x}_{r_j c_{j+1}} \underline{C}_{r_j s_j} \underline{1}_{s_j} k_{\delta\delta_j}) \underline{1}^{T}_{s_j} \underline{C}_{s_j r_j} \underline{r}^{x}_{r_j c_{j+1}}$$

$$+ (\underline{C}_{r_j s_j} \underline{1}_{s_j} k_{\gamma\gamma_j} + \underline{r}^{x}_{r_j c_{j+1}} \underline{C}_{r_j s_j} \underline{1}_{s_j} k_{\delta\gamma_j}) \underline{1}^{T}_{s_j} \underline{C}_{s_j r_j}$$

$$- (\underline{C}_{r_j s_{j-1}} \underline{1}_{s_{j-1}} k_{\delta\gamma_{j-1}} + \underline{r}^{x}_{r_j c_j} \underline{C}_{r_j s_{j-1}} \underline{1}_{s_{j-1}} k_{\delta\delta_{j-1}}) \underline{1}^{T}_{s_{j-1}} \underline{C}_{s_{j-1} r_j} \underline{r}^{x}_{r_j c_j}$$

$$+ (\underline{C}_{r_j s_{j-1}} \underline{1}_{s_{j-1}} k_{\gamma\gamma_{j-1}} + \underline{r}^{x}_{r_j c_j} \underline{C}_{r_j s_{j-1}} \underline{1}_{s_{j-1}} k_{\delta\gamma_{j-1}}) \underline{1}^{T}_{s_{j-1}} \underline{C}_{s_{j-1} r_j}$$

$$\underline{K}_{\alpha_j\alpha_{j+1}} = (\underline{C}_{r_j s_j} \underline{1}_{s_j} k_{\delta\gamma_j} + \underline{r}^{x}_{r_j c_{j+1}} \underline{C}_{r_j s_j} \underline{1}_{s_j} k_{\delta\delta_j}) \underline{1}^{T}_{s_j} \underline{C}_{s_j r_{j+1}} \underline{r}^{x}_{r_{j+1} c_{j+1}}$$

$$- (\underline{C}_{r_j s_j} \underline{1}_{s_j} k_{\gamma\gamma_j} + \underline{r}^{x}_{r_j c_{j+1}} \underline{C}_{r_j s_j} \underline{1}_{s_j} k_{\delta\gamma_j}) \underline{1}^{T}_{s_j} \underline{C}_{s_j r_{j+1}}$$

†Here $j \varepsilon (1,\ldots,m)$, provided that the following definitions are noted: for $j = 1$, $j - 1 \triangleq m$ and for $j = m$, $j + 1 \triangleq 1$.

Table 2.5

Partitioning† of the Input Matrix, $\underline{B}$

$$
\begin{bmatrix}
\underline{0} & \underline{0} & \underline{0} & \cdot & \cdot & \underline{0} & \underline{0} & \underline{0} & \underline{0} & \underline{0} & \underline{0} & \underline{0} & \cdot & \cdot & \underline{0} & \underline{0} \\
\underline{0} & \underline{0} & \underline{0} & \cdot & \cdot & \underline{0} & \underline{0} & \underline{0} & \underline{0} & \underline{0} & \underline{0} & \underline{0} & \cdot & \cdot & \underline{0} & \underline{0} \\
\underline{B}_{r_1 c_2} & \underline{0} & \underline{0} & \cdot & \cdot & \underline{0} & \underline{0} & \underline{B}_{r_1 c_1} & \underline{B}_{r_1 s_m} & \underline{B}_{r_1 s_1} & \underline{0} & \underline{0} & \cdot & \cdot & \underline{0} & \underline{0} \\
\underline{B}_{r_2 c_2} & \underline{B}_{r_2 c_3} & \underline{0} & \cdot & \cdot & \underline{0} & \underline{0} & \underline{0} & \underline{0} & \underline{B}_{r_2 s_1} & \underline{B}_{r_2 s_2} & \underline{0} & \cdot & \cdot & \underline{0} & \underline{0} \\
\cdot & \underline{B}_{r_3 c_3} & \underline{B}_{r_3 c_4} & \underline{0} & \cdot & \cdot & \cdot & \cdot & \cdot & \cdot & \underline{B}_{r_3 s_2} & \underline{B}_{r_3 s_3} & \cdot & \cdot & \cdot & \cdot \\
\cdot & \cdot & \underline{B}_{r_4 c_4} & \times & \cdot & \cdot & \cdot & \cdot & \cdot & \cdot & \cdot & \underline{B}_{r_4 s_3} & \times & \cdot & \cdot & \cdot \\
\cdot & \cdot & \cdot & \times & \times & \underline{0} & \underline{0} & \cdot & \cdot & \cdot & \cdot & \cdot & \times & \times & \underline{0} & \underline{0} \\
\cdot & \cdot & \cdot & \cdot & \times & \underline{B}_{r_{m-2} c_{m-1}} & \underline{0} & \cdot & \cdot & \cdot & \cdot & \cdot & \cdot & \times & \underline{B}_{r_{m-2} s_{m-2}} & \underline{0} \\
\cdot & \cdot & \cdot & \cdot & \cdot & \underline{B}_{r_{m-1} c_{m-1}} \; \underline{B}_{r_{m-1} c_m} & & \cdot & \cdot & \cdot & \cdot & \cdot & \cdot & \cdot & \underline{B}_{r_{m-1} s_{m-2}} & \underline{B}_{r_{m-1} s_{m-1}} \\
\underline{0} & \underline{0} & \underline{0} & \cdot & \cdot & \underline{0} & \underline{B}_{r_m c_m} & \underline{B}_{r_m c_1} & \underline{B}_{r_m s_m} & \underline{0} & \underline{0} & \underline{0} & \cdot & \cdot & \underline{0} & \underline{B}_{r_m s_{m-1}}
\end{bmatrix}
$$

†see Table 2.6 for individual elements

× a series of nonzero elements

· a series of zero elements

Table 2.6

Expressions for Partitioned Elements in $\underline{\mathcal{B}}$

(see Table 2.5)

$$\underline{\mathcal{B}}_{r_j c_{j+1}} = \frac{1}{\ell_{s_j}} \underline{r}^{x}_{r_j c_{j+1}} \underline{C}_{r_j s_j} \underline{1}^{x}_{s_j}$$

$$\underline{\mathcal{B}}_{r_j c_j} = -\frac{1}{\ell_{s_{j-1}}} \underline{r}^{x}_{r_j c_j} \underline{C}_{r_j s_{j-1}} \underline{1}^{x}_{s_{j-1}}$$

$$\underline{\mathcal{B}}_{r_j s_j} = -\frac{1}{\ell_{s_j}} \underline{r}^{x}_{r_j s_j} \underline{C}_{r_j s_j} \underline{1}^{x}_{s_j}$$

$$\underline{\mathcal{B}}_{r_j s_{j-1}} = -\frac{1}{\ell_{s_{j-1}}} \underline{r}^{x}_{r_j s_{j-1}} \underline{C}_{r_j s_{j-1}} \underline{1}^{x}_{s_{j-1}}$$

Table 2.7

Expression for Elements in the Disturbance Vector $\underline{u}_d$

[see equation (2.87)]

$$\underline{g}_{\alpha_j} = \underline{\delta}_{\alpha_j} + \underline{C}_{r_j s_j} \underline{g}_{s_j} + \underline{r}^{x}_{r_j s_j} \underline{C}_{r_j s_j} \underline{f}_{s_j}$$

$$- \underline{C}_{r_j s_j} \underline{1}_{s_j} \delta_{\gamma_j} - \underline{r}^{x}_{r_j c_{j+1}} \underline{C}_{r_j s_j} \underline{1}_{s_j} \delta_{\delta_j}$$

$$+ \underline{C}_{r_j s_{j-1}} \underline{1}_{s_{j-1}} \delta_{\gamma_{j-1}} + \underline{r}^{x}_{r_j c_j} \underline{C}_{r_j s_{j-1}} \underline{1}_{s_{j-1}} \delta_{\delta_{j-1}}$$

$$+ \frac{1}{\ell_{s_j}} \underline{r}^{x}_{r_j c_{j+1}} \underline{C}_{r_j s_j} \underline{1}^{x}_{s_j} \underline{g}_{s_j} - \frac{1}{\ell_{s_{j-1}}} \underline{r}^{x}_{r_j c_j} \underline{C}_{r_j s_{j-1}} \underline{1}^{x}_{s_{j-1}} \underline{g}_{s_{j-1}}$$

the ongoing detailed-design procedure. It is noteworthy that for the present DAISY design, no torque exists about o_{s_j} and o_{c_j}, in directions perpendicular to $\underline{1}_{s_j}$. Hence, the product $\underline{B}\underline{u}_b$, where $\underline{B}$ and $\underline{u}_b$ are given by Table 2.5 and Equation (2.86), vanishes.

A number of other system matrices must still be specified — a damping matrix $\underline{D}$, a gyroscopic matrix $\underline{G}$, an output matrix $\underline{P}$, a measurement matrix $\underline{C}$, a regulation cost matrix $\underline{Q}$, and a control cost matrix $\underline{R}$. However, a great deal of information can be gleaned from (2.84) in its present form, provided that the values for the various matrices associated with each substructure are known. This subject is dealt with in Section 4.

3. DISTURBANCE MODELS

In this section, two sources of environmental disturbance important to the dynamics of DAISY are modeled. They are gravitational and aerodynamic forces and torques.

3.1 Gravitational Disturbances

Earth's gravity plays a key role in the design of DAISY. As explained in Appendix A, the preload in the out-of-plane spirator spring at each rib root is governed by gravitational forces. In fact, provided DAISY remains motionless, this spring balances the gravitational torque about the rib root. However, once DAISY is set in motion (via external excitation) gravitational disturbing forces and torques will arise. In an attempt to predict these disturbances a gravitational force and torque model is assumed for each substructure. Simply, neglecting the finite size of each structure relative to the radius of Earth, the gravitational force acting on body $i \in \{h, r_j, s_j\}$, expressed in F_i (recall Fig. 2.2), is

$$\underline{f}_{Gi} = -a_G m_i \underline{C}_{iI} \hat{\underline{R}}_i \tag{3.1}$$

Here a_G (= 9.8 m/s) is the acceleration of gravity at Earth's surface, m_i is the mass of body i, $\underline{C}_{iI}$ is the rotation matrix that transforms frame F_I

into frame F_i, and $\hat{\underline{R}}_i$ is the unit vector from the mass center of Earth to O_i. $\hat{\underline{R}}_i$ is expressed in F_I, where F_I is taken to have its origin at Earth's mass center. Furthermore, it is assumed that the hub frame F_h and F_I are related via the first order rotation matrix

$$\underline{C}_{hI} = \begin{bmatrix} 1 & \theta_3 & -\theta_2 \\ -\theta_3 & 1 & \theta_1 \\ \theta_2 & -\theta_1 & 1 \end{bmatrix} \tag{3.2}$$

where the order for the hub rotation angles $\underline{\theta}_h = (\theta_1, \theta_2, \theta_3)$ is θ_1 about x_h, followed by θ_2 about y_h and finally θ_3 about z_h.

To be consistent with the decision to neglect the finite size of each substructure relative to Earth's radius, it is also assumed that

$$\hat{\underline{R}} = \hat{\underline{R}}_h \doteq \hat{\underline{R}}_{r_j} \doteq \hat{\underline{R}}_{s_j} \tag{3.3}$$

Whence

$$\underline{f}_{Gi} = -a_G m_i \underline{C}_{ih} \hat{\underline{R}} \tag{3.4}$$

where

$$\hat{\underline{R}} = \underline{C}_{hI} \hat{\underline{R}} = [\theta_2 \quad -\theta_1 \quad -1]^T \tag{3.5}$$

That is, z_h (the hub axis perpendicular to the X-Y plane shown in Fig. 1.1) is aligned with $-\hat{\underline{R}}$ when DAISY is motionless. It also is assumed that the x_h and y_h axes of F_h are aligned with the x_I and y_I axes of F_I initially. In other words, the nominal rest state for DAISY is $\underline{\theta}_h \equiv \underline{0}$.

Now, given (3.3), the torque caused by gravity about F_i, expressed in O_i, takes the form

$$\underline{g}_{Gi} = -a_G \underline{c}_i^x \underline{C}_{ih} \hat{\underline{R}} \tag{3.6}$$

where $\underline{c}_i^x$ is the first moment of inertia of body i. Also, recalling (2.38) and (2.47), the generalized 'elastic' gravitational forces and torques

acting on each rib and strut can be determined. These are summarized in Table 3.1, along with $\underline{f}_{Gi}$ and $\underline{g}_{Gi}$ for each substructure described in Section 2.1.1.

3.2 Aerodynamic Disturbances

The details of the aerodynamic disturbance models assumed for DAISY are described in [Sincarsin and Hughes, 1983]. As a consequence, only a brief summary of the two models is presented here. The first considers a flexible body i immersed in an incompressible frictionless fluid (a high Reynolds number model). The inertial resistance of the fluid to the translational, rotational and 'elastic' accelerations of the body takes the form

$$\begin{bmatrix} \underline{f}_{Ri} \\ \underline{g}_{Ri} \\ \underline{f}_{Ri} \end{bmatrix} = - \begin{bmatrix} \underline{M}_{Ri} & \underline{C}_{Ri}^T & \underline{P}_{Ri} \\ \underline{C}_{Ri} & \underline{J}_{Ri} & \underline{H}_{Ri} \\ \underline{P}_{Ri}^T & \underline{H}_{Ri}^T & \underline{M}_{RRi} \end{bmatrix} \begin{bmatrix} \ddot{\underline{w}}_i \\ \ddot{\underline{\theta}}_i \\ \ddot{\underline{q}}_i \end{bmatrix} \tag{3.7}$$

where

$$\underline{M}_{Ri} = \rho \int_{S_i} \underline{n}_i \underline{\xi}_{wi}^T dS_i \quad ; \quad \underline{P}_{Ri} = \rho \int_{S_i} \underline{n}_i \underline{\xi}_{qi}^T \underline{\Psi}_i dS_i$$

$$\underline{C}_{Ri} = \rho \int_{S_i} \underline{r}_i^X \underline{n}_i \underline{\xi}_{wi}^T dS_i \quad ; \quad \underline{H}_{Ri} = \rho \int_{S_i} \underline{r}_i^X \underline{n}_i \underline{\xi}_{qi}^T \underline{\Psi}_i dS_i \tag{3.8}$$

$$\underline{J}_{Ri} = \rho \int_{S_i} \underline{r}_i^X \underline{n}_i \underline{\xi}_{\theta i}^T dS_i \quad ; \quad \underline{M}_{RRi} = \rho \int_{S_i} \underline{\Psi}_i^T \underline{n}_i \underline{\xi}_{qi}^T \underline{\Psi}_i dS_i$$

and

$$\phi_i = \underline{\xi}_{wi}^T \underline{w}_i + \underline{\xi}_{\theta i}^T \underline{\theta}_i + \underline{\xi}_{qi}^T \underline{\Psi}_i \underline{q}_i \tag{3.9}$$

$$\underline{d}_i(\underline{r}_i, t) = \underline{w}_i - \underline{r}_i^X \underline{\theta}_i + \underline{\Psi}_i \underline{q}_i \tag{3.10}$$

Table 3.1

Gravitational Force and Torque on Each Substructure

Hub:

$$\underline{f}_{Gh} = - a_G m_h \hat{\underline{R}}$$

$$\underline{g}_{Gh} = - a_G \underline{c}^{x}_{h} \hat{\underline{R}}$$

Rib_j:

$$\underline{f}_{Gr_j} = - a_G m_{r_j} \underline{C}_{r_j h} \hat{\underline{R}}$$

$$\underline{g}_{Gr_j} = - a_G \underline{c}^{x}_{r_j} \underline{C}_{r_j h} \hat{\underline{R}}$$

$$\underline{\mathcal{G}}_{G\alpha_j} = \underline{g}_{Gr_j}$$

$Strut_j$:

$$\underline{f}_{Gs_j} = - a_G m_{s_j} \underline{C}_{s_j h} \hat{\underline{R}}$$

$$\underline{g}_{Gs_j} = - a_G \underline{c}^{x}_{s_j} \underline{C}_{s_j h} \hat{\underline{R}}$$

$$\mathcal{G}_{G\delta_j} = \underline{1}_j^T \underline{f}_{Gs_j}$$

$$\mathcal{G}_{G\gamma_j} = \underline{1}_j^T \underline{g}_{Gs_j}$$

Here $\underline{f}_{Ri}$, $\underline{g}_{Ri}$ and $\underline{f}_{Ri}$ are the inertial resistance force, torque and generalized 'elastic' force acting at some arbitrarily chosen point O_i in the body. $\underline{M}_{Ri}$, $\underline{C}_{Ri}$, $\underline{J}_{Ri}$ and $\underline{M}_{RRi}$ are hydrodynamic inertia matrices, and $\underline{P}_{Ri}$ and $\underline{H}_{Ri}$ are hydrodynamic momentum matrices. The absolute displacement of a point on the surface S_i of body i is given by $\underline{d}_i$, where $\underline{r}_i$ is measured from O_i. As in the previous section, $\underline{w}_i$ is the absolute displacement of O_i relative to some inertial frame and $\underline{\theta}_i$ is the absolute rotation of a frame F_i with origin at O_i. The elastic displacements of body i are represented by the product of a rectangular shape function matrix $\underline{\Psi}_i$ with a set of generalized coordinates $\underline{q}_i$. The velocity potential ϕ_i associated with the fluid flow (of density ρ) past body i is stated by (3.9). It is expressed as a superposition of the vector potentials $\underline{\xi}_{wi}$, $\underline{\xi}_{\theta i}$ and $\underline{\xi}_{qi}$ associated with each type of displacement in $\underline{d}_i$. Finally, $\underline{n}_i$ is the normal to the surface S_i.

A second areodynamic model, where the fluid (in this case air) instead is assumed viscous, is also presented in [Sincarsin and Hughes, 1983]. This model, which is applicable for low Reynolds numbers, culminates in the following resistive forces, torques and generalized 'elastic' forces for body i:

$$\begin{bmatrix} \underline{f}_{vi} \\ \underline{g}_{vi} \\ \underline{f}_{vi} \end{bmatrix} = - \begin{bmatrix} \underline{M}_{vi} & \underline{C}_{vi}^T & \underline{P}_{vi} \\ \underline{C}_{vi} & \underline{J}_{vi} & \underline{H}_{vi} \\ \underline{P}_{vi}^T & \underline{H}_{vi}^T & \underline{M}_{vvi} \end{bmatrix} \begin{bmatrix} \dot{\underline{w}}_i \\ \dot{\underline{\theta}}_i \\ \dot{\underline{q}}_i \end{bmatrix} \tag{3.11}$$

where

$$\underline{M}_{vi} = -\mu \int_{S_i} \underline{N}_{wi} dS_i \quad ; \quad \underline{P}_{vi} = -\mu \int_{S_i} \underline{N}_{qi} dS_i$$

$$\underline{C}_{vi} = -\mu \int_{S_i} \underline{r}_i^X \underline{N}_{wi} dS_i \quad ; \quad \underline{H}_{vi} = -\mu \int_{S_i} \underline{r}_i^X \underline{N}_{qi} dS_i \tag{3.12}$$

$$\underline{J}_{vi} = -\mu \int_{S_i} \underline{r}_i^X \underline{N}_{\theta i} dS_i \quad ; \quad \underline{M}_{vvi} = -\mu \int_{S_i} \underline{\Psi}_i^T \underline{N}_{qi} dS_i$$

and $\underline{N}_z$, $z \in \{w_i, \theta_i, q_i\}$ is the portion of the normal component of the stress tensor at the surface of body i associated with $\underline{z}$. Here, $\underline{f}_{Vi}$, $\underline{g}_{Vi}$ and $\underline{f}_{Vi}$ are the force, torque and generalized 'elastic' force caused by viscous effects ($\underline{g}_{Vi}$ is taken about $\underline{O}_i$). $\underline{M}_{Vi}$, $\underline{C}_{Vi}$, $\underline{J}_{Vi}$ and $\underline{M}_{VVi}$ are hydrodynamic inertia-rate matrices, and $\underline{P}_{Vi}$ and $\underline{H}_{Vi}$ are hydrodynamic momentum-rate matrices. The remaining undefined symbol μ is the viscocity of the fluid. Both (3.7) and (3.11) are expressed in F_i.

In order to apply the above two aerodynamic models to DAISY, the hydrodynamic matrices given in (3.8) and (3.12) must be determined for each substructure cited in Section 2.1.1.

3.2.1 Hub Hydrodynamic Matrices

Since the hub is a rigid substructure, only $\underline{M}_z$, $\underline{C}_z$ and $\underline{J}_z$, $z \in \{Rh, Vh\}$, need to be specified. We choose to model the hub as a thin disk parallel to the x_h-y_h plane (where F_h is as shown in Fig. 4.1), centered about the z_h axis, a distance $\frac{1}{2}h$ above O_h, where h is the height of the hub. This model is reasonable provided that $\hat{\ell}_h >> \frac{1}{2}$, where $\hat{\ell}_h (= a_h/h_h)$ is the ratio of the hub radius a_h to the hub height. For DAISY, $\hat{\ell}_h \doteq 3$, hence this model should be adequate. If for some reason this does not prove to be the case, the much more complicated hydrodynamic matrices for an oblate spheroid can be used. A disk is the limiting case for this quadric.

Rather than belabor the details of the integrations cited in (3.8) and (3.12), a sample calculation for a typical rib is given instead, in Appendix B. The hub hydrodynamic matrices are simply stated here without proof (see Tables 3.2 and 3.3). For further details, the interested reader should consult [Lamb, 1945], [Milne and Thomson, 1955] and [Brenner, 1974].

The form of the matrices provided in Tables 3.2 and 3.3 is chosen to highlight the matrix components parallel to (denoted by the subscript $\parallel$) and perpendicular to (denoted by the subscript $\perp$) the symmetry axis $\underline{1}_i$, $i \in \{h, r_j, s_j\}$, for each substructure. This axis, expressed in F_i, also is specified in the tables. The final hydrodynamic matrices are expressed relative to O_i, instead of relative to the substructure's geometric

Table 3.2

Inertial-Resistance Hydrodynamic Matrices

Formulas:

$$i \in \{h, r_j, s_j\}$$

$$\underline{M}_{Ri} = \underline{1}_i \underline{1}_i^T M_{R\|i} - \underline{1}_i^X \underline{1}_i^X M_{R\perp i}$$

$$\underline{C}_{Ri} = \underline{1}_i^X C_{Ri}$$

$$\underline{J}_{Ri} = \underline{1}_i \underline{1}_i^T J_{R\|i} - \underline{1}_i^X \underline{1}_i^X J_{R\perp i}$$

Hub:

$$\underline{1}_h = [0 \quad 0 \quad 1]^T$$

$$M_{R\|h} = \frac{8}{3} \rho a_h^3 \qquad M_{R\perp h} = 0$$

$$J_{R\|h} = 0 \qquad J_{R\perp h} = \frac{16}{45} \rho a_h^5$$

$$C_{Rh} = 0$$

Rib j:

$$\underline{1}_{rj} = [1 \quad 0 \quad 0]^T$$

$$M_{R\|r_j} = 0 \qquad M_{R\perp r_j} = \rho \pi a_{r_j}^2 \ell_{r_j}$$

(cont'd)

$$J_{R\|r_j} = 0 \qquad J_{R\perp r_j} = \tfrac{1}{3} M_{R\perp r_j} \ell_{r_j}^2$$

$$C_{Rr_j} = \tfrac{1}{2} M_{R\perp r_j} \ell_{r_j}$$

$$\underline{P}_{Rr_j} = -\underline{C}_{Rr_j} \qquad \underline{H}_{Rr_j} = \underline{J}_{Rr_j}$$

$$\underline{M}_{RRr_j} = \underline{J}_{Rr_j}$$

Strut j:

$$\underline{1}_{s_j} = [0 \quad 1 \quad 0]^T$$

$$M_{R\|s_j} = 0 \qquad M_{R\perp s_j} = \rho \pi a_{s_j}^2 \ell_{s_j}$$

$$J_{R\|s_j} = 0 \qquad J_{R\perp s_j} = \tfrac{1}{3} M_{R\perp s_j} \ell_{s_j}^2$$

$$C_{Rs_j} = \tfrac{1}{2} M_{R\perp s_j} \ell_{s_j}$$

$$\underline{P}_{Rs_j} = \underline{O} \qquad \underline{H}_{Rs_j} = \underline{O}$$

$$\underline{M}_{RRs_j} = \underline{O}$$

Table 3.3

Viscous-Resistance Hydrodynamic Matrices

Formulas:

$$i \in \{h, r_j, s_j\}$$

$$\underline{M}_{vi} = \underline{1}_i \underline{1}_i^T M_{v||i} - \underline{1}_i^X \underline{1}_i^X M_{v\perp i}$$

$$\underline{C}_{vi} = \underline{1}_i^X C_{vi}$$

$$\underline{J}_{vi} = \underline{1}_i \underline{1}_i^T J_{v||i} - \underline{1}_i^X \underline{1}_i M_{v\perp i}$$

Hub:

$$\underline{1}_h = [0 \quad 0 \quad 1]^T$$

$$M_{v||h} = 16 \mu a_h \qquad M_{v\perp h} = \tfrac{32}{3} \mu a_h$$

$$J_{v||h} = \tfrac{32}{3} \mu a_h^3 \qquad J_{v\perp h} = J_{v||h} + \tfrac{1}{4} M_{v\perp h} h_h^2$$

$$C_{vh} = \tfrac{1}{2} M_{v\perp h} h_h$$

Rib j:

$$\underline{1}_{r_j} = [1 \quad 0 \quad 0]^T \qquad \hat{\ell}_{r_j} = \ell_{r_j} / a_{r_j}$$

$$M_{v||r_j} = 4\pi\mu\ell_{r_j} / (\ell n 2\hat{\ell}_{r_j} - \tfrac{3}{2}) \qquad M_{v\perp r_j} = 8\pi\mu\ell_{r_j} / (\ell n 2\hat{\ell}_{r_j} - \tfrac{1}{2})$$

(cont'd)

$$J_{v\|r_j} = \frac{2}{3}\mu \qquad J_{v\perp r_j} = \frac{\mu}{18}\left[\hat{\ell}_{r_j}^2\left(\ell n\hat{\ell}_{r_j} - 1\right)/\left(\ell n\left(\hat{\ell}_{r_j}/2\right)\right)^2 + 16.35/(4\pi)\right] + \frac{1}{4}M_{v\perp r_j}\ell_{r_j}^2$$

$$C_{vr_j} = \frac{1}{2}M_{v\perp r_j}\ell_{r_j}$$

$$\underline{P}_{vr_j} = -\underline{C}_{vr_j} \qquad \underline{H}_{vr_j} = \underline{J}_{vr_j}$$

$$\underline{M}_{vvr_j} = \underline{J}_{vr_j}$$

Strut j:

$$\underline{1}_{s_j} = [0 \quad 1 \quad 0]^T \qquad \hat{\ell}_{s_j} = \ell_{s_j}/a_{s_j}$$

$$M_{v\|s_j} = 4\pi\mu\ell_{s_j}/\left(\ell n2\hat{\ell}_{s_j} - \frac{3}{2}\right) \qquad M_{v\perp s_j} = 8\pi\mu\ell_{s_j}/\left(\ell n2\hat{\ell}_{s_j} - \frac{1}{2}\right)$$

$$J_{v\|s_j} = \frac{2}{3}\mu \qquad J_{v\perp s_j} = \frac{\mu}{18}\left[\hat{\ell}_{s_j}^2\left(\ell n\hat{\ell}_{s_j} - 1\right)/\left(\ell n\left(\hat{\ell}_{s_j}/2\right)\right)^2 + 16.35/(4\pi)\right] + \frac{1}{4}M_{v\perp s_j}\ell_{s_j}^2$$

$$C_{vs_j} = \frac{1}{2}M_{v\perp s_j}\ell_{s_j}$$

(cont'd)

$$\underline{P}_{V\delta_j} = \underline{M}_{VS_j}\underline{1}_{S_j} \qquad \underline{H}_{V\delta_j} = \underline{O}$$

$$\underline{P}_{V\gamma_j} = \underline{O} \qquad \underline{H}_{V\gamma_j} = \underline{J}_{VS_j}\underline{1}_{S_j}$$

$$M_{VV\delta\delta_j} = M_{V||S_j}$$

$$M_{VV\delta\gamma_j} = M_{VV\gamma\delta_j} = 0$$

$$M_{VV\gamma\gamma_j} = J_{V||S_j}$$

center. Hence extensive use has been made of the parallel-axis theorems cited in [Sincarsin and Hughes, 1983].

It should be noted that, for a disk immersed in an ideal fluid and subjected to either longitudinal translations (i.e. in the x_h- or y_h-directions) or a rotation about its perpendicular (z_h in the present case), the resultant flow has no velocity component perpendicular to the surface of the disk. The flow simply *slips* tangentially across the disk's surface. For a viscous fluid this is no longer the case, a fact reflected by the disappearance of several zero entries between the inertial resistance and viscous-resistance hydrodynamic matrices for the disk.

3.2.2 Rib Hydrodynamic Matrices

Unlike the hub, each rib is modeled as a 'flexible', rather than a rigid, substructure. Thus the entire complement of hydrodynamic matrices $\underline{M}_z$, $\underline{C}_z$, $\underline{J}_z$, $\underline{P}_z$, $\underline{H}_z$ and $\underline{M}_{zz}$, $z = \{Rr_j, Vr_j\}$, must be specified. To determine these matrices, the rib is modeled by an 'infinite' cylinder. A typical rib is shown in Fig. 4.2. The assumed rib frame, F_{r_j}, also is shown in that figure.

As previously mentioned, the detailed derivation of the hydrodynamic matrices for rib j is relegated to Appendix B. Here only the results of that process are summarized (see Tables 3.2 and 3.3). Again, the components parallel to, and perpendicular to, the symmetry axis $\underline{1}_{r_j}$ are highlighted in the form of the final matrices.

In a manner analogous to that for the hub, certain motions of rib j result in no normal velocity component to the surface, for a rib immersed in an ideal fluid. For F_{r_j} as shown in Fig. 4.2, these motions are translations along the x_{r_j}-direction and rotations about the x_{r_j}-axis. For a finite cylinder moving along x_{r_j}, this is not strictly true. However, since the rib is a thin open-ended tube the inertial resistance in this direction should be negligible. As before, these statements do not apply

for viscous fluids, hence the extra nonzero entries in the viscous-resistance hydrodynamic matrices for rib j.

3.2.3 Strut Hydrodynamic Matrices

Strut j (see Fig. 4.3) is geometrically similar to rib j; thus an 'infinite' cylinder model also is used to determine the strut hydrodynamic matrices. Again, since the strut is a 'flexible' substructure, all the matrices defined by (3.8) and (3.12) must be determined. The exact procedure is analogous to that given in Appendix B, except that the 'elastic' displacements for rib j ($\underline{\alpha}_j$) and their corresponding shape functions ($-\underline{r}^x_{r_j}$) are replaced by those for strut j ($[\delta_j \quad \gamma_j]^T$ and $[\underline{1}_{s_j} \quad -\underline{r}^x_{s_j}\underline{1}_{s_j}]$). The resulting hydrodynamic matrices, expressed in F_{s_j} (recall Fig. 4.3) are shown in Tables 3.2 and 3.3. Once again, the matrix components along the symmetry axis $\underline{1}_{s_j}$ and in the cross-axis directions are emphasized.

Since an infinite-cylinder model is used for both rib j and strut j, it follows that comments similar to those for the motion of rib j, when immersed in an ideal fluid, will also apply to strut j. The only difference is that F_{s_j} is oriented with y_{s_j} along the strut's symmetry axis, while F_{r_j} is oriented with x_{r_j} along the rib's symmetry axis. Hence translations along the y_{s_j}-direction and rotations about the y_{s_j}-axis yield no velocity component normal to the surface of strut j. In fact, since the end of each strut is essentially blocked by a rib, the assumption that the inertial resistance in the direction of the symmetry axis is negligible is even more valid for strut j. However, once viscosity is included, a substantial resistance results in the y_{s_j} direction, not because of 'end effects', but because of tangential viscous forces acting along the length of the strut. The result, as for the hub and rib, is the appearance of several nonzero elements in the viscous-resistance matrices, that are zero in the corresponding inertial-resistance matrices.

3.3 Total Disturbing Forces and Torques

It is useful at this juncture to summarize the total external environmental disturbance acting on each substructure of DAISY. This permits one major component of the external disturbance vector $\underline{u}_d$ (recall 2.87) to be identified. That is, $\underline{u}_d$ can be written as the sum of two components, as follows:

$$\underline{u}_d = \underline{u}_{dE} + \underline{u}_{dI} \tag{3.13}$$

where $\underline{u}_{dE}$ denotes external environmental disturbances and $\underline{u}_{dI}$ represents known external 'input' disturbances. 'Input' disturbances means those disturbances introduced during control studies and used to define the initial uncontrolled state, or as adversaries during the performance verification of a particular control strategy.

To accomplish the separation implied in (3.13) it is necessary to write the total external force and torque on each substructure in a similar form ($i \varepsilon \{h, r_j, s_j\}$):

$$\underline{f}_i = \underline{f}_{Ei} + \underline{f}_{Ii} \tag{3.14}$$

$$\underline{g}_i = \underline{g}_{Ei} + \underline{g}_{Ii} \tag{3.15}$$

$$\underline{\mathcal{M}}_i = \underline{\mathcal{M}}_{Ei} + \underline{\mathcal{M}}_{Ii} \qquad i \neq h \tag{3.16}$$

Then, given the information in the previous two sections, the following definitions apply:

$$\underline{f}_{Ei} = \underline{f}_{Gi} + \underline{f}_{Ri} + \underline{f}_{vi} \tag{3.17}$$

$$\underline{g}_{Ei} = \underline{g}_{Gi} + \underline{g}_{Ri} + \underline{g}_{vi} \tag{3.18}$$

Also, for rib j,

$$\underline{\mathcal{M}}_{E\alpha_j} = \underline{g}_{Er_j} \tag{3.19}$$

and, for strut j

$$\mathcal{E}_{E\delta_j} = \underline{1}_{s_j}^T \underline{f}_{Es_j} \; ; \qquad \mathcal{E}_{E\gamma_j} = \underline{1}_{s_j}^T \underline{g}_{Es_j} \tag{3.20}$$

The exact forms for $\underline{f}_{Ii}$, $\underline{g}_{Ii}$ and $\underline{\mathcal{A}}_{Ii}$ are still to be determined. They, of course, will depend greatly on the exact locations and directions of action of the peripherial actuators for DAISY, the sources for the 'input' disturbances.

4. SUBSTRUCTURE INERTIA MODELS

To further complete the motion equations provided in Section 2, a detailed set of inertia models for the various substructures is required. Since the 'elastic' mass and the momentum matrices associated with a typical rib [recall (2.35) - (2.37)] and a typical strut [recall (2.47)] are functions of the *rigid* inertias of each respective structure, it is necessary only to specify the mass m_i, the first moment of inertia $\underline{c}_i$, and the second moment of inertia $\underline{J}_i$ about O_i, expressed in F_i, for each substructure $i\varepsilon\{h,r_j,s_j\}$. In the following, the alignment chosen for F_i and the components of the attachment point vectors for the various O_i's (recall Section 2.1.4) also will be given.

Let each substructure i consist of n_i components. Futhermore assume that in each component k there is some reference point O_k, located relative to O_i by $\underline{r}_{ik}$, that acts as the origin for a reference frame F_k. Hence F_k and F_i are related by the rotation matrix $\underline{C}_{ik}$. Then denoting the mass, first moment of inertia and second moment of inertia of k about O_k, expressed in F_k, by m_k, $\underline{c}_k$ and $\underline{J}_k$, respectively, the inertias of substructure i are given by

$$m_i = \sum_{k=1}^{n_i} m_k \tag{4.1}$$

$$c_i = \sum_{k=1}^{n_i} (m_k \underline{r}_{ik} + \underline{C}_{ik}\underline{c}_k) \tag{4.2}$$

$$\underline{J}_i = \sum_{k=1}^{n_i} (\underline{C}_{ik}\underline{J}_k\underline{C}_{ki} - \underline{C}_{ik}\underline{c}_k^x\underline{C}_{ki}\underline{r}_{ik}^x$$

$$- \underline{r}_{ik}^x\underline{C}_{ik}\underline{c}_k^x\underline{C}_{ki} - m_k\underline{r}_{ik}^x\underline{r}_{ik}^x) \qquad (4.3)$$

Rather than write (4.1) through (4.3) explicitly for each substructure, only r_{ik}, $\underline{C}_{ik}$, and the individual component inertias will be provided in what follows.

4.1 Inertia Model for the Hub

As stated in Section 2.1.1, the hub is assumed to be rigid. To be more specific, it is assumed that the hub consists of five basic components: a bottom cover plate, a central cylinder, a top cover plate, a group of reaction wheels (3) and a set of rib mounts (m = the number of ribs). Hence for the hub (i = h), $n_h = 6 + m$, where the above components are denoted by k = (B, C, T, RX, RY, RZ and Mr_j), respectively. A diagram highlighting the various hub components is given in Fig. 4.1.

4.1.1 Bottom Cover Plate

The bottom cover plate is a solid circular disk of uniform density. The local reference frame F_B, with origin O_B at the geometric center of the plate, is taken to be aligned with F_h. The physical parameters of interest are the disk radius a_B, height h_B, and density ρ_B. Given these quantities the inertias for the bottom cover plate, relative to O_B and expressed in F_B, are

$$m_B = \rho_B \pi a_B^2 h_B$$

$$\underline{c}_B = \underline{0}$$

$$J_{B11} = J_{B22} = \tfrac{1}{12} m_B(3a_B^2 + h_B^2) \qquad (4.4)$$

$$J_{B33} = \tfrac{1}{2} m_B a_B^2$$

$$J_{B12} = J_{B13} = J_{B23} = 0$$

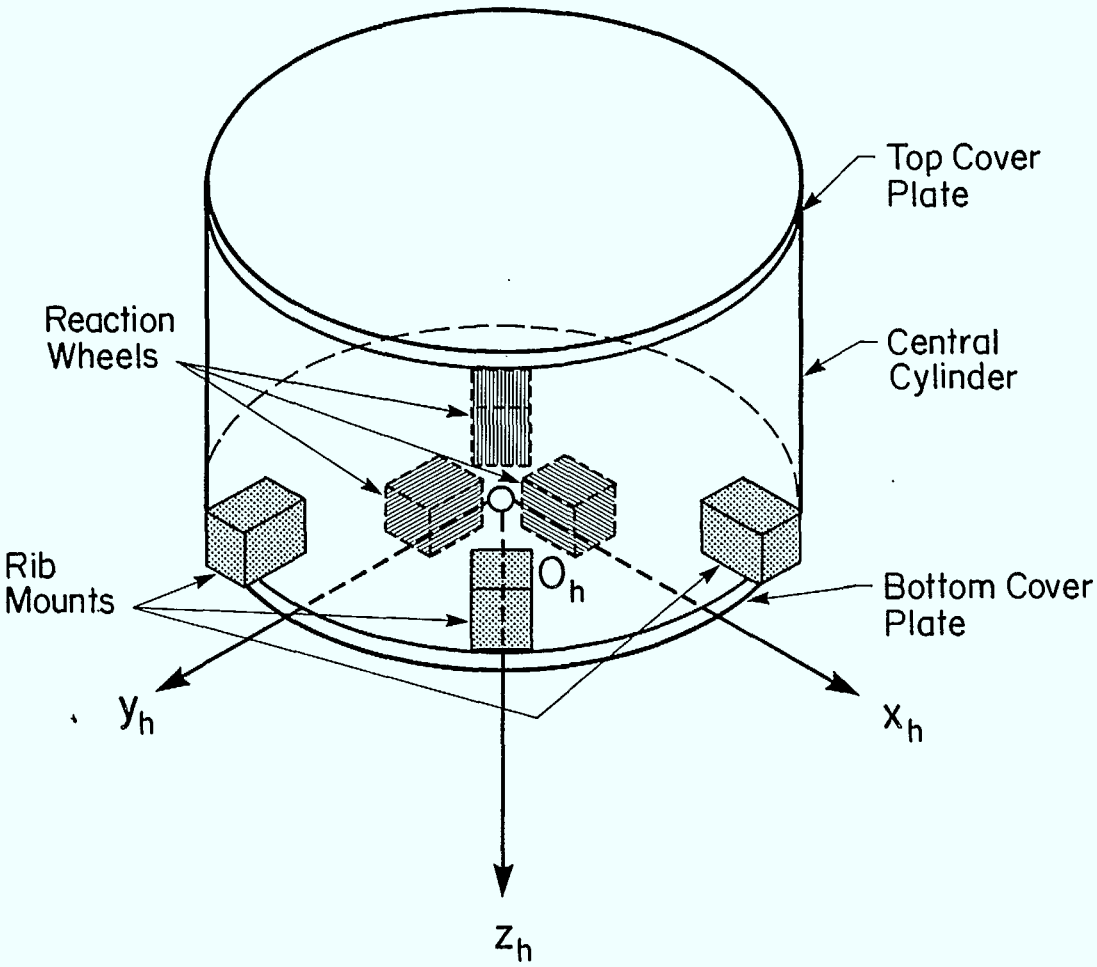

Figure 4.1: Hub Components

Also, the location of O_B relative to O_h and the rotation matrix relating F_B to F_h are

$$\underline{r}_{hB} = [0 \quad 0 \quad \tfrac{1}{2}h_B]^T \tag{4.5}$$

$$\underline{C}_{hB} = \underline{1} \tag{4.6}$$

These relations imply that O_h is located at the center of the lower surface of the bottom cover plate. Furthermore, F_h is chosen such that the $x_h - y_h$ plane coincides with this surface and z_h is the downward facing normal. The directions of x_h and y_h are fixed by choosing x_h to lie along one of the rib axes, as shown in Fig. 1.1.

4.1.2 Central Cylinder

The central portion of the hub is modeled by a thick-walled cylinder (necessary to accept the bolt-on cover plates) of uniform density. The cavity within the hub created by this component is used to hold the reaction wheels. Here the local reference frame F_c has its origin at the cylinder's geometric center and it is aligned with F_h. The geometric center is chosen, rather than the mass center, because creating holes to accept the rib joints, or any other such removal of mass, will shift the center of mass, but leave the geometric center unchanged.

The physical parameters required to determine the inertias of the central cylinder are: the outer radius of the cylinder, a_c; the wall thickness, t_c; the cylinder height, h_c; the density, ρ_c; and the inertias associated with the mass removed to permit the rib joint to interface with the hub (see Fig. 4.4 and Section 4.4). In fact, these 'hole' inertias are more easily dealt with as part of the rib-mount inertias and therefore they are included in the section that considers the rib mounts. Hence the inertias for the central cylinder, relative to O_c and expressed in F_c, are

$$m_C = \rho_C \pi (a_C^2 - b_C^2) h_C$$

$$\underline{c}_C = \underline{0}$$

$$J_{C11} = J_{C22} = \tfrac{1}{12} m_c (3a_C^2 + 3b_C^2 + h_C^2) \tag{4.7}$$

$$J_{C33} = \tfrac{1}{2} m_C (a_C^2 + b_C^2)$$

$$J_{C12} = J_{C13} = J_{C23} = 0$$

where

$$b_C = a_C - t_C \tag{4.8}$$

Here the location of O_C relative to O_h and the rotation matrix relating F_C to F_h are given by

$$\underline{r}_{hC} = [0 \quad 0 \quad (h_B + \tfrac{1}{2} h_C)]^T \tag{4.9}$$

$$\underline{C}_{hC} = \underline{1} \tag{4.10}$$

This completes the inertia model for the central cylinder.

4.1.3 Top Cover Plate

The top cover plate model is identical to that for the bottom cover plate although, to permit different dimensions and materials to be used in each case, the physical parameters of the two plates are not assumed to be the same. This is indicated by changing the subscript B in (4.4) to the subscript T. Also, while O_T and F_T are defined in a manner analogous to O_B and F_B, so that (4.6) still applies (with B replaced by T), the location of O_T is given by

$$\underline{r}_{hT} = [0 \quad 0 \quad (h_B + h_C + \tfrac{1}{2} h_T)]^T \tag{4.11}$$

rather than by (4.5).

4.1.4 Reaction Wheels

It is assumed that three reaction wheels are contained within the hub, one with its spin axis aligned along the x_h-axis (RX), another with its spin axis aligned along the y_h-axis (RY), and the last one with its spin axis aligned along the z_h-axis (RZ). At present, the detailed design of these components has not been performed. Hence, from the viewpoint of obtaining a preliminary inertia model for the hub, only the inertia about each wheel's spin axis J_τ, $\tau\varepsilon\{RX11,RY22,RZ33\}$, and the mass m_k, $k\varepsilon\{RX,RY,RZ\}$, of each reaction wheel are included. Furthermore, it is assumed that O_k, the origin of the local frame F_k, is at the mass center of each wheel, hence $\underline{c}_k = \underline{0}$. The location of each wheel's mass center relative to O_h is represented by

$$\underline{r}_{hk} = [\xi_k \quad \eta_k \quad \zeta_k]^T \tag{4.12}$$

while F_k is related to F_h according to

$$\underline{C}_{hk} = \underline{1} \tag{4.13}$$

One advantage of the component-by-component analysis of each substructure is that, once a more detailed component model or an undated component model becomes available, the entire substructure's new inertia can be computed in a straightforward manner via (4.1) through (4.3). One obvious application for this procedure is the case in point. As more detailed inertia models for the reaction wheels become available, the hub inertia will be recomputed.

4.1.5 Rib Joint Mounts

It suffices to consider a typical mount, that corresponding to rib j, rather than the entire set of m. Each mount is, in fact, two mounts, one external to the central cylinder wall and one inside the wall (see Fig. 4.4). A common shaft hole is shared by both mounts and there is, of course, an identical hole through the wall of the central cylinder at the appropriate position.

A similar set of mounts exists for each strut attached to rib j (recall Fig. 1.1). Hence a certain commonality can be maintained for all mounts (and all joints). One can use identical mount and joint models throughout, provided appropriate subscripts are adopted. To this end, a general mount and joint model is provided in Section 4.4. To obtain the inertias corresponding to the rib j mounts on the hub, one simply substitutes $(\tau, t, \rho) = (r_j, t_C, \rho_C)$ in the formulas contained in the mount section found therein.

The locations of the various mounts are unique and must be treat individually. For the rib mount Mr_j it is assumed that O_{Mr_j} lies on the center line of the mount hole at the outer surface of the central cylinder wall. Then

$$\underline{r}_{hMr_j} = [a_C\cos\Lambda_j \quad a_C\sin\Lambda_j \quad \zeta_{Mr_j}] \tag{4.14}$$

where

$$\Lambda_j = 2\pi(j - 1)/m \tag{4.15}$$

is measured about z_h in the positive right-hand-sense (starting at the x_h-axis) and ζ_{Mr_j} is the z_h-component of O_{Mr_j}. Furthermore, F_{Mr_j} is taken to be aligned with F_h, except for the above rotation. Whence

$$\underline{C}_{hMr_j} = \begin{bmatrix} \cos\Lambda_j & -\sin\Lambda_j & 0 \\ \sin\Lambda_j & \cos\Lambda_j & 0 \\ 0 & 0 & 1 \end{bmatrix} \tag{4.16}$$

This implies that x_{Mr_j} always points radially outward along a rib and would be the rib centerline if the ribs did not droop under gravity. (Given (4.15), the ribs have been assumed equidistantly spaced around the circumference of the hub.)

4.2 Inertia Model for a Typical Rib

Since the flexibility of each rib is localized at the rib

root (or, to be more specific, in the rib joint — see Section 4.4), the 'elastic' rib inertias are all related to the rigid rib inertias. Consequently the rib can be considered as a rigid body for the purposes of obtaining its inertia model. A typical rib consists of five main components, as shown for rib j in Fig. 4.2. These are: a rib joint, of which only the attachment bracket is shown in Fig. 4.2 (a more complete illustration is given in Fig. 4.4); a rib tube; an accelerometer group; and two sets of strut mounts. Therefore, for each rib j ($i = r_j$), we have $n_{r_j} = 5$, where the appropriate component subscripts are $k = (J_{r_j}, R_j, A_j, M_{s_j}$ and $M_{c_j})$, respectively.

As shown in Fig. 4.2, rib j droops through an angle θ_{oj} relative to the horizontal (i.e., the $x_h - y_h$ plane). The primed F_h axes shown in the figure correspond to the prerotated joint axes F_{Ur_j} given in Section 4.4. They are aligned with F_{Mr_j} of the previous section; however, their origin o_{r_j} is offset a distance d_{r_j} (defined in Section 4.4.2) in the positive x_{Mr_j} (x'_h) direction. Thus

$$\underline{r}_{hr_j} = [(a_C + d_{r_j})\cos\Lambda_j \quad (a_C + d_{r_j})\sin\Lambda_j \quad \zeta_{r_j}]^T \tag{4.17}$$

$$\underline{C}_{hh'} = \underline{C}_{hMr_j} \tag{4.18}$$

Now as shown in Fig. 4.2, o_{r_j} is also the origin of F_{r_j}. Therefore, (4.17) locates the origin for this substructure relative to o_h. The rotation matrix relating F_{r_j} to F_h follows from the realization that the rotation matrix relating F_{r_j} to F'_h is

$$\underline{C}_{h'r_j} = \begin{bmatrix} \cos\theta_{oj} & 0 & -\sin\theta_{oj} \\ 0 & 1 & 0 \\ \sin\theta_{oj} & 0 & \cos\theta_{oj} \end{bmatrix} \tag{4.19}$$

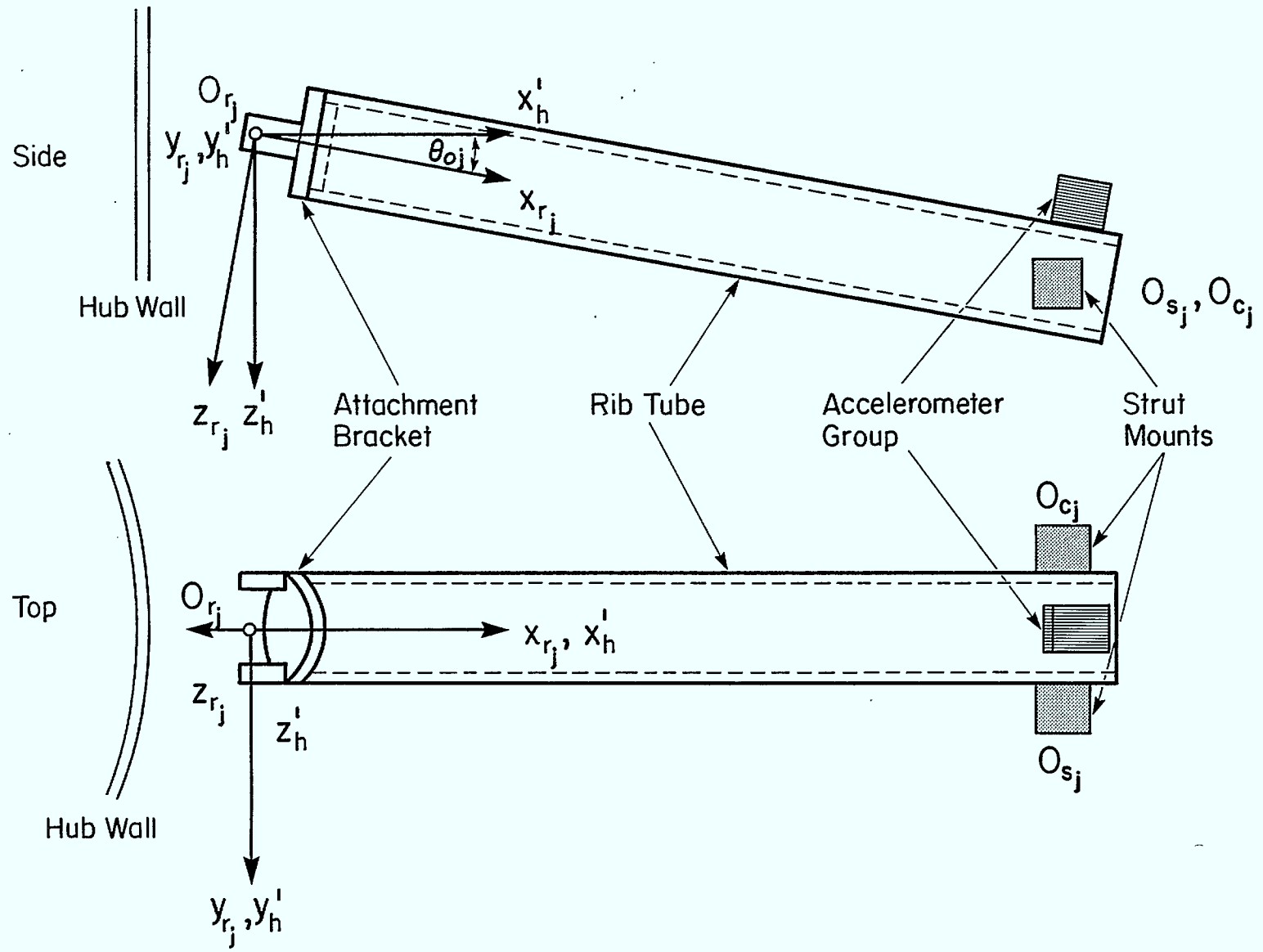

Figure 4.2: Rib j Components

Whence, recalling (2.1),

$$\underline{C}_{hr_j} = \underline{C}_{hh'}\,\underline{C}_{h'r_j} \tag{4.20}$$

Both (4.17) and (4.20) play key roles in the dynamical equations for DAISY presented in Section 2. (The use of $F_{h'}$ rather than F_{Ur_j} in Fig. 4.2 was motivated by the desire for a briefer notation and to emphasize the relationship of F_{Ur_j} to F_h.)

4.2.1 Rib Joint

Each rib joint (excluding the joint mounts) consists of a universal mechanism and a circular attachment bracket. Details of local reference frames, appropriate physical parameters, and inertias for a typical rib joint are discussed at length in Section 4.4. The appropriate variable set for this case is $(\tau, \lambda) = (r_j, \theta_{oj})$.

Given the inertias from the above procedure, it only remains to note that

$$\underline{r}_{r_j Jr_j} = \underline{0} \tag{4.21}$$

$$\underline{C}_{r_j Jr_j} = \underline{1} \tag{4.22}$$

which are consistent with the comments made in Section 4.2.

4.2.2 Rib Tube

The rib tube is modeled as a thin-walled circular cylinder of uniform density. This hollow design minimizes the mass and is capable of accepting the accelerometer leads. Once again the local reference frame, here denoted F_{R_j}, is chosen to have its origin o_{R_j} at the geometric center of the component. However, now F_{r_j} is the substructural reference frame of importance and thus F_{R_j} is chosen to be aligned with F_{r_j}.

The physical parameters necessary to establish the rib tube inertias are: the outer radius of the tube, a_{R_j}; the wall thickness, t_{R_j}; the length of the rib, ℓ_{r_j}; the distance from O_{r_j} to the edge of the rib tube, ξ_{Jr_j} (from Section 4.4); the density, ρ_{R_j}; and the inertias associated with the mass removed to permit the strut joints to interface with the rib (see Fig. 4.4 and Section 4.4). As before, these 'hole' inertias are most easily dealt with as part of the strut mount inertias and hence they will not be included in the inertias given below. Given the above parameters, the inertias for the rib tube, relative to O_{R_j} and expressed in F_{R_j}, are

$$
\begin{aligned}
m_{R_j} &= \rho_{R_j}\pi(a_{R_j}^2 - b_{R_j}^2)\ell_{R_j} \\
\underline{c}_{R_j} &= \underline{0} \\
\underline{J}_{R_j}11 &= \tfrac{1}{2} m_{R_j}(a_{R_j}^2 + b_{R_j}^2) \\
J_{R_j}22 &= J_{R_j}33 = \tfrac{1}{12} m_{R_j}(3a_{R_j}^2 + 3b_{R_j}^2 + \ell_{R_j}^2) \\
J_{R_j}12 &= J_{R_j}13 = J_{R_j}23 = 0
\end{aligned}
\tag{4.23}
$$

where

$$b_{R_j} = a_{R_j} - t_{R_j} \tag{4.24}$$

$$\ell_{R_j} = \ell_{r_j} - \xi_{Jr_j} \tag{4.25}$$

Also, the location of O_{R_j} relative to O_{r_j} and the rotation matrix relating F_{R_j} to F_{r_j} are given by

$$\underline{r}_{r_jR_j} = [\xi_{Jr_j} + \tfrac{1}{2}\ell_{R_j} \quad 0 \quad 0]^T \tag{4.26}$$

$$\underline{C}_{r_jR_j} = \underline{1} \tag{4.27}$$

It should be noted that no end cap has been assumed for the rib tube. There are three main reasons for this decision: less weight, less aerodynamic resistance, and easy access to mounts and accelerometer leads.

4.2.3 Accelerometer Group

The accelerometer group is presently modeled by a point mass m_{R_j}. The location of this mass relative to o_{r_j} is represented by

$$\underline{r}_{r_j A_j} = [\xi_{A_j} \quad \eta_{A_j} \quad \zeta_{A_j}]^T \tag{4.28}$$

If a more detailed accelerometer inertia model becomes necessary it can easily be implemented via equations (4.1) through (4.3).

4.2.4 o_{s_j} Strut Joint Mounts

As discussed in Section 4.1.5, a universal joint-mount inertia model is adopted for DAISY. The details of this model are presented in Section 4.4. Using the parameter set $(\tau, t, \rho) = (s_j, t_{R_j}, \rho_{R_j})$ in the equations found therein one obtains the inertias corresponding to the joint-mount inertias associated with the o_{s_j} strut (recall Fig. 2.1). However, since each strut joint is oriented such that the 'U' of the joint universal (see Fig. 4.4) lies in the horizontal plane (the $x_h - y_h$ plane), rather than being vertical like the rib joint, a transformation is required to redefine the inertias about the appropriate axes. The problem is further complicated by the fact that different axes are assigned for the symmetry axis of the rib and the strut (for each rib the symmetry axis is the x-axis, while for each strut the symmetry axis is the y-axis). This change in axes simplifies the final rotation matrices and ultimately the physical interpretations of DAISY's various motions; however, it complicates the transformation required to realign the inertias from Section 4.4. In any case, the final transformation has a relatively simple form:

$$\underline{T}_S = \begin{bmatrix} 0 & 0 & -1 \\ 1 & 0 & 0 \\ 0 & -1 & 0 \end{bmatrix} \tag{4.29}$$

whence

$$\begin{aligned} m_{Ms_j} &= m_{M\tau} \\ \underline{c}_{Ms_j} &= \underline{T}_S \underline{c}_{M\tau} \\ \underline{J}_{Ms_j} &= \underline{T}_S \underline{J}_{M\tau} \underline{T}_S^T \end{aligned} \tag{4.30}$$

where the subscripted τ-quantities are those from Section 4.4.

The local reference frame for the O_{s_j} mounts, F_{Ms_j}, has its origin located relative to O_{r_j} by

$$\underline{r}_{r_j Ms_j} = [\xi_{s_j} \quad a_{R_j} \quad 0]^T \tag{4.31}$$

where ξ_{s_j} is the distance to the centerline of the mount holes from O_{r_j}. The above equation implies that O_{Ms_j} lies on the outer surface of the rib tube, on the centerline of the mount holes, which lies in the $x_{r_j} - y_{r_j}$ plane and is aligned with y_{r_j}. F_{Ms_j} is taken to be aligned with F_h', from Figure 4.2. Therefore,

$$\underline{C}_{r_j Ms_j} = \underline{C}_{r_j h'} \tag{4.32}$$

This completes the information required for the O_{s_j} mounts.

4.2.5 O_{C_j} Strut Joint Mounts

In a manner analogous to the previous section, the joint-mount inertias associated with the O_{C_j} strut (recall Fig. 2.1) are obtained

by setting $(\tau, t, \rho) = (c_j, t_{R_j}, \rho_{R_j})$ in the formulas of Section 4.4. A transformation similar to (4.29) is required here also, for the same reasons:

$$\underline{T}_c = \begin{bmatrix} 0 & 0 & -1 \\ -1 & 0 & 0 \\ 0 & 1 & 0 \end{bmatrix} \tag{4.32a}$$

Then,

$$\begin{aligned} m_{Mc_j} &= m_{M\tau} \\ \underline{c}_{Mc_j} &= \underline{T}_c \underline{c}_{M\tau} \\ \underline{J}_{Mc_j} &= \underline{T}_c \underline{J}_{M\tau} \underline{T}_{c_j}^T \end{aligned} \tag{4.32b}$$

where, again, the subscripted τ-quantities come from Section 4.4.

The origin of the local reference frame for the o_{c_j} mounts, o_{Mc_j}, is located relative to o_{r_j} by the vector

$$\underline{r}_{r_j cM_j} = [\xi_{c_j} \quad -a_{R_j} \quad 0]^T$$

where ξ_{c_j} is the distance to the centerline of the mount holes from o_{r_j}. That is, o_{Mc_j} lies on the outer surface of the rib tube on the centerline of the mount holes. As for the o_{s_j} mounts, this centerline lies in the $x_{r_j} - y_{r_j}$ plane and is aligned with the y_{r_j}-axis. Also, the local reference frame F_{Mc_j} is taken to be aligned with F_h'. Hence,

$$\underline{C}_{r_j Mc_j} = \underline{C}_{r_j h'} \tag{4.32c}$$

It is notable that, ideally, all the strut mounts should be located the

same distance from O_{r_j}. Therefore, it will be assumed henceforth that $\xi_{s_j} = \xi_{c_j} = \xi_j$.

4.3 Inertia Model for a Typical Strut

Each strut has its flexibility localized in springs at the joints and in a pair of linear springs on the guide ram shaft (see Fig. 4.3). As a consequence, this substructure's 'elastic' inertias, like those of the rib, are all related to its rigid inertias. Thus one need concentrate only on the latter. In this regard, five strut-component inertia models must be developed, one for each component shown in Fig. 4.3. Therefore, in the notation adopted in the introduction to Section 4, $i = s_j$, $n_{s_j} = 5$ and $k = (J_{s_j}, E_j, G_j, S_j \text{ and } J_{c_{j+1}})$, where the k subscripts respectively refer to the O_{s_j} strut joint, the end plate, the guide ram (keyed not to rotate), the strut tube, and the $O_{c_{j+1}}$ strut joint components.

The F_h'' frame shown in Fig. 4.3 corresponds to the prerotated joint axes $F_{U\tau}$ given in Section 4.4 for the O_{s_j} strut joint. Again, a simplified notation that emphasizes the relationship of this frame to F_h is adopted. The $x_h'' - y_h''$ plane is parallel to the $x_h - y_h$ plane, hence the z_h'' axis is parallel to the z_h axis. Now, F_h' is aligned with F_{Ms_j}; however, O_{s_j} is offset a distance d_{s_j} (defined in Section 4.4) in the positive y_{Mr_j} (y_h'') direction. Therefore,

$$\underline{r}_{r_j s_j} = [\xi_j \quad a_{R_j} + d_{s_j} \quad 0]^T \tag{4.33}$$

$$\underline{C}_{r_j h''} = \underline{C}_{r_j Ms_j} \tag{4.34}$$

Furthermore, O_{s_j} is also the origin of F_{s_j}, so that (4.33) locates the origin for the strut substructural frame relative to O_{r_j}. The strut substructural frame F_{s_j} is obtained from F_h'' by a rotation of $\bar{\Lambda}$ about z_h'', where

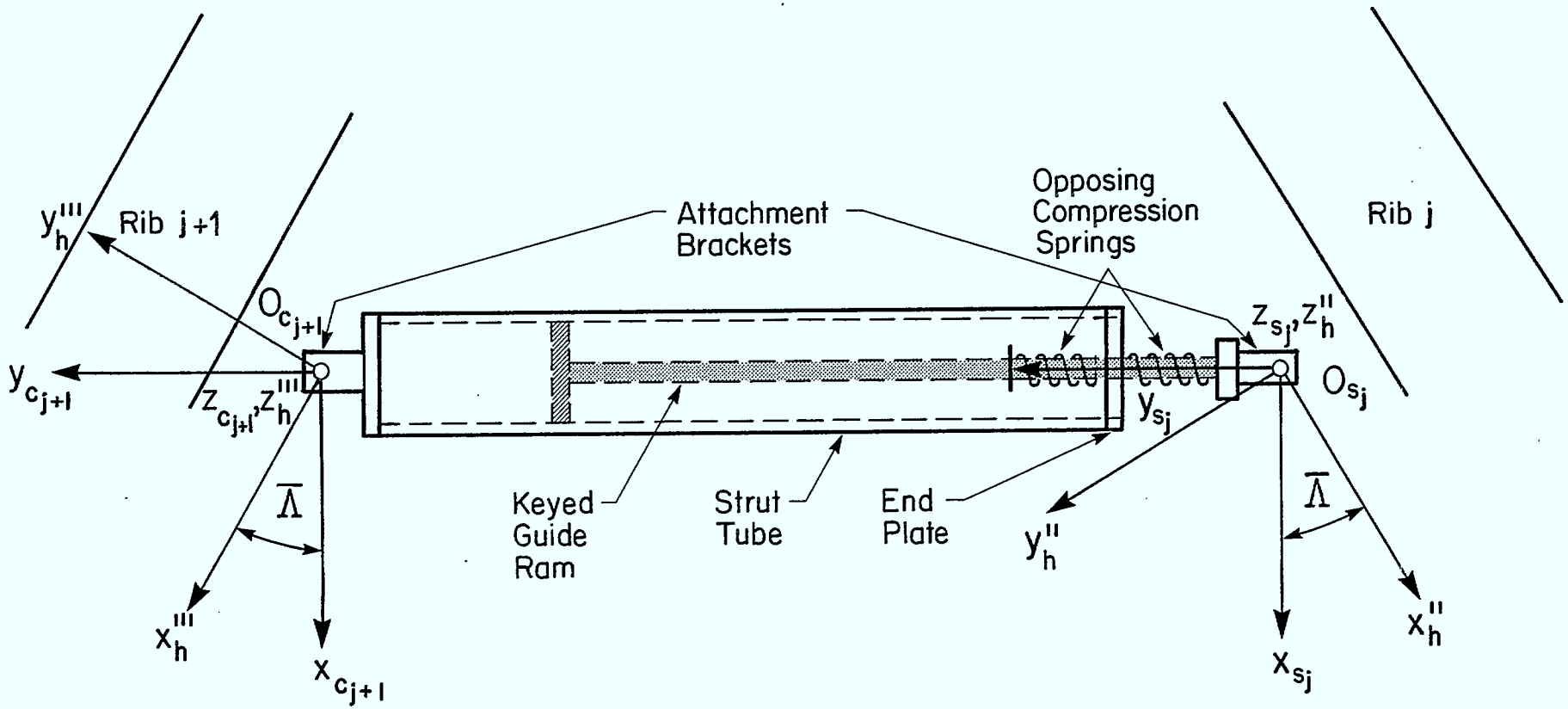

Figure 4.3: Strut j Components

$$\bar{\Lambda} = \tfrac{1}{2}(\Lambda_{j+1} - \Lambda_j) = \pi/m \tag{4.35}$$

given (4.15). Equation (4.35) results from the geometry of a set of ribs equidistantly spaced around the circumference of the hub and a set of struts whose ends are located at the same radial distance from the z_h-axis. More general relations can be proved which permit the modeling of geometric errors caused by manufacturing tolerances. Although not included in this report, an unpdated description of the inertia model will be issued should such be required later in the design process.

Given (4.35), the rotation matrix relating F_{s_j} to F_h'' is

$$\underline{C}_{h''s_j} = \begin{bmatrix} \cos\bar{\Lambda} & -\sin\bar{\Lambda} & 0 \\ \sin\bar{\Lambda} & \cos\bar{\Lambda} & 0 \\ 0 & 0 & 1 \end{bmatrix} \tag{4.36}$$

Hence the rotation matrix relating F_{s_j} to F_{r_j} is

$$\underline{C}_{r_j s_j} = \underline{C}_{r_j h''} \underline{C}_{h'' s_j} \tag{4.37}$$

This relation also holds for $F_{C_{J+1}}$ which is aligned with F_{s_j} but has its origin $O_{C_{J+1}}$ given by

$$\underline{r}_{r_{J+1} c_{j+1}} = [\xi_{j+1} \quad -(a_{R_{j+1}} + d_{s_{j+1}}) \quad 0]^T \tag{4.38}$$

or

$$\underline{r}_{r_j c_{j+1}} = \underline{r}_{r_j s_j} + \underline{C}_{r_j s_j} [0 \quad \ell_{s_j} \quad 0]^T \tag{4.39}$$

instead of by (4.33). Here ℓ_{s_j} is the length of the strut which, given the assumptions used to obtain (4.35), is the same for all struts.

4.3.1 O_{s_j} Strut Joint

This joint consists of a universal mechanism and a rectangular bracket (shown side-on in Fig. 4.3). As with the rib joint, the details governing the inertias assumed for the O_{s_j} strut joint are provided by substituting $(\tau, \lambda) = (s_j, \bar{\Lambda})$ into the formulas contained in Section 4.4. However, as explained in 4.2.4, the inertias resulting from this process must be subjected to a transformation analogous to that in (4.30). To be specific,

$$\begin{aligned} m_{Js_j} &= m_{J\tau} \\ \underline{C}_{Js_j} &= \underline{T}_S \underline{C}_{M\tau} \\ \underline{J}_{Js_j} &= \underline{T}_S \underline{J}_{M\tau} \underline{T}_S^T \end{aligned} \tag{4.40}$$

where $\underline{T}_S$ is given by (4.29) and the subscripted τ-quantities are those obtained from Section 4.4.

To complete the O_{s_j} strut joint inertia model it must be noted that O_{Js_j} coincides with O_{r_j} and that F_{Js_j} is aligned with F_{s_j}. Thus

$$\underline{r}_{s_j Js_j} = \underline{0} \tag{4.41}$$

$$\underline{C}_{s_j Js_j} = \underline{1} \tag{4.42}$$

These results are required in (4.2) and (4.3).

4.3.2 End Plate

The end plate of each strut j is a circular disk of uniform density. A hole is drilled along its symmetry axis so as to permit the translational motion δ_j of the keyed guide ram (see Fig. 4.3). The local frame F_{E_j} is again chosen to have its origin O_{E_j} at the geometric center of the disk, and is aligned with F_{s_j}. Thus

$$\underline{r}_{s_j E_j} = [0 \quad \xi_{Js_j} + \Delta_{E_j} + \tfrac{1}{2} h_{E_j} \quad 0]^T \tag{4.43}$$

$$\underline{C}_{s_j E_j} = \underline{1} \tag{4.44}$$

where ξ_{Js_j} is the distance from O_{r_j} to the edge of the rectangular bracket closest to the end plate (see Section 4.4), Δ_{E_j} is the gap between this edge and the end plate and h_{E_j} is the height of the end plate.

The remaining physical parameters for the end plate are: the radius of the disk, a_{E_j}; the radius of the hole, a_{H_j}; and the density, ρ_{E_j}. The required inertias then become

$$\begin{aligned} m_{E_j} &= \rho_{E_j} \pi (a_{E_j}^2 - a_{H_j}^2) h_{E_j} \\ \underline{c}_{E_j} &= \underline{0} \\ J_{E_j 11} &= J_{E_j 22} = \tfrac{1}{12} m_{E_j} (3a_{E_j}^2 + 3a_{H_j}^2 + h_{E_j}^2) \\ J_{E_j 22} &= \tfrac{1}{2} m_{E_j} (a_{E_j}^2 + a_{H_j}^2) \\ J_{E_j 12} &= J_{E_j 13} = J_{E_j 23} = 0 \end{aligned} \tag{4.45}$$

relative to O_{E_j} and expressed in F_{E_j}. For the present, any difference between the bushing density (a bushing exists in the end-plate hole to assist the motion of the keyed ram) and that of the end plates is neglected.

4.3.3 Guide Ram

The guide ram shown in Fig. 4.3 consists of a disk with a threaded center hole, into which a shaft is threaded. Even though this shaft is welded to the rectangular end plate, it is still considered to be part of the guide ram. This ability to unscrew the two components (and to remove the strut end plate) is necessary to be able to access and preload the shaft springs. A retainer ring is also required to force the interior shaft spring to maintain its compressive load against the end plate. The rectangular attachment bracket plays the same role for the exterior shaft spring.

Here the physical parameters of interest are: the radius of the disk, a_{G_j}; the height of the disk, h_{G_j}; the density of the disk, ρ_{G_j}; the radius of the guide shaft, a_{Gs_j}; its length, ℓ_{Gs_j}; and its density, ρ_{Gs_j}. One must also know the distance to the retainer ring, d_{RR_j}; its mass, m_{RR_j}; and the masses of the interior and exterior springs, m_{Is_j} and m_{Es_j}. Then the appropriate inertias are

$$
\begin{aligned}
m_{G_j} &= m_{GD_j} + m_{GS_j} + m_{RR_j} \\
&\quad + m_{IS_j} + m_{ES_j} \\
c_{G_j 2} &= -\tfrac{1}{2} m_{GS_j}(\ell_{GS_j} - h_{G_j}) \\
&\quad - m_{RR_j}(\ell'_{GS_j} - \Delta'_{E_j} - d_{RR_j}) \\
&\quad - m_{IS_j}(\ell'_{GS_j} - \Delta'_{E_j} - \tfrac{1}{2} d_{RR_j}) \\
&\quad - m_{ES_j}(\ell'_{GS_j} - \tfrac{1}{2}\Delta_{E_j}) \\
c_{G_j 1} &= c_{G_j 3} = 0
\end{aligned}
\tag{4.46}
$$

$$
\begin{aligned}
J_{G_j 11} = J_{G_j 33} &= \tfrac{1}{12} m_{GD_j}(3a_{G_j}^2 + 3a_{GS_j}^2 + h_{G_j}^2) \\
&\quad + \tfrac{1}{12} m_{GS_j}(3a_{G_j}^2 + \ell_{GS_j}^2) \\
&\quad + \tfrac{1}{4} m_{GS_j}(\ell_{GS_j} - h_{G_j})^2 \\
&\quad + m_{RR_j}(\ell'_{GS_j} - \Delta'_{E_j} - d_{RR_j})^2 \\
&\quad + m_{IS_j}(\ell'_{GS_j} - \Delta'_{E_j} - \tfrac{1}{2} d_{RR_j})^2 \\
&\quad + m_{ES_j}(\ell'_{GS_j} - \tfrac{1}{2}\Delta_{E_j})^2 \\
J_{G_j 22} &= \tfrac{1}{2} m_{GD_j} a_{G_j}^2 + \tfrac{1}{2} m_{GS_j} a_{GS_j}^2 \\
J_{G_j 12} &= J_{G_j 13} = J_{G_j 23} = 0
\end{aligned}
$$

where

$$m_{GD_j} = \rho_{G_j}\pi(a_{G_j}^2 - a_{GS_j}^2)h_{G_j}$$

$$m_{GS_j} = \rho_{GS_j}\pi a_{GS_j}^2 \ell_{GS_j}$$

$$\ell'_{GS_j} = \ell_{GS_j} - \tfrac{1}{2}h_{G_j}$$

$$\Delta'_{E_j} = \Delta_{E_j} + h_{E_j}$$

and the inertias are taken relative to O_{G_j} and expressed in F_{G_j}. Here it is assumed that O_{G_j} is at the geometric center of the guide ram disk and that F_{G_j} is aligned with F_{s_j}. Thus

$$\underline{r}_{s_j G_j} = [0 \quad \xi_{Js_j} + \ell'_{Gs_j} \quad 0]^T \tag{4.47}$$

$$\underline{C}_{s_j G_j} = \underline{1} \tag{4.48}$$

It should be noted that the self-inertias of the retainer ring and both shaft springs have been neglected in obtaining the above results.

4.3.4 Strut Tube

The strut tube is modeled as a thin-walled circular cylinder of uniform density. The local reference frame F_{S_j} is taken to be aligned with F_{s_j} and to have its origin O_{S_j} located at the geometric center of the tube.

$$\underline{r}_{s_j S_j} = [0 \quad \xi_{s_j} + \Delta_{E_j} + h_{E_j} + \tfrac{1}{2}\ell_{S_j} \quad 0]^T \tag{4.49}$$

$$\underline{C}_{s_j S_j} = \underline{1} \tag{4.50}$$

where

$$\ell_{S_j} = \ell_{s_j} - \xi_{s_j} - \xi_{c_{j+1}} - \Delta_{E_j} - h_{E_j} \tag{4.51}$$

and $\xi_{c_{j+1}}$ is the distance from $O_{c_{j+1}}$ to the edge of the circular attachment bracket on the strut end nearest rib $j+1$. Also, given the assumptions cited in the introduction to Section 4.3, ℓ_{s_j} can be written as a function of variables that have already been discussed:

$$\ell_{s_j} = 2[\{(a_C + d_{r_j}) + \xi_j \cos\theta_{o_j}\}\sin\bar{\Lambda} + (a_{R_j} + d_{s_j})\cos\bar{\Lambda}] \tag{4.52}$$

The only remaining physical parameters of interest are the outer radius of the tube, a_{S_j}, the wall thickness, t_{S_j}, and the density, ρ_{S_j}. Then the inertias for the strut tube take the form

$$\begin{aligned} m_{S_j} &= \rho_{S_j}\pi(a_{S_j}^2 - b_{S_j}^2)\ell_{S_j} \\ \underline{c}_{S_j} &= \underline{0} \\ J_{S_j 11} &= J_{S_j 33} = \tfrac{1}{12} m_{S_j}(3a_{S_j}^2 + 3b_{S_j}^2 + \ell_{S_j}^2) \\ J_{S_j 22} &= \tfrac{1}{2} m_{S_j}(a_{S_j}^2 + b_{S_j}^2) \\ J_{S_j 12} &= J_{S_j 13} = J_{S_j 23} = 0 \end{aligned} \tag{4.53}$$

where

$$b_{S_j} = a_{S_j} - t_{S_j} \tag{4.54}$$

A lubricated lining to aid the translational motion of the guide ram is also anticipated to be necessary; however, any difference between the density of this lining and that of the rib tube is neglected, for the present. Also, holes may have to be drilled in the rib tube, above and below the displacement range of the guide-ram disk, to relieve the air pressure on this disk. If this should prove to be the case, then some modification

of (4.53) would be required.

4.3.5 $O_{c_{j+1}}$ Strut Joint

Unlike the O_{s_j} strut joint (recall Section 4.3.1), this joint employs a circular, rather than a rectangular, attachment bracket. Again the inertias for this joint are found by substituting $(\tau, \lambda) = (c_{j+1}, \bar{\Lambda})$ directly into the equations of Section 4.4 and then performing a transformation to realign the inertias, so as to be consistent with the joint orientation adopted for the struts. In particular,

$$\begin{aligned} m_{Jc_{j+1}} &= m_{J\tau} \\ \underline{c}_{Jc_{j+1}} &= \underline{T}_c \underline{c}_{M\tau} \\ \underline{J}_{Jc_{j+1}} &= \underline{T}_c \underline{J}_{M\tau} \underline{T}_c^T \end{aligned} \tag{4.55}$$

where $\underline{T}_c$ is given by (4.32a) and the quantities with the subscript τ are those from Section 4.4.

To complete the $O_{c_{j+1}}$ strut joint inertia model it must be noted that $O_{Jc_{j+1}}$ coincides with $O_{c_{j+1}}$ and is located relative to O_{s_j} by

$$\underline{r}_{s_j Jc_{j+1}} = [0 \quad \ell_{s_j} \quad 0]^T \tag{4.56}$$

and that $F_{Jc_{j+1}}$ coincides with $F_{c_{j+1}}$, which in turn is aligned with F_{s_j}. Therefore, the necessary rotation matrix is

$$\underline{C}_{s_j Jc_{j+1}} = \underline{1} \tag{4.57}$$

This enables equations (4.2) and (4.3) to be applied for the $O_{c_{j+1}}$ strut joint.

4.4 Inertia Model for a Typical Joint

In this section an inertial model for the joint shown in Fig. 4.4

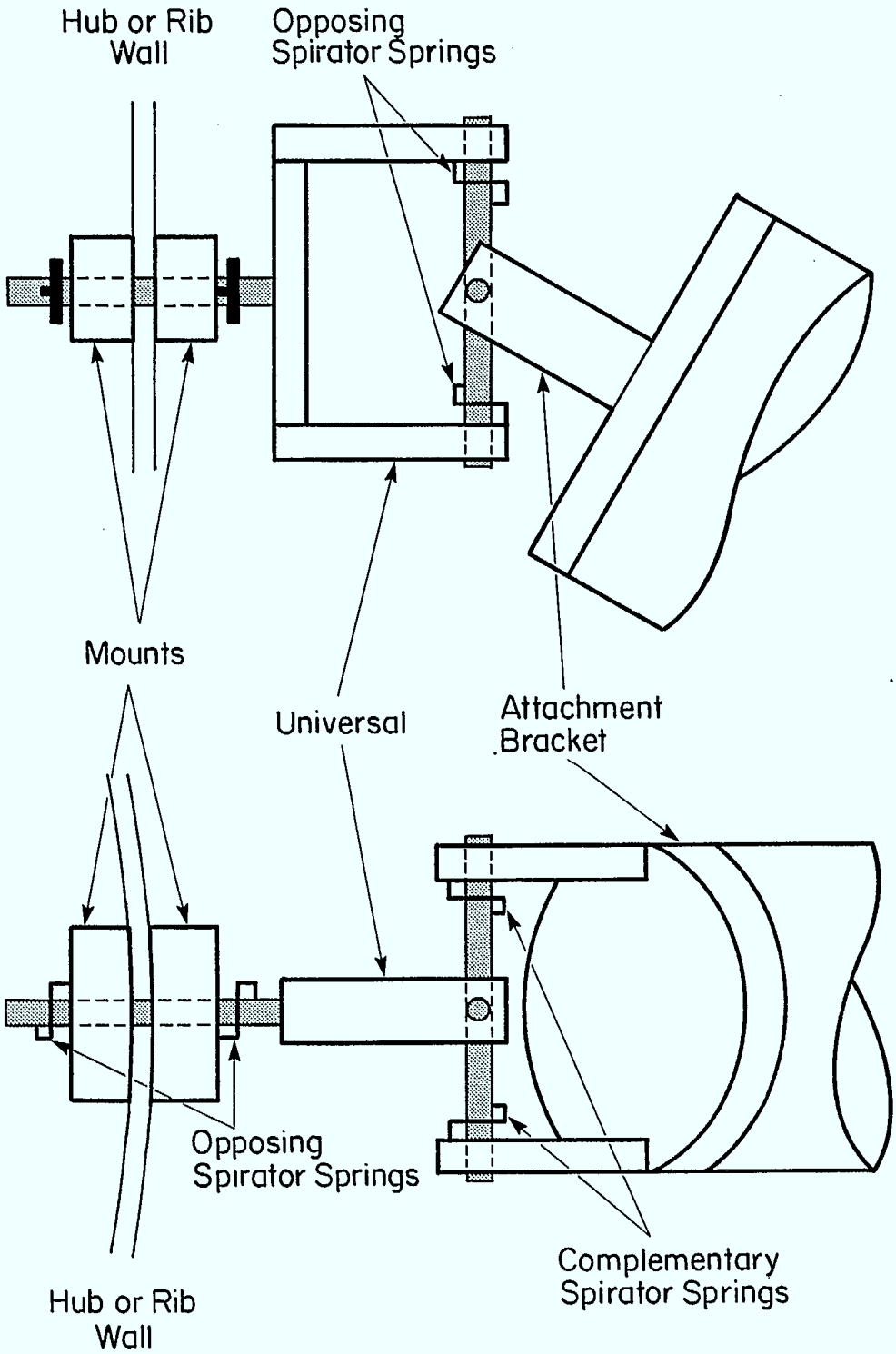

Figure 4.4: A Typical Joint

is presented. A joint strictly is defined as a universal plus either a circular (shown) or a rectangular (not shown) attachment bracket. Each joint is considered to be part of the substructure to which the attachment bracket is fastened. Hence each rib has one joint, while each strut has two. The joint mounts are also shown in Fig. 4.4 and will be discussed in what follows. They also are considered as part of the substructure to which they are attached.

The orientation of each joint depends on the particular substructure to which it is attached. For each rib, the top drawing in Fig. 4.4 is in a vertical plane aligned with the z_h axis, while the bottom drawing is the top view of the joint. For each strut, the top drawing lies in a horizontal plane parallel to $x_h - y_h$ so that the bottom drawing is a side view of the joint. The dimensions of the mounts are also altered for the strut joint so that the two views shown in Fig. 4.4 are reversed.

4.4.1 Mounts

A dimensioned schematic of a typical pair of joint mounts is presented in Fig. 4.5, where a general notation employing the subscript τ has been adopted. In fact, the physical parameters for the mounts also employ this notation (see Table 4.1). There are, however, two unsubscripted 'global' quantities, the thickness t of the wall separating the exterior and interior mounts, and the density ρ of the wall material. These two variables are determined by the type of mount (rib or strut). For example, the set $(\tau, t, \rho) = (r_j, t_C, \rho_C)$ specifies a rib mount, while the set $(\tau, t, \rho) = (s_j, t_{R_j}, \rho_{R_j})$ specifies a strut mount.

The local frame $F_{M\tau}$, chosen for the purpose of inertia calculations, also is shown in Fig. 4.5. Its origin $O_{M\tau}$ is located on the centerline of the mount holes at the wall-edge of the exterior mount. The mounts are positioned relative to $F_{M\tau}$ (as shown). The alignment of $F_{M\tau}$ again depends on the type of mount considered. These alignments have been discussed previously and will not be repeated here (see Sections 4.1.5, 4.2.4 and 4.2.5).

Given these facts, the inertias for the rib mounts, relative to $O_{M\tau}$ and expressed in $F_{M\tau}$, are

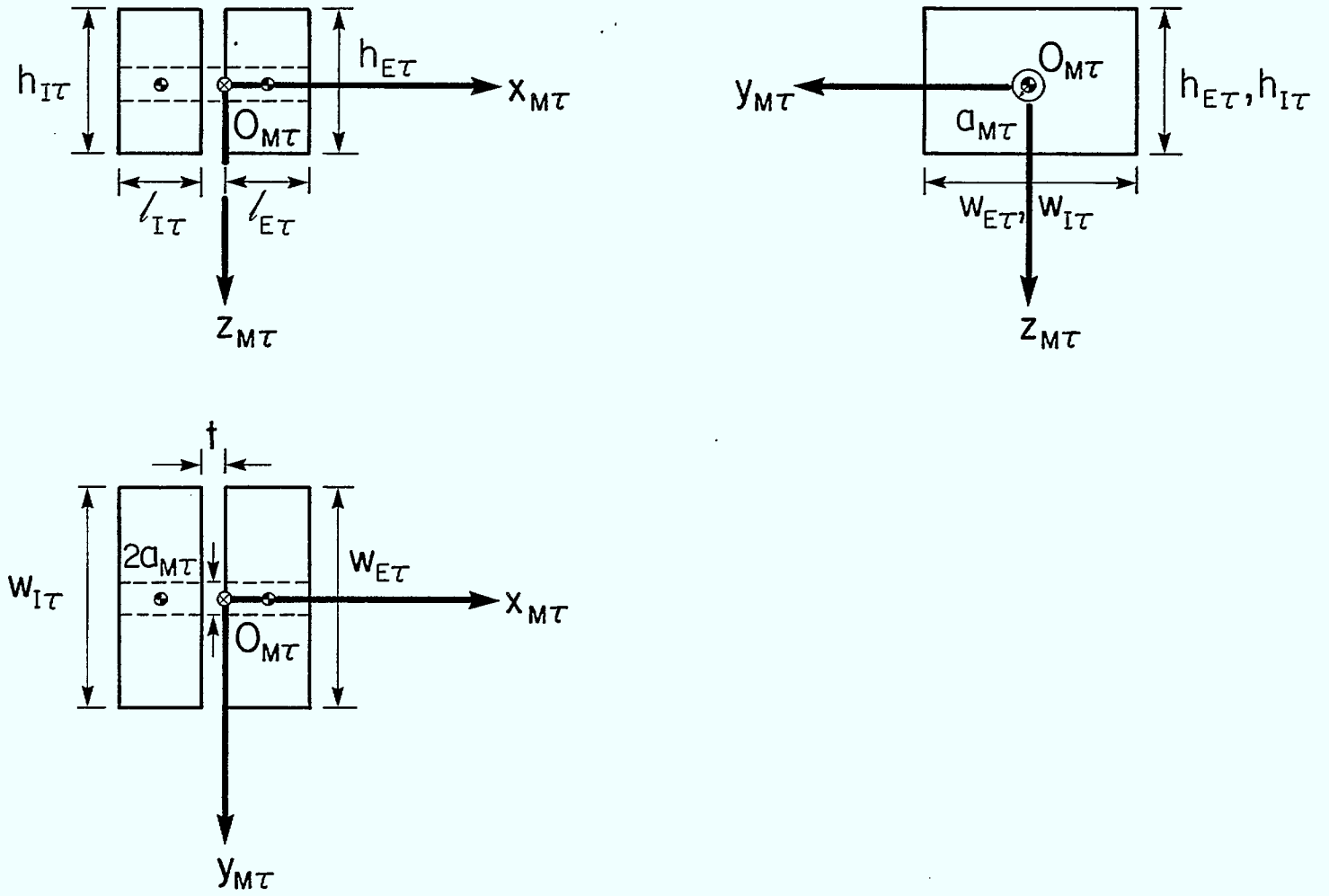

Figure 4.5: Joint Mounts

Table 4.1

Mount and Joint Physical Parameters

Mounts:

Exterior (Interior)

$\ell_{E(I)\tau}$ — length

$w_{E(I)\tau}$ — width

$h_{E(I)\tau}$ — height

$\rho_{E(I)\tau}$ — density

a_{τ} — hole radius

$m_{ms\tau}$ — mass of each opposing spring

Global

t — wall thickness

ρ — wall density

Joint:

Universal

$a_{C\tau}$ — radius of cross shafts (4)

$a_{M\tau}$ — radius of mount shaft (1)

$\ell_{C\tau}$ — length of cross shafts

$\ell_{M\tau}$ — length of mount shaft

$\rho_{S\tau}$ — density of shafts

$\ell_{P\tau}$ — length of cross-shaft support plates (2)

$w_{P\tau}$ — width

$t_{P\tau}$ — thickness

$\ell_{B\tau}$ — length of back plates

$w_{B\tau}$ — width

$t_{B\tau}$ — thickness

(cont'd)

Table 4.1 (Continued)

$\rho_{P\tau}$ — density of plates

$\Delta_{C\tau}$ — gap between cross shafts and back plate

$\Delta_{M\tau}$ — gap between back plate and exterior mount

$t_{U\tau}$ — see below

$m_{OS\tau}$ — mass of each opposing spring

$m_{CS\tau}$ — mass of each complementary

Circular Attachment Bracket

$\ell_{U\tau}$ — length of uprights (2)

$w_{U\tau}$ — width

$t_{U\tau}$ — thickness

$a_{D\tau}$ — radius of disk

$h_{D\tau}$ — height

$\rho_{B\tau}$ — density of bracket

$\xi_{J\tau}$ — distance from centerline of bracket holes to farthest edge of disk

$a_{C\tau}$ — as above

Rectangular Attachment Bracket

$\ell_{R\tau}$ — length of rectangular plate

$w_{R\tau}$ — width

$h_{R\tau}$ — height

$\ell_{U\tau}$, $w_{U\tau}$, $t_{U\tau}$, $\rho_{B\tau}$, $a_{C\tau}$ — as above

$\xi_{J\tau}$ — as above, except now to farthest edge of plate

Global

λ — angle between $x_{U\tau}$ and $x_{J\tau}$ axes

$$m_{M\tau} = m_{E\tau} + m_{I\tau} - m_{EH\tau} - m_{IH\tau} + m_{ES\tau} + m_{IS\tau}$$

$$\underline{c}_{M\tau} = \begin{bmatrix} \tfrac{1}{2}(m_{E\tau} - m_{EH\tau})\ell_{E\tau} + (m_{IH\tau} - m_{I\tau})(\tfrac{1}{2}\ell_{I\tau} + t) \\ + m_{MS\tau}\ell_{E\tau} - m_{MS\tau}(\ell_{I\tau} + t) \\ 0 \\ 0 \end{bmatrix} \tag{4.58}$$

$$J_{M\tau 11} = \tfrac{1}{12} m_{E\tau}(h_{E\tau}^2 + w_{E\tau}^2) + \tfrac{1}{12} m_{I\tau}(h_{I\tau}^2 + w_{I\tau}^2) - \tfrac{1}{2} m_{EH\tau} a_\tau^2 - \tfrac{1}{2} m_{IH\tau} a_\tau^2$$

$$J_{M\tau 22} = \tfrac{1}{12} m_{E\tau}(\ell_{E\tau}^2 + h_{E\tau}^2) + \tfrac{1}{12} m_{I\tau}(\ell_{I\tau}^2 + h_{I\tau}^2) + J_M$$

$$J_{M\tau 33} = \tfrac{1}{12} m_{E\tau}(\ell_{E\tau}^2 + w_{E\tau}^2) + \tfrac{1}{12} m_{I\tau}(\ell_{I\tau}^2 + w_{I\tau}^2) + J_M$$

$$J_{M\tau 12} = J_{M\tau 13} = J_{M\tau 23} = 0$$

where

$$m_{E(I)\tau} = \rho_{E(I)\tau} \ell_{E(I)\tau} w_{E(I)\tau} h_{E(I)\tau} \tag{4.59}$$

$$m_{E(I)H\tau} = \rho_{E(I)\tau} \pi a_\tau^2 \ell_{E(I)\tau} \tag{4.60}$$

$$J_M = -\tfrac{1}{12} m_{EH\tau}(3a_\tau^2 + \ell_{E\tau}^2) - \tfrac{1}{12} m_{IH\tau}(3a_\tau^2 + \ell_{I\tau}^2) + \tfrac{1}{4}(m_{E\tau} - m_{EH\tau})\ell_{E\tau}^2 + (m_{I\tau} - m_{IH\tau})(\tfrac{1}{2}\ell_{I\tau} + t)^2 + m_{MS\tau}\ell_{E\tau}^2 + m_{MS\tau}(\ell_{I\tau} + t)^2 \tag{4.61}$$

Also, the *corrections* to the inertias of the substructure supporting the mounts (either the hub or rib j) required because a mount hole must be drilled through the wall of that substructure, are

$$
\begin{aligned}
m_{C\tau} &= \pi\rho a_\tau^2 t \\
\underline{c}_{C\tau} &= [-\tfrac{1}{2}m_{C\tau}t \quad 0 \quad 0]^T \\
J_{C\tau 11} &= \tfrac{1}{2}m_{C\tau}a_\tau^2 \\
J_{C\tau 22} &= J_{C\tau 33} = \tfrac{1}{12}\, m_{C\tau}(3a_\tau^2 + t^2) + \tfrac{1}{4}\, m_{C\tau}t^2 \\
J_{C\tau 12} &= J_{C\tau 13} = J_{C\tau 23} = 0
\end{aligned}
\tag{4.62}
$$

where the above inertias are taken relative to $O_{M\tau}$ and expressed in $F_{M\tau}$. These inertias are most easily incorporated into the overall inertia model for DAISY by subtracting them from the inertias given in (4.58).

4.4.2 Universal

The universal portion of a typical joint is shown dimensioned in Fig. 4.6. Again, the same τ-subscript notation as that adopted for the mounts is used both in the figure and in the physical parameters given in Table 4.1. However, now only one global quantity is required, namely λ, the angle between the universal and joint frames, $F_{U\tau}$ and $F_{J\tau}$ (also shown in Fig. 4.6). Therefore, a rib universal is specified by setting $(\tau, \lambda) = (r_j, \theta_{o_j})$ in the equations that follow, while a strut universal is obtained for $(\tau, \lambda) = (s_j, \bar{\Lambda})$.

In what follows, the universal inertias will first be expressed in $F_{U\tau}$ and then transformed into $F_{J\tau}$. As can be seen from Fig. 4.6 these two frames share the same origin; however, $F_{J\tau}$ is rotated relative to $F_{U\tau}$ by an angle of $-\lambda$ about $y_{U\tau}$. Whence

$$
\underline{C}_{J\tau U\tau} = \begin{bmatrix} \cos\lambda & 0 & \sin\lambda \\ 0 & 1 & 0 \\ -\sin\lambda & 0 & \cos\lambda \end{bmatrix}
\tag{4.63}
$$

Note that the origin of these frames corresponds to either O_{r_j}, O_{s_j} or O_{c_j}.

It should also be noted that $O_{M\tau}$ is a distance

$$
d_\tau = \xi_{M\tau} + \ell_{E\tau}
\tag{4.64}
$$

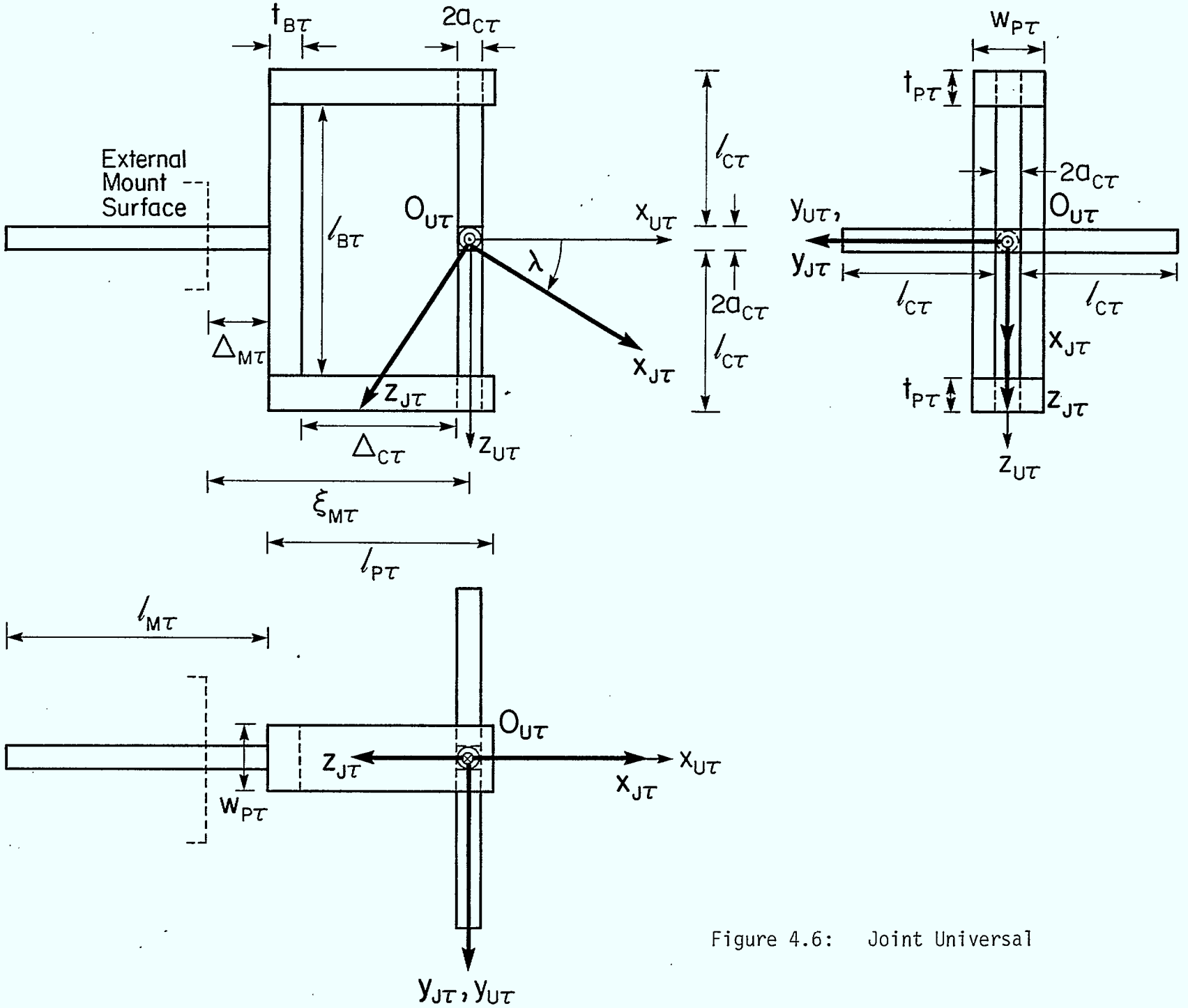

Figure 4.6: Joint Universal

behind $O_{U\tau}$ ($O_{J\tau}$) in the negative $x_{U\tau}$ direction, where

$$\xi_{M\tau} = \Delta_{M\tau} + t_{B\tau} + \Delta_{C\tau} + a_{C\tau} \tag{4.65}$$

from Fig. 4.6.

Now, the inertias of the universal, relative to $O_{U\tau}$ and expressed in $F_{U\tau}$, are

$$m_\tau = 2m_{P\tau} + m_{B\tau} + m_{CC\tau} + 4m_{C\tau} + m_{S\tau} - 2m_{H\tau} + 2m_{Os\tau} + 2m_{CS\tau}$$

$$\underline{c}_\tau = \begin{bmatrix} -2m_{P\tau}(\xi'_M - \tfrac{1}{2}\ell_{P\tau}) - m_{B\tau}(\xi'_{M\tau} - \tfrac{1}{2}t_{B\tau}) \\ \quad - m_{S\tau}(\xi'_{M\tau} + \tfrac{1}{2}\ell_{M\tau}) \\ 0 \\ 0 \end{bmatrix} \tag{4.66}$$

$$\begin{aligned} J_{\tau 11} &= \tfrac{1}{6} m_{P\tau}(t_{P\tau}^2 + w_{P\tau}^2) + \tfrac{1}{12} m_{B\tau}(\ell_{B\tau}^2 + w_{B\tau}^2) \\ &\quad + \tfrac{2}{3} m_{CC\tau} a_{C\tau}^2 + \tfrac{1}{3} m_{C\tau}(3a_{C\tau}^2 + \ell_{C\tau}^2) \\ &\quad + \tfrac{1}{2} m_{S\tau} a_{M\tau}^2 - \tfrac{1}{6} m_{H\tau}(3a_{C\tau}^2 + t_{P\tau}^2) \\ &\quad + \tfrac{1}{2}(m_{P\tau} - m_{H\tau})(\ell_{B\tau} + t_{P\tau})^2 + 4m_{C\tau}(\tfrac{1}{2}\ell_{C\tau} + a_{C\tau}^2) \\ &\quad + 2m_{OS\tau}(\ell_{C\tau} + a_{C\tau} - t_{P\tau})^2 + 2m_{CS\tau}(\ell_{C\tau} + a_{C\tau} - t_{U\tau})^2 \end{aligned}$$

$$\begin{aligned} J_{\tau 22} &= \tfrac{1}{6} m_{P\tau}(\ell_{P\tau}^2 + t_{P\tau}^2) + \tfrac{1}{12} m_{B\tau}(\ell_{B\tau}^2 + t_{B\tau}^2) \\ &\quad - \tfrac{1}{6} m_{H\tau}(3a_{C\tau}^2 + t_{P\tau}^2) + \tfrac{1}{2}(m_{P\tau} - m_{H\tau})(\ell_{B\tau} + t_{P\tau})^2 \\ &\quad + 2m_{OS\tau}(\ell_{C\tau} + a_{C\tau} - t_{P\tau})^2 + J_\tau \end{aligned}$$

$$\begin{aligned} J_{\tau 33} &= \tfrac{1}{6} m_{P\tau}(\ell_{P\tau}^2 + w_{P\tau}^2) + \tfrac{1}{12} m_{B\tau}(w_{B\tau}^2 + t_{B\tau}^2) - m_{H\tau} r_{C\tau}^2 \\ &\quad + 2m_{CS\tau}(\ell_{C\tau} + a_{C\tau} - t_{U\tau})^2 + J_\tau \end{aligned}$$

$$J_{\tau 12} = J_{\tau 13} = J_{\tau 23} = 0$$

where

$$m_{P(B)\tau} = \rho_{P\tau} \ell_{P(B)\tau} w_{P(B)\tau} t_{P(B)\tau} \tag{4.67}$$

$$m_{CC\tau} = 8\rho_{S\tau} a_{C\tau}^3 \tag{4.68}$$

$$m_{C\tau} = \rho_{S\tau} \pi a_{C\tau}^2 \ell_{C\tau} \tag{4.69}$$

$$m_{S\tau} = \rho_{S\tau} \pi a_{M\tau}^2 \ell_{M\tau} \tag{4.70}$$

$$m_{H\tau} = \rho_{P\tau} \pi a_{C\tau}^2 t_{P\tau} \tag{4.71}$$

$$\begin{aligned} J_\tau = {} & \tfrac{2}{3} m_{CC\tau} a_{C\tau}^2 + m_{C\tau} a_{C\tau}^2 \\ & + \tfrac{1}{6} m_{C\tau}(3a_{C\tau}^2 + \ell_{C\tau}^2) + \tfrac{1}{12} m_{S\tau}(3a_{M\tau}^2 + \ell_{M\tau}^2) \\ & + 2m_{P\tau}(\xi'_{M\tau} - \tfrac{1}{2}\ell_{P\tau})^2 + m_{B\tau}(\xi'_{M\tau} - \tfrac{1}{2}t_{B\tau})^2 \\ & + 2m_{C\tau}(\tfrac{1}{2}\ell_{C\tau} + a_{C\tau})^2 + m_{S\tau}(\xi'_{M\tau} + \tfrac{1}{2}\ell_{M\tau})^2 \end{aligned} \tag{4.72}$$

$$\xi'_{M\tau} = \xi_{M\tau} - \Delta_{M\tau} \tag{4.73}$$

Whence the inertias for the universal, expressed in $F_{J\tau}$, are

$$\begin{aligned} m_{U\tau} &= m_\tau \\ \underline{c}_{U\tau} &= \underline{C}_{J\tau U} \underline{c}_\tau \\ \underline{J}_{U\tau} &= \underline{C}_{J\tau U\tau} \underline{J}_\tau + \underline{C}_{U\tau J\tau} \end{aligned} \tag{4.75}$$

It remains to establish the attachment bracket inertias before the total joint inertias can be determined.

4.4.3 Circular Attachment Bracket

A typical circular bracket is shown in Fig. 4.7. It consists of two uprights and a flat circular disk, dimensioned as indicated in the figure. Also shown is the orientation of the attachment bracket relative

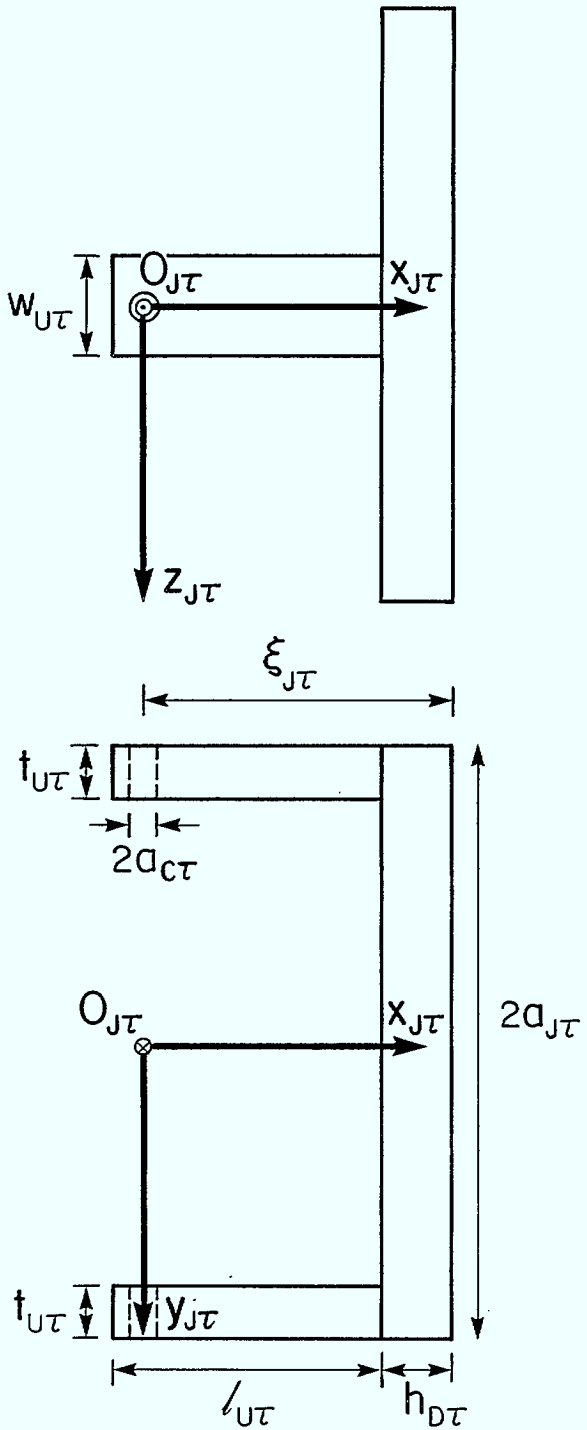

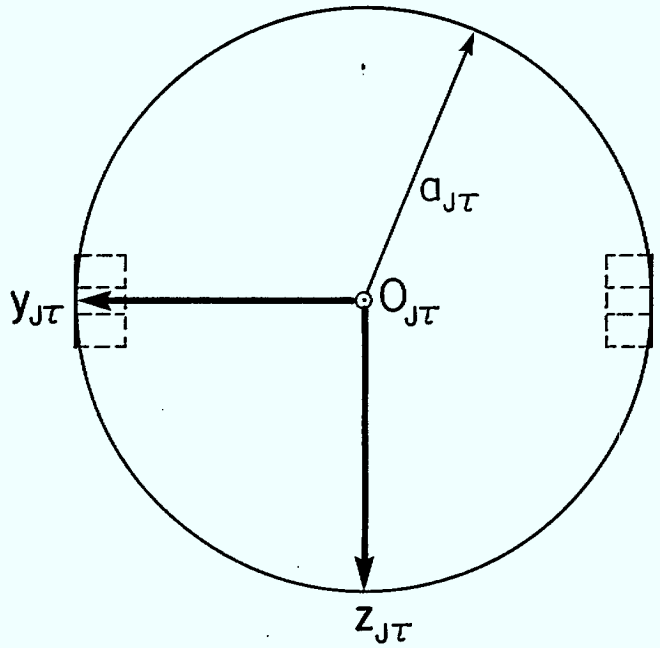

Figure 4.7: Circular Attachment Bracket (CAB)

to the joint axes $F_{J\tau}$ and the origin of that frame $O_{J\tau}$. Given the geometry shown in Fig. 4.7 and the parameter definitions from Table 4.1, the appropriate inertias for the circular attachment bracket, relative to $O_{J\tau}$ and expressed in $F_{J\tau}$, are

$$m_{B\tau} = m_{D\tau} + 2m_{U\tau} - 2m_{D\tau}$$

$$\underline{c}_{B\tau} = \begin{bmatrix} m_{D\tau}(\xi_{J\tau} - \tfrac{1}{2}h_{D\tau}) + 2m_{U\tau}(\xi_{J\tau} - h_{D\tau} - \tfrac{1}{2}\ell_{U\tau}) \\ 0 \\ 0 \end{bmatrix} \tag{4.76}$$

$$J_{B\tau 11} = \tfrac{1}{2} m_{D\tau} a_{J\tau}^2 + \tfrac{1}{6} m_{U\tau}(t_{U\tau}^2 + w_{U\tau}^2) + J_{B\tau}$$

$$J_{B\tau 22} = \tfrac{1}{12} m_{D\tau}(3a_{J\tau}^2 + h_{D\tau}^2) + \tfrac{1}{6} m_{U\tau}(\ell_{U\tau}^2 + w_{U\tau}^2) - m_{D\tau} a_{C\tau}^2 + m_{D\tau}(\xi_{J\tau} - \tfrac{1}{2}h_{D\tau})^2 + 2m_{U\tau}(\xi_{J\tau} - h_{D\tau} - \tfrac{1}{2}\ell_{U\tau})^2$$

$$J_{B\tau 33} = \tfrac{1}{2} m_{D\tau}(3a_{J\tau}^2 + h_{D\tau}^2) + \tfrac{1}{6} m_{U\tau}(\ell_{U\tau}^2 + t_{U\tau}^2) + m_{D\tau}(\xi_{J\tau} - \tfrac{1}{2}h_{D\tau})^2 + 2m_{U\tau}(\xi_{J\tau} - h_{D\tau} - \tfrac{1}{2}\ell_{U\tau})^2 + J_{B\tau}$$

$$J_{B\tau 12} = J_{B\tau 13} = J_{B\tau 33} = 0$$

where

$$m_{D\tau} = \rho_{B\tau} \pi a_{D\tau}^2 h_{D\tau} \tag{4.77}$$

$$m_{U\tau} = \rho_{B\tau} \ell_{U\tau} w_{U\tau} t_{U\tau} \tag{4.78}$$

$$m_{O\tau} = \rho_{B\tau} \pi a_{C\tau}^2 t_{U\tau} \tag{4.79}$$

$$J_{B\tau} = -\tfrac{1}{6} m_{O\tau}(3a_{C\tau}^2 + t_{U\tau}^2) + 2(m_{U\tau} - m_{O\tau})(a_{J\tau} - \tfrac{1}{2}t_{U\tau})^2 \tag{4.80}$$

The total joint inertias are then the sum of (4.75) and (4.76).

4.4.4 Rectangular Attachment Bracket

This bracket, which is used at the O_{S_j} strut joint to reduce weight, still has two uprights, but now a rectangular plate replaces the circular disk of the previous design. The same local reference frame $F_{J\tau}$ and origin $O_{J\tau}$ are used for this bracket. Furthermore, the orientation of the bracket relative to the local frame remains unchanged (see Fig. 4.8).

Noting the slightly different physical parameter set from Table 4.1, and taking the inertias relative to $O_{J\tau}$, the inertias for this bracket, expressed in $F_{J\tau}$, are

$$m_B = m_{R\tau} + 2m_{U\tau} - 2m_{O\tau}$$

$$\underline{c}_{B\tau} = \begin{bmatrix} m_{R\tau}(\xi_{J\tau} - \tfrac{1}{2}h_{R\tau}) + 2m_U(\xi_{J\tau} - h_{R\tau} - \tfrac{1}{2}\ell_{U\tau}) \\ 0 \\ 0 \end{bmatrix} \tag{4.81}$$

$$J_{B\tau 11} = \tfrac{1}{12} m_{R\tau}(\ell_{R\tau}^2 + w_{R\tau}^2) + \tfrac{1}{6} m_{U\tau}(t_{U\tau}^2 + w_{U\tau}^2) + J_{B\tau}$$

$$J_{B\tau 22} = \tfrac{1}{12} m_{R\tau}(h_{R\tau}^2 + w_{R\tau}^2) + \tfrac{1}{6} m_{U\tau}(\ell_{U\tau}^2 + w_{U\tau}^2) - m_{O\tau}a_{C\tau}^2 + m_{R\tau}(\xi_{J\tau} - \tfrac{1}{2}h_{R\tau})^2 + 2m_{U\tau}(\xi_{J\tau} - h_{R\tau} - \tfrac{1}{2}\ell_{U\tau})^2$$

$$J_{B\tau 33} = \tfrac{1}{12} m_{R\tau}(\ell_{R\tau}^2 + h_{R\tau}^2) + \tfrac{1}{6} m_{U\tau}(\ell_{U\tau}^2 + t_{U\tau}^2) + m_{R\tau}(\xi_{J\tau} - \tfrac{1}{2}h_{R\tau})^2 + 2m_{U\tau}(\xi_{J\tau} - h_{R\tau} - \tfrac{1}{2}\ell_{U\tau})^2 + J_{B\tau}$$

$$J_{B\tau 12} = J_{B\tau 13} = J_{B\tau 23} = 0$$

where

$$m_{R\tau} = \rho_{B\tau}\ell_{R\tau}w_{R\tau}h_{R\tau} \tag{4.82}$$

$$J_{B\tau} = -2m_{O\tau}(3a_{C\tau}^2 + t_{U\tau}^2) + 2(m_{U\tau} - m_{O\tau})(\ell_{R\tau} - \tfrac{1}{2}t_{U\tau})^2 \tag{4.83}$$

and the remaining variables are as given in Section 4.4.3. Once again, the

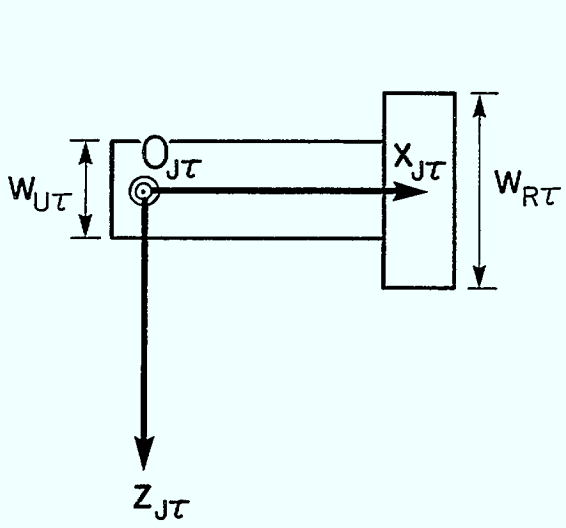

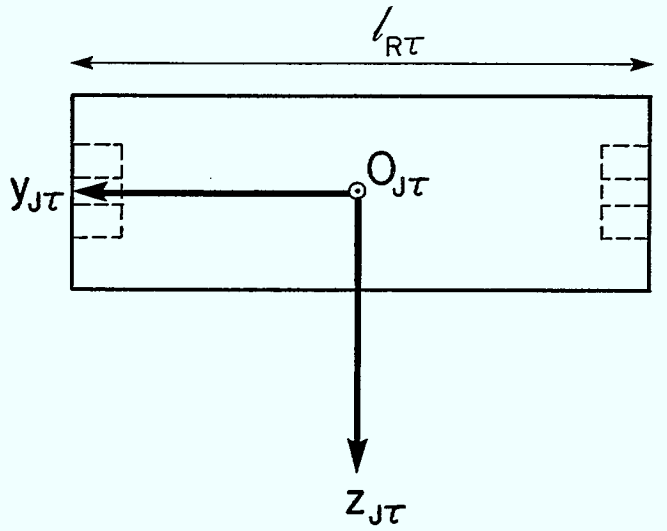

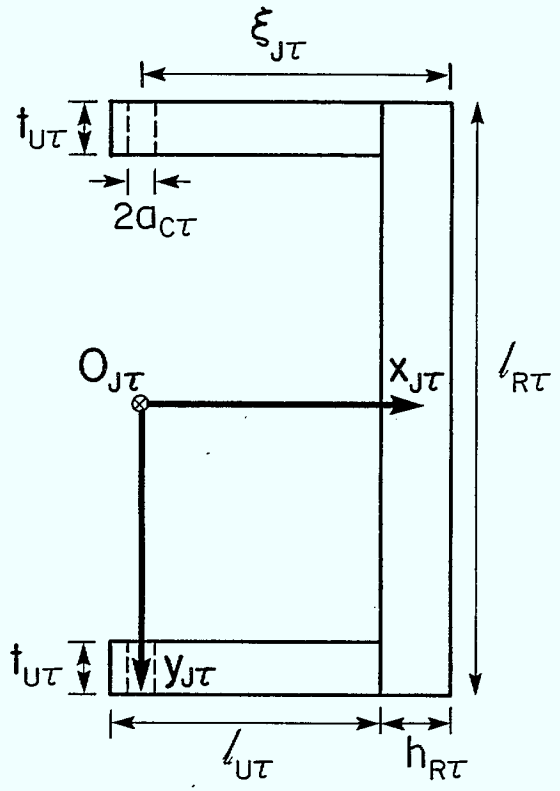

4.8: Rectangular Attachment Bracket (RAC)

total joint inertias are found by summing the bracket inertias from (4.81) with the universal inertias given by (4.75).

4.4.5 Joint Springs

It should be noted that a number of spring masses appear in the joint inertia model presented in the previous sections. These springs, which always occur in pairs, are shown conceptually in Fig. 4.4. Two sets of opposing springs and one set of complementary springs are found in each rib joint. If the joint is a strut joint then only the opposing spring-set on the mount shaft should be retained in the earlier inertia model [i.e., $m_{OS_\tau} = m_{CS_\tau} = 0$ in (4.66)].

The opposing springs occur in pairs to permit preloading of the springs. This shifts the equilibrium position for the springs away from zero, thus avoiding a potential hysteresis problem. To accomplish this each spring of an opposing pair is mounted so that its stored energy, if released, would generate a torque equal in magnitude to its counterpart but in the opposite direction. As a consequence, each spring 'torque' just balances the other, resulting in a preloaded pair.

The complementary spring pair is chosen to maintain an inertia balance rather than to create a preloaded condition. As explained in Appendix A, gravity provides the preloading torque for these springs.

4.4.6 Joint Damping

In the present design it is more likely that one might wish to reduce damping, rather than to increase it. If, however, this does not prove to be the case, a simple means for including additional damping in a controlled manner does exit. (There also is the opportunity to conduct control experiments for a variety of damping ratios.) It is a straightforward matter to mount Houdaille dampers on the ends of the universal mount and cross-shafts.

A typical Houdaille damper is shown in Fig. 4.9. It consists of a free rotational mass within a cylindrical cavity filled with viscous fluid [Thomson, 1972]. The only dynamical coupling between the free mass and the rotation of the shaft on which the damper is mounted is provided by the

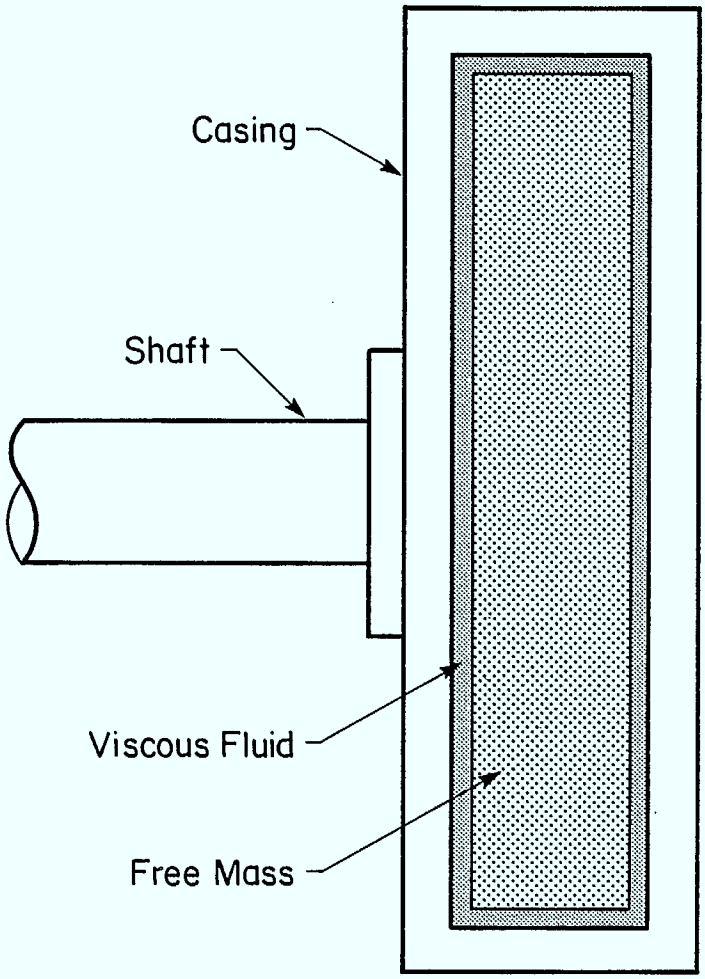

Figure 4.9: A Typical Houdaille Damper

viscosity of the fluid. The motion equations for this damper are well known (for further details, the interested reader is referred to [Thomson, 1972]).

5. CONCLUDING REMARKS

Substantial progress has been documented towards completing the detailed design for the flexible structure DAISY. A comprehensive dynamics model, based on a linear combination of individual substructural models, has been developed. Furthermore, preliminary designs for each substructure have been proposed and a detailed inertia model prepared. Gravitational and aerodynamic disturbance models also have been presented for each substructure. Upon such a foundation the major effort of iterating to an acceptable final structural design can be built. It remains, however, to model in detail the peripheral actuator and sensor inputs and outputs to the model. Although straightforward in concept, the details are greatly aided by the information provided in Section 2. Moreover, much dynamical data can be gleaned from the present model. For example, natural frequencies, mode shapes, maximum deflections, accelerations and loads on the structure can be predicted. The programning and simulations required to accomplish this task are now actively underway within Dynacon.

6. REFERENCES

Brenner, H. "Rheology of a Dilute Suspension of Axisymmetric Brownian Particles," *Int. J. Multiphase Flow*, Vol. 1, No. 2, 1974, pp. 195 - 341.

Hughes, P. C. "Structural Dynamics Modeling Plan for Control System Design and Evaluation," Dynacon Report MSAT-3, December, 1981.

Lamb, H. *Hydrodynamics* (6th ed.), Dover Publications, New York, 1945.

Milne, L. M.
Thomson, C. B. E. *Theoretical Hydrodynamics* (3rd. ed.), MacMillan, New York, 1955.

Sincarsin, G. B. "Facility to Study the Control of Flexible Space Structures — Conceptual Design," Dynacon Report DAISY-1, January, 1983.

Sincarsin, G. B.
Hughes, P. C. "Aerodynamics of a Vibrating Ribbed Structure," Dynacon Report DAISY-3, February, 1983.

Thomson, W. T. *Theory of Vibration with Applications*, Prentice-Hall, New Jersey, 1972.

Appendix A

Spirator Spring Design Considerations

As alluded to in Chapter 3, gravity can be used to preload the out-of-plane spirator spring at each rib root. This preload permits the working range of the spring to be shifted away from zero along the torque - vs - deflection curve (see Fig. A.1). Thus, a potential problem, that caused by the hysteresis often associated with torque reversals as the spring deflection passes through zero, can be avoided. To accomplish this, let us consider the 'dangling' rib shown in Fig. A.2. The root spirator spring is wound counterclockwise about the pivot and then attached to the rib, which is held securely. The rib is then released and moves clockwise, as a consequence of the spring torque, until the torque generated by gravity equals that applied by the spring. For the rib to be in equilibrium the angle from the vertical $\Theta = \Theta_o$ is given by

$$ma_G c \sin\Theta_o = k(\Theta_o - \Theta_r) \qquad (A.1)$$

where m is the mass of the rib, a_G is the acceleration of gravity, c is the distance to the mass center from the pivot, k is the torsional spring constant and Θ_r is the reference angle for the spring (i.e. the total spring angle in the counterclockwise direction prior to releasing the rib). This relation follows by direct substitution of $\Theta = \Theta_o$, a constant, into the motion equation for the rib

$$J\ddot{\Theta} + m a_G c \sin\Theta - k(\Theta - \Theta_r) = 0 \qquad (A.2)$$

where J is the second moment of inertia of the rib about the pivot.

To test the stability of the equilibrium $\Theta = \Theta_o$, one substitutes $\Theta = \Theta_o + \delta$ into (A.2), where δ is a first-order perturbation about Θ_o. The resulting requirement for stability is

$$ma_G c \cos\Theta_o > k \qquad (A.3)$$

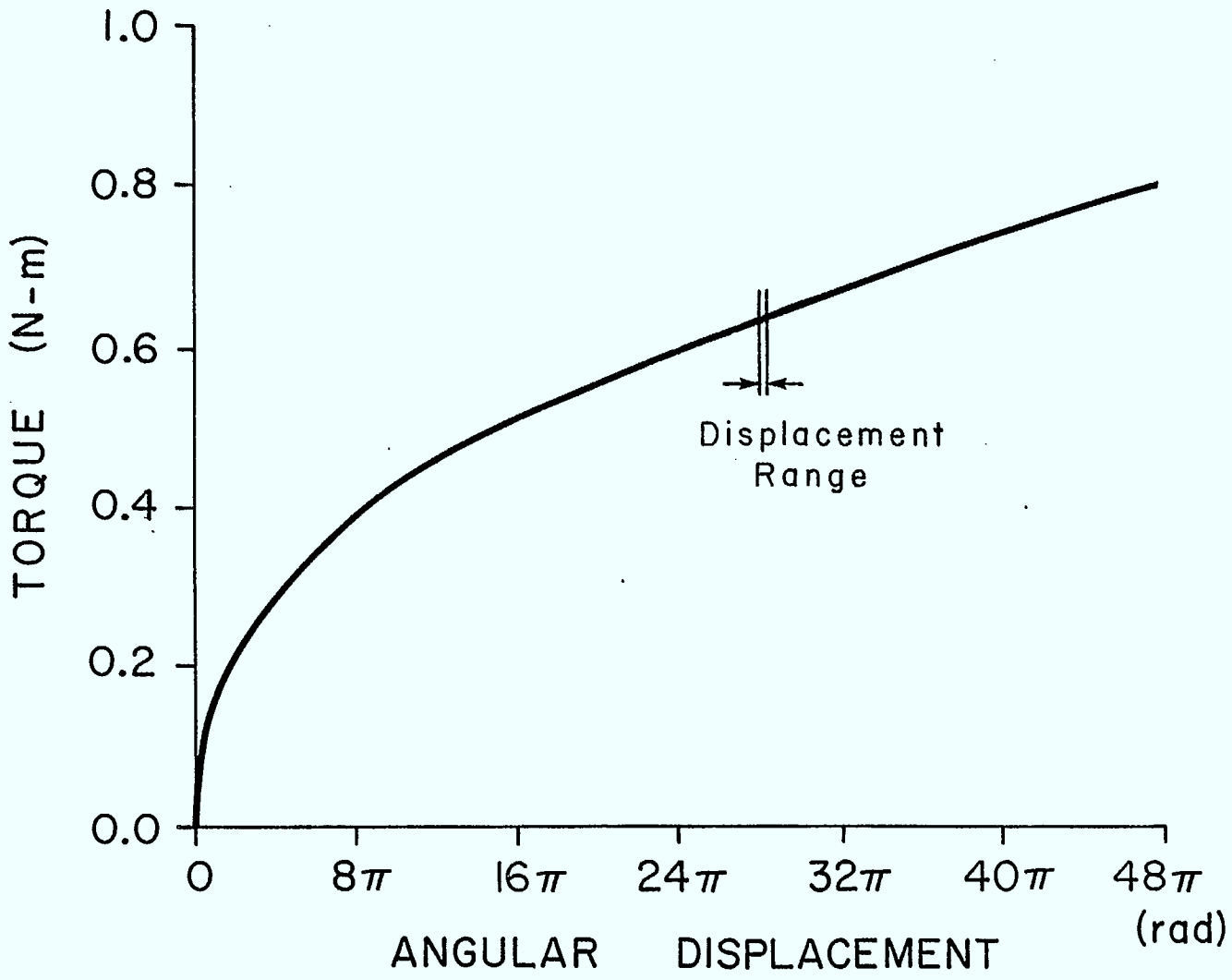

Figure A.1: Typical Torque versus Angular Displacement Characteristic for a 'Spirator Spring'

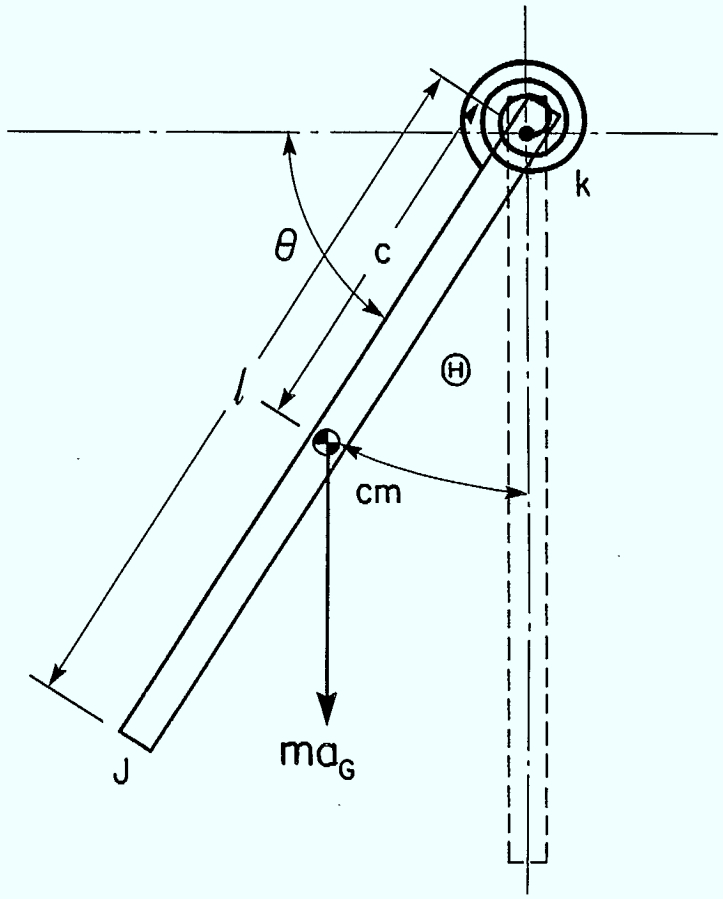

Figure A.2: A 'Drooping' Rib

Now letting the natural frequency of the out-of-plane rib vibration be denoted by ω, it follows that

$$\Theta_o = \cos^{-1}[J(\omega^2 + k)/ma_G c] \tag{A.4}$$

which, for a uniform rod ($c = \ell/2$, $J = m\ell^2/3$) and a spirator spring ($k \cong 0$), becomes

$$\Theta_o \cong \cos^{-1}(2\ell\omega^2/3a_G) \tag{A.5}$$

Therefore, the lower the natural frequency the smaller the angle Θ_o, and the larger the *droop angle* $\theta = (\pi/2) - \Theta_o$ (see Fig. A.2). It must be ensured, of course, that the chosen droop angle exceeds the anticipated half-amplitude of the rib vibration (i.e. $|\theta| > |\alpha|$). In other words, the first-order perturbation of primary interest here is the oscillation of the rib about Θ_o.

Relation (A.5) is most useful as a design tool for estimating the final equilibrium postion for each of DAISY's ribs. A better value for Θ_o then can be determined from (A.4) once the actual rib inertias (see Section 4.2) and spirator spring stiffnesses are known.

The remaining spirator rib springs, the spirator strut springs and the linear strut springs also are preloaded, but not by gravity. Instead they occur in opposing pairs in which each spring of the pair generates a torque or force equal in magnitude but opposite in direction to the other member of the pair. Hence the 'forces' balance and there is a static equilibrium with energy stored in each spring.

Appendix B

Calculation of Rib Hydrodynamic Matrices

In what follows, it will be assumed that rib j and F_{r_j} are as shown in Fig. 4.2. Futhermore, from Section 2.2.3, recall that the absolute displacement of an arbitrary point in rib j can be written (to first order) in the form

$$\underline{d}_{r_j}(\underline{r}_{r_j},t) = \underline{w}_{r_j}(t) - \underline{r}^{X}_{r_j}\underline{\theta}_{r_j}(t) + \underline{\Delta}_{r_j}(\underline{r}_{r_j},t) \tag{B.1}$$

where

$$\underline{\Delta}_{r_j}(\underline{r}_{r_j},t) \triangleq \underline{\Psi}_{r_j}(\underline{r}_j)\underline{q}_{r_j}(t) \tag{B.2}$$

$$\underline{\Psi}_{r_j}(\underline{r}_j) = -\underline{r}^{X}_{r_j} \tag{B.3}$$

$$\underline{q}_{r_j}(t) = \underline{\alpha}_j \tag{B.4}$$

Hence the velocity of an arbitrary point in rib j is

$$\underline{u}_{r_j}(\underline{r}_{r_j},t) = \dot{\underline{w}}_{r_j} - \underline{r}^{X}_{r_j}(\dot{\underline{\theta}}_{r_j} + \dot{\underline{\alpha}}_j) \tag{B.5}$$

The individual velocity components given by this expression play a key role in determining the rib hydrodynamic matrices.

B.1 Inertial-Resistance Matrices

As stated in Section 3.2.2, it is assumed that, for the purposes of modeling aerodynamic disturbances, rib j can be approximated by an 'infinite' cylinder. Thus for an ideal fluid, the appropriate velocity potential is

$$\phi_{r_j} = \frac{a_{r_j}}{R}(u_1\cos\lambda + u_2\sin\lambda) \tag{B.6}$$

where, as shown in Fig. B.1, u_1 and u_2 are the x_1 and x_2 components of the fluid flow at some arbitrary point, given by the polar coordinates (R, λ), and a_{r_j} is the radius of the rib. Thus the bracketed quantity in (B.6) is the fluid velocity component normal to the surface of the rib. It should be noted that the potential given by (B.6) assumes that the fluid is at rest at infinity. Furthermore, fluid flow along the symmetry axis of the rib is not permitted. This is consistent with the earlier arguments (recall Section 3.2.2) that inertial – resistance forces should be negligible in this direction.

For a rib oriented as shown in Fig. 4.2, x_1 and x_2 become y_{r_j} and z_{r_j}, and thus

$$\phi_{r_j} = \frac{a_{r_j}}{R}(u_y \cos\lambda + u_z \sin\lambda) \tag{B.7}$$

where from (B.5)

$$u_y = w_y + x(\dot{\theta}_z + \dot{\alpha}_z) - z(\dot{\theta}_x + \dot{\alpha}_x) \tag{B.8}$$

$$u_z = w_z - x(\dot{\theta}_y + \dot{\alpha}_y) + y(\dot{\theta}_x + \dot{\alpha}_x) \tag{B.9}$$

given

$$\underline{r}_{r_j} = [x \quad y \quad z]^T \tag{B.10}$$

expressed in F_{r_j}. Also, the normal to the rib's surface, $\underline{n}$, has the components

$$\underline{n}_{r_j} = [0 \quad \cos\lambda \quad \sin\lambda]^T \tag{B.11}$$

where

$$\cos\lambda = y/R \tag{B.12}$$

$$\sin\lambda = z/R \tag{B.13}$$

$$R^2 = x^2 + y^2 \tag{B.14}$$

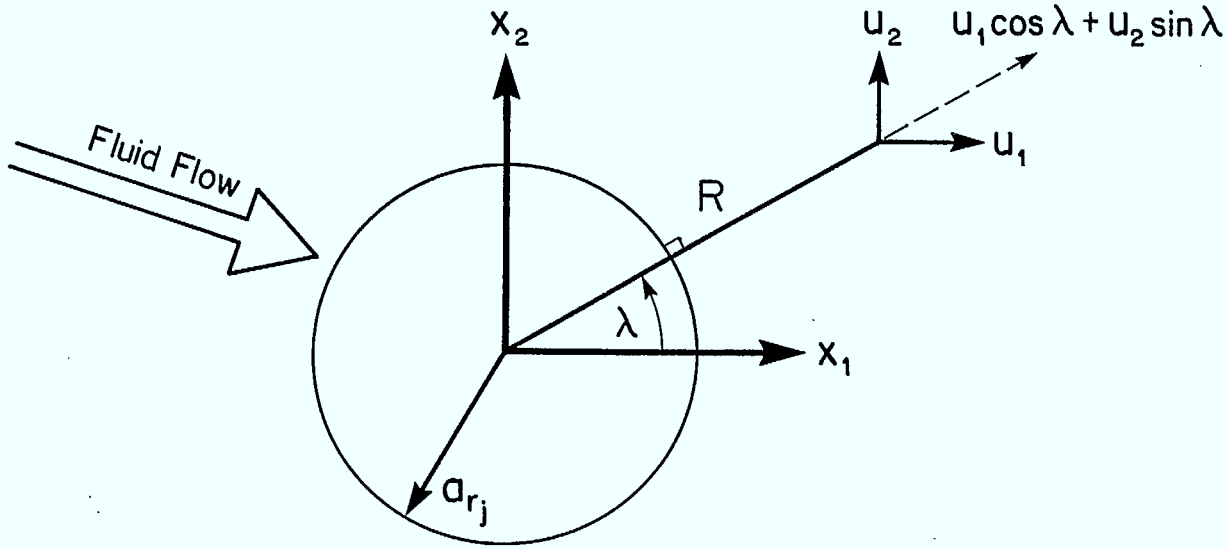

Figure B.1: Velocity Components for a Rib Immersed in an Ideal Fluid

Hence (B.7) can be rewritten in the form

$$\phi_{r_j} = \frac{a_{r_j}^2}{R}(\underline{n}^T\dot{\underline{w}} + \underline{n}^T\underline{1}^{\times}_{r_j}\underline{1}^{\times}_{r_j}\underline{r}^{\times}_{r_j}\dot{\underline{\theta}}_{r_j} + \underline{n}^T\underline{1}^{\times}_{r_j}\underline{1}^{\times}_{r_j}\underline{r}^{\times}_{r_j}\dot{\underline{\alpha}}_j) \tag{B.15}$$

with the knowledge, from Section 3.2.2, that

$$\underline{1}_{r_j} = [1 \quad 0 \quad 0]^T \tag{B.16}$$

Finally, recalling equation (3.9), namely,

$$\phi_{r_j} = \underline{\xi}^T_{w_{r_j}}\dot{\underline{w}}_{r_j} + \underline{\xi}^T_{\theta_{r_j}}\dot{\underline{\theta}}_{r_j} + \underline{\xi}^T_{q_{r_j}}\underline{\psi}_{r_j}\dot{\underline{q}}_{r_j} \tag{B.17}$$

the following relations become obvious:

$$\underline{\xi}^T_{w_{r_j}} = \frac{a_{r_j}^2}{R}\underline{n}^T_{r_j} \tag{B.18}$$

$$\underline{\xi}^T_{\theta_{r_j}} = \frac{a_{r_j}^2}{R}\underline{n}^T_{r_j}\underline{1}^{\times}_{r_j}\underline{1}^{\times}_{r_j}\underline{r}^{\times}_{r_j} \tag{B.19}$$

$$\underline{\xi}^T_{q_{r_j}} = -\frac{a_{r_j}^2}{R}\underline{n}^T_{r_j}\underline{1}^{\times}_{r_j}\underline{1}^{\times}_{r_j} \tag{B.20}$$

On surface S_{r_j}, $R = a_{r_j}$ and (B.18) through (B.20) become

$$\underline{\xi}^T_{w_{r_j}} = a_{r_j}\underline{n}^T \; ; \qquad \underline{\xi}^T_{\theta_{r_j}} = \underline{n}^T\underline{1}^{\times}_{r_j}\underline{1}^{\times}_{r_j}\hat{\underline{r}}^{\times}_{r_j} \tag{B.21}$$

$$\underline{\xi}^T_{q_{r_j}} = -a_{r_j}\underline{n}^T_{r_j}\underline{1}^{\times}_{r_j}\underline{1}^{\times}_{r_j}$$

where

$$\hat{\underline{r}}_{r_j} = \underline{r}_{r_j}/a_{r_j} = [x/a_{r_j} \quad \cos\lambda \quad \sin\lambda]^T \tag{B.22}$$

Then upon application of the integrals given by (3.8), namely,

$$\underline{M}_{Rr_j} = \rho\int_{S_{r_j}} \underline{n}_{r_j}\underline{\xi}_{w_{r_j}}^T \, dS_{r_j} \; ; \qquad \underline{P}_{Rr_j} = \rho\int_{S_{r_j}} \underline{n}_{r_j}\underline{\xi}_{q_{r_j}}^T \underline{\Psi}_{r_j} \, dS_{r_j}$$

$$\underline{C}_{Rr_j} = \rho\int_{S_{r_j}} \underline{r}_{r_j}^X \underline{n}_{r_j}\underline{\xi}_{w_{r_j}}^T \, dS_{r_j} \; ; \qquad \underline{H}_{Rr_j} = \rho\int_{S_{r_j}} \underline{r}_{r_j}^X \underline{n}_{r_j}\underline{\xi}_{q_{r_j}}^T \underline{\Psi}_{r_j} \, dS_{r_j} \tag{B.23}$$

$$\underline{J}_{Rr_j} = \rho\int_{S_{r_j}} \underline{r}_{r_j}^X \underline{n}_{r_j}\underline{\xi}_{\theta_{r_j}}^T \, dS_{r_j} \; ; \qquad \underline{M}_{RRr_j} = \rho\int_{S_{r_j}} \underline{\Psi}_{r_j}^T \underline{n}_{r_j}\underline{\xi}_{q_{r_j}}^T \underline{\Psi}_{r_j} \, dS_{r_j}$$

given

$$dS_{r_j} = a_{r_j} \, d\lambda \, dx \tag{B.24}$$

where $0 \leq \lambda \leq 2\pi$ and $0 \leq x \leq \ell_{r_j}$ (ℓ_{r_j} is the length of the rib, $\hat{\ell}_{r_j} = \ell_{r_j}/a_{r_j} >> 1$), the following inertial-resistance hydrodynamic matrices result ($m_{r_j} = \rho\pi a_{r_j}^2 \ell_{r_j}$):

$$\underline{M}_{Rr_j} = \begin{bmatrix} 0 & 0 & 0 \\ 0 & m_{r_j} & 0 \\ 0 & 0 & m_{r_j} \end{bmatrix} ; \qquad \underline{P}_{Rr_j} = \begin{bmatrix} 0 & 0 & 0 \\ 0 & 0 & \frac{1}{2}m_{r_j}\ell_{r_j} \\ 0 & -\frac{1}{2}m_{r_j}\ell_{r_j} & 0 \end{bmatrix}$$

$$\underline{C}_{Rr_j} = \begin{bmatrix} 0 & 0 & 0 \\ 0 & 0 & -\frac{1}{2}m_{r_j}\ell_{r_j} \\ 0 & \frac{1}{2}m_{r_j}\ell_{r_j} & 0 \end{bmatrix} ; \qquad \underline{H}_{Rr_j} = \begin{bmatrix} 0 & 0 & 0 \\ 0 & \frac{1}{3}m_{r_j}\ell_{r_j}^3 & 0 \\ 0 & 0 & \frac{1}{3}m_{r_j}\ell_{r_j}^3 \end{bmatrix} \tag{B.25}$$

(cont'd)

$$\underline{J}_{Rr_j} = \begin{bmatrix} 0 & 0 & 0 \\ 0 & \frac{1}{3}m_{r_j}\ell^3_{r_j} & 0 \\ 0 & 0 & \frac{1}{3}m_{r_j}\ell^3_{r_j} \end{bmatrix}; \quad \underline{M}_{RRr_j} = \begin{bmatrix} 0 & 0 & 0 \\ 0 & \frac{1}{3}m_{r}\ell^3_{r_j} & 0 \\ 0 & 0 & \frac{1}{3}m_{r_j}\ell^3_{r_j} \end{bmatrix} \tag{B.25}$$

These are the matrices cited for rib j in Table 3.2 of Section 3.2.2.

B.2 Viscous-Resistance Matrices

A very detailed derivation of the viscous-resistance hydrodynamic matrices for a variety of shapes is provided by [Brenner, 1974] and the references cited therein. Rather than repeat the derivation for an 'infinite' *rigid* cylinder here, the interested reader is referred to the above papers. The extension of Brenner's results to the case of a *flexible* rib, however, deserves further comment. From (B.5), we know that the 'elastic' coordinates $\underline{\alpha}_j$ behave the same as the rigid rotations $\underline{\theta}_{r_j}$, as far as determining the velocity of an arbitrary point in the rib is concerned. (This is true because the flexibility associated with each rib of DAISY is all localized in torsional spirator springs located at the rib root.) Therefore, in terms of the normal stress components associated with $\dot{\underline{\alpha}}_j$ and $\dot{\underline{\theta}}_{r_j}$,

$$\underline{N}_{\alpha_j} = \underline{N}_{\theta r_j} \tag{B.26}$$

For a detailed discussion of the exact form of the stress tensor the reader is referred to [Sincarsin and Hughes, 1983]. Here it is sufficient to recognize only that (B.26) is true. Then given (3.12), it immediately follows that

$$\underline{H}_{Vr_j} = -\mu\int_{S_{r_j}} \underline{r}^X_{r_j}\underline{N}_{\alpha_j}\, dS_{r_j} = -\mu\int_{S_{r_j}} \underline{r}^X_{r_j}\underline{N}_{\theta r_j}\, dS_{r_j} = \underline{J}_{Vr_j} \tag{B.27}$$

$$\underline{M}_{vvr_j} = -\mu\int_{S_{r_j}} \underline{\Psi}^T \underline{N}_{\alpha_j} dS_{r_j} = -\mu\int_{S_{r_j}} \underline{r}^x_{r_j} \underline{N}_{\theta r_j} dS_{r_j} = \underline{J}_{vr_j} \tag{B.28}$$

Also, from [Sincarsin and Hughes, 1983], it is known that

$$\underline{C}_v^T = -\mu\int \underline{N}_\theta dS_B \tag{B.29}$$

Whence

$$\underline{P}_{vr_j} = -\mu\int_{S_{r_j}} \underline{N}_{\alpha_j} dS_{r_j} = -\mu\int_{S_{r_j}} \underline{N}_{\theta r_j} dS_{r_j} = \underline{C}^T_{vr_j} \tag{B.20}$$

Thus, for DAISY, no extra computations are required to obtain the viscous-resistance hydrodynamic matrices associated with the elastic motion of rib j.

SINCARSIN, G.B.

Facility to study the control of flexible space structures: detailed design (preliminary).